

POLITECNICO DI TORINO

Corso di Laurea Magistrale
in Ingegneria Meccanica

Tesi di Laurea Magistrale



Techno-economic analysis of energy storage for best
utilization of surplus of thermal and electrical energy

Relatori:

Prof. Vittorio Verda

Prof. Elisa Guelpa

Supervisor esterno :

Prof. Adriano Sciacovelli

Candidato:

Luca Abatemarco

Matr. s241975

Anno Accademico 2018/2019



POLITECNICO DI TORINO

Joint work with :



UNIVERSITY OF BIRMINGHAM

Abstract

In this work, a model of an Organic Rankine Cycle (ORC) able to produce electricity thanks Waste Heat Recovery (WHR) from an industrial process has been developed. To compute all the steps a coupled use of MatLab and Engineer Equations Solver (EES) is used.

Very common target in the whole society is energy saving. It is performed with several forms; the present work aims to investigate in the world of the industrial processes and how can be possible the best utilization of a surplus of energy existing during them. The concept of “Waste Heat Recovery” (WHR) is important, waste heat is present in large quantities in several sectors, such as the manufacturing industry, commercial and residential buildings, power plants and transportation systems. Waste Heat Recovery (WHR) systems basically transfer waste energy to a heat carrier or storage system.

It's impossible to perform work without waste heat: wherever goods are produced, and machines are operated, waste heat is produced and released either via radiation, cooling fluid, exhaust gas or air. These streams often contain large amounts of exergy and would be able to perform work through one of the many waste heat usage technologies. The dominant one in these technologies is the TES (Thermal Energy Storage). The using of TES allows also to manipulate the differences between demand and supply and obtain the best utilization of this surplus of energy. The most suitable waste heat sources for power generation are found in energy-intensive industrial processes. All these sources very often experience fluctuations of the available thermal power. To obtain work from the WHR, there is a complication of the plant in terms of components which means adding costs. Furthermore, must be necessary to evaluate how the system is able to use the WHR with a fluctuating source which means operate mainly in off-design. The focus of this study is the coupling of the use of those sources with the ORC using also a TES in order to understand when its techno-economic impact is relevant. That represents an enormous opportunity to increase the energy efficiency of various industry sectors and to reduce emissions and waste of primary sources.

Table of Contents

ABSTRACT	2
INTRODUCTION	14
1.1 STRUCTURE OF THE THESIS	15
1.2 ENERGY'S WORLD SCENARIO AND THE RELEVANCE OF THE WHR	16
1.3 HOW TO PRODUCE ELECTRICAL ENERGY FROM WHR	18
1.4 THERMAL ENERGY STORAGE AND HOW IS POSSIBLE TO IMPROVE THE PROCESSES WITH IT	23
1.5 AIMS AND OBJECTIVES	24
2. O.R.C. – MODELLING AND THERMODYNAMIC BEHAVIOR OF THE COMPONENTS IN DESIGN AND OFF-DESIGN CONDITIONS	26
2.1 DEFINITION OF THE THERMODYNAMIC CYCLE AND GENERAL ASSUMPTIONS.....	26
2.2 GOVERNING EQUATIONS OF THE COMPONENTS IN DESIGN-CONDITIONS	30
2.2.1 EVAPORATOR	30
2.2.2 TURBINE.....	33
2.2.3 INTERMEDIATE HEAT EXCHANGER	33
2.2.4 CONDENSER.....	34
2.2.5 PUMP	34
2.3 OFF-DESIGN CONSIDERATIONS.....	35
2.4 VALIDATION, THE FEASIBILITY OF THE RESULTS, AND ASSESSMENT OF THE WORKING CONDITIONS	37
2.4.1 VALIDATION OF THE THERMODYNAMIC MODEL	37
2.4.2 DEFINITION OF THE DESIGN CONDITIONS	38
2.4.3 THE RESPONSE OF THE SYSTEM AT THE VARIABILITY OF THE SOURCE	40
2.5 EXERGY'S ANALYSIS.....	43

3. MODEL DEVELOPMENT OF DIFFERENT TYPOLOGIES OF THERMAL ENERGY STORAGE (TES).	46
3.1.1 TWO-TANK	47
3.1.2 SINGLE THERMOCLINE	50
3.1.3 DUAL-MEDIA THERMOCLINE	52
3.1.4 GOVERNING EQUATIONS AND CONSIDERATIONS OF MOLTEN SALT PUMPS	56
3.2 VALIDATION	58
4. ECONOMICS CORRELATIONS FOR THE EVALUATION OF THE INVESTMENT	62
4.1 ORGANIC RANKINE CYCLE	62
4.2 THERMAL ENERGY STORAGE	65
4.3 TECHNO-ECONOMIC PARAMETERS	66
4.3.1 LCOE	66
4.3.2 NCOTES	66
4.3.3 NET PRESENT VALUE	66
4.3.4 CAPACITY FACTOR	67
5. TECHNO-ECONOMIC ANALYSIS – RESULTS OF DIFFERENT CASES FOR THE EVALUATION OF THE INFLUENCE OF WORKING CONDITIONS HAVING A FLUCTUATING SOURCE.	68
5.1 PRESENTATION OF SCENARIOS	68
5.1.1 SCENARIO 1: HYPOTHETIC SINUSOIDAL TREND OF SOURCE	68
5.1.2 SCENARIO 2: CLINKER COOLING	69
5.1.3 SCENARIO 3: PERIODIC ANALYSIS	70
5.2 SIZING OF THERMAL ENERGY STORAGE	70
5.2.1 ONLY HTF AS THERMAL STORAGE MEDIUM	71
5.2.2 DUAL MEDIA SENSIBLE THERMAL STORAGE, SOLID AND HTF	71
5.2.3 GEOMETRY DEFINITION AND SIZING OF THE TANKS IN DIFFERENT SCENARIOS AND CONFIGURATIONS	72
5.3 COMPARISONS BETWEEN THE SCENARIOS WITH AND WITHOUT THE STORAGE FOCUSING ON THE DIFFERENCES IN TERMS OF THERMAL LOAD	76

5.4	ORC'S ANALYSIS	84
5.5	EXERGY'S RESULTS OF THE PLANT	96
5.6	TECHNO-ECONOMIC ANALYSIS.....	98
5.6.1	COST ANALYSIS OF THE INVESTMENT - LCOE & NCOTES EVALUATION	98
5.6.2	PRELIMINARY STUDY OF THE INVESTMENT'S FEASIBILITY - NPV & PBP EVALUATION	111
5.6.3	UTILISATION OF THE TES	114
5.7	MISCELLANEOUS RESULTS – SURFACE HEAT EXCHANGERS	118
6.	<u>CONCLUSIONS AND FUTURE DEVELOPMENTS</u>	<u>119</u>
6.1	RESUME AND DISCUSSION OF THE RESULTS	120
6.2	ADDITIONAL SCENARIOS – POST ANALYSIS.....	125
6.2.1	SCENARIO 4 – PERIODIC ANALYSIS WITHOUT OVERSIZE OF THE TESS'S TANKS (20% OF REDUCTION) 125	
6.2.2	SCENARIO 5 – PERIODIC ANALYSIS WITH A MODIFIED UNDERLOAD SOURCE-PROFILE (5 % OF REDUCTION)	128
6.3	FUTURE WORK.....	130
7.	<u>REFERENCES.....</u>	<u>132</u>

Figures

Figure 1 - Schematic representation of the chapter-by-chapter structure.....	15
Figure 2 - Comparisons of the T-s diagram with some organic fluids and water.....	20
Figure 3 - Recuperator or Internal Heat Exchanger configuration with T-s diagram.....	21
Figure 4 - Multiple superheating configuration with the T-s diagram.....	22
Figure 5 - Dual Pressure configuration with the T-s diagram.....	22
Figure 6 - Scheme of the plant with the denomination of state point	28
Figure 7 - Scheme of the evaporator.....	31
Figure 8 - Recovery Heat Exchanger (IXE)	34
Figure 9 - Theoretical trend of the source	39
Figure 10 - Temperature/Entropy diagram of the R123 at the design conditions.....	40
Figure 11 - Pie graphs of the Exergy's Destruction	44
Figure 12 - TES systems subdivision: a) Two tank direct b) two tank indirect c)Thermocline system d) Concrete block system - [37]	47
Figure 13 - Two tank TES - Operating principle of the integration between components of the plant.....	49
Figure 14 - Thermocline thermal storage using a heat transfer fluid only (A) Thermocline; (B) hot and cold fluid separated with a baffle. [39].....	51
Figure 15 - Single Thermocline TES - Operating principle of the integration between components of the plant.....	52
Figure 16 - Scheme of the packed bed TES and a control volume for analysis.....	54
Figure 17 - Comparisons between thw Van Lew's work (dashed line) and the results obtained with the model.....	59
Figure 18 - Time-independent study, Adimensional coordinates (Time and space)	60
Figure 19 - Time-independent study,Trend of the percentage error	60
Figure 20 - Time-independent study, Trend of the maximum and average percentage error	60
Figure 21 - From [9], Overview of the specific investment costs of ORGANIC RANKINE CYCLE	64
Figure 22 - Scenario 1) Source-profile representation	69

Figure 23 - Scenario 2) Source-profile representation	69
Figure 24 - Scenario 3) Source-profile representation	70
Figure 25 - Volumes of the different configurations regarding SCENARIO 1	73
Figure 26 - Breakdown of the volume of the tank between HTF and Filler – SCENARIO 1	73
Figure 27 - Volumes of the different configurations regarding - SCENARIO 2	74
Figure 28 - Breakdown of the volume of the tank between HTF and Filler – SCENARIO 2	74
Figure 29 - Volumes of the different configurations regarding - SCENARIO 3	75
Figure 30 - Breakdown of the volume of the tank between HTF and Filler – SCENARIO 3	75
Figure 31 - T-s representation of Nominal conditions (GREEN) and limit conditions (YELLOW)	78
Figure 32 - Different phases of the source-profile: SCENARIO 1	79
Figure 33 - Different phases of the source-profile: SCENARIO 2	79
Figure 34 - Different phases of the source-profile: SCENARIO 3	80
Figure 35 - Comparisons of the work conditions with/without storage in terms of Thermal Load in different configurations – SCENARIO 1	81
Figure 36 - Comparisons of the work conditions with/without storage in terms of Thermal Load in different configurations – SCENARIO 2	81
Figure 37 - Comparisons of the work conditions with/without storage in terms of Thermal Load in different configurations – SCENARIO 3	82
Figure 38 - Comparisons of POWER NET with/without storage in different configurations – SCENARIO 1	83
Figure 39 - Comparisons of POWER NET with/without storage in different configurations – SCENARIO 2	83
Figure 40 - Comparisons of POWER NET with/without storage in different configurations – SCENARIO 3	84
Figure 41 - Orc average efficiency for different configurations – SCENARIO 1	85
Figure 42 - Orc average efficiency for different configurations – SCENARIO 2	85
Figure 43 - Orc average efficiency for different configurations – SCENARIO 3	86
Figure 44 - Orc Efficiency trend along the time analysis – SCENARIO 1	86
Figure 45 - Orc Efficiency trend along the time analysis – SCENARIO 2	87
Figure 46 - Orc Efficiency trend along the time analysis – SCENARIO 3	87

Figure 47 - No storage case, ORC and GLOBAL efficiency comparisons – SCENARIO 1.....	88
Figure 48 - No storage case, ORC and GLOBAL efficiency comparisons – SCENARIO 2.....	88
Figure 49 - No storage case, ORC and GLOBAL efficiency comparisons – SCENARIO 3.....	89
Figure 50 - Electrical energy production on daily time analysis – SCENARIO 1.....	90
Figure 51 - Surplus of Electrical power production on yearly time-analysis - SCENARIO 1 ...	90
Figure 52- Electrical energy production on daily time analysis – SCENARIO 2	91
Figure 53 - Surplus of Electrical power production on yearly time-analysis - SCENARIO 2...	91
Figure 54 - Electrical energy production on daily time analysis – SCENARIO 3.....	92
Figure 55 - Surplus of Electrical power production on yearly time-analysis - SCENARIO 3....	92
Figure 56 - Isentropic average efficiency Turbine – SCENARIO 1.....	93
Figure 57 - Trend of isentropic efficiency of the turbine – SCENARIO 1	93
Figure 58 - Isentropic average efficiency Turbine – SCENARIO 2	94
Figure 59 - Trend of isentropic efficiency of the turbine – SCENARIO 2	94
Figure 60 - Isentropic average efficiency Turbine – SCENARIO 3	95
Figure 61 - Trend of isentropic efficiency of the turbine – SCENARIO 3	95
Figure 62 - Destruction of exergy breakdown - SCENARIO 1	96
Figure 63 - Destruction of exergy breakdown - SCENARIO 2	96
Figure 64 - Destruction of exergy breakdown - SCENARIO 3	97
Figure 65 - Cost of the materials for the tank - Breakdown between HTF and Filler – SCENARIO 1.....	102
Figure 66 - Cost TES per kWhth of thermal energy storage capacity – SCENARIO 1	103
Figure 67 – LCOE results – SCENARIO 1	103
Figure 68 – Deviation of the LCOE respect the conditions without storage – SCENARIO 1 .	104
Figure 69 - NCOTES results – SCENARIO 1	104
Figure 70 - Cost of the materials for the tank - Breakdown between HTF and Filler – SCENARIO 2.....	105
Figure 71 - Cost TES per kWhth of thermal energy storage capacity – SCENARIO 2	105
Figure 72 - LCOE results – SCENARIO 2	106
Figure 73 - Deviation of the LCOE respect the conditions without storage – SCENARIO 2..	106
Figure 74 - NCOTES results – SCENARIO 2	107

Figure 75 - Cost of the materials for the tank - Breakdown between HTF and Filler – SCENARIO 3.....	108
Figure 76 - Cost TES per kWhth of thermal energy storage capacity – SCENARIO 3	108
Figure 77 - LCOE results - SCENARIO 3	109
Figure 78 - Deviation of the LCOE respect the conditions without storage – SCENARIO 3.	109
Figure 79 - NCOTES results - SCENARIO 3	110
Figure 80 – Pay Back Period results - SCENARIO 1.....	111
Figure 81 - Net Present Value – SCENARIO 1	111
Figure 82 – Pay Back Period results - SCENARIO 2.....	112
Figure 83 - Net Present Value – SCENARIO 2	112
Figure 84 - Pay Back Period results - SCENARIO 3	113
Figure 85 – Net Present Value – SCENARIO 3	113
Figure 86 - Capacity factor - Results - SCENARIO 1.....	114
Figure 87 - State of the TESs - Therminol VP-1 - SCENARIO 1	114
Figure 88 - State of the TESs - Hitec - SCENARIO 1	115
Figure 89 - - Capacity factor - Results - SCENARIO 2	115
Figure 90 - State of the TESs - Therminol VP-1 - SCENARIO 2	116
Figure 91 - State of the TESs - Hitec - SCENARIO 2	116
Figure 92 - - Capacity factor - Results - SCENARIO 3	117
Figure 93 - State of the TESs - SCENARIO 3	117
Figure 94 - Differences between Scenario 3 and Scenario 4	126
Figure 95 - Differences between Scenario 4 and Scenario 5 – Dimensionless T.L. representation	128
Figure 96 - Differences between Scenario 4 and Scenario 5 – State of TES.....	129

Tables

Table 1 - Resume of working fluids.....	19
Table 2 - Values of the independent variables for the design conditions	29
Table 3 – Comparisons for Validation of the ORC model	38
Table 4 - Information of the source of the plant: flue gas exiting an industrial process (Cement Industry).....	39
Table 5 - Operational Design Parameters of the Organic Rankine Cycle.....	40
Table 6 – Operational Parameters - Comparison between nominal and off-design conditions (50% of the source at the evaporator)	41
Table 7 - Heat transfer surfaces - Comparison between nominal and off-design conditions (50% of the source at the evaporator)	42
Table 8 – Resume of Exergy balances.....	43
Table 9 - Exergy's parameters in the comparison between nominal and off-design conditions (50% source at the evaporator)	44
Table 10 - Main HTF and Filler material for Sensible Heat TESs	53
Table 11 - Results of the pump in the TES-Loop.....	57
Table 12 - Material properties (HTF and filler) present in the tank.....	58
Table 13 - Data used for the validation	58
Table 14 - The unit cost of the storage medium.....	65
Table 15 - Formulations for tank estimation cost.....	65
Table 16 - Input fixed for the determination of the geometry of the tank	72
Table 17 - Breakdown of the costs of TESs – THERMINOL VP1 - SCENARIO 1	99
Table 18 - Breakdown of the costs of TESs –HITEC - SCENARIO 1	99
Table 19 - Breakdown of the costs of TESs – THERMINOL VP1 - SCENARIO 2	100
Table 20 - Breakdown of the costs of TESs – HITEC – SCENARIO 2	100
Table 21 - Breakdown of the costs of TESs – THERMINOL VP-1 as HTF – SCENARIO 3	101
Table 22 - Breakdown of the costs of TESs – HITEC – SCENARIO 3	101
Table 23 - Surfaces heat exchange – Nominal Conditions	118
Table 24 - LCOE'scenarios results	120
Table 25 – Capacity factor's scenarios results.	121

Table 26 – PBP’s scenarios results.....	122
Table 27 – NPS’s scenarios results.....	122
Table 28- NCOTES’s scenarios results.....	123
Table 29 – Cost TES of scenarios results	124
Table 30 - Lcoe's results - Scenario 4.....	126
Table 31 - NPV's results - Scenario 4	127
Table 32 - PBP's results - Scenario 4.....	127
Table 33 - Lcoe's results - Scenario 5.....	129
Table 34 - NPV's results - Scenario 5	129
Table 35 - PBP's results - Scenario 5	130

Nomenclature

A	Area/surface of heat exchanger
CF	Capacity Factor
CAES	Compressed Air Energy Storage
C	Costs
DMT	Dual-Media Thermocline
EES	Engineering Equations Solver
Ft	Geometrical parameter
Cp	Heat capacity at constant pressure
Q	Heat exchanged
HRSG	Heat Recovery Steam Generator
HTF	Heat Transfer Fluid
H	Height of the tank
HP	High Pressure
IXE	Interanal Heat Exchanger
LCOE	Levelized cost of Electricity
LMTD	Logarithmic method temperature difference
LP	Low Pressure
m	Mass flow rate
NPV	Net Present Value
NCOTES	Normalized cost of thermal energy storage
Pr	Number of Prandtl
Re	Number of Reynilds
ORC	Organic Rankine Cycle
U	Overall coefficient of heat exchanger
PCM	Phase Change Material
W	Power
P	Pressure
PHPS	Pumped Hydro-Power Storage
R	Radius of the tank
ST	Single Thermocline
h	Specific enthalpy
s	Specific entropy
SIC	Specific Investment Cost
E	Specific exergy
TEA	Techno-Economic Approach
T	Temperature
k	Thermal Conductivity
T.L.	Dimensionless Thermal Load
TFC	Trilateral Flash Cycle
TT	Two-Tank
u	Velocity along the pipe
V	Volume

WHR	Waste Heat Recovery
z	Dimensionless space

Greek Symbols

β	Pressure ratio in the turbine
ε	Void factor
η	Efficiency
θ	Dimensionless Temperature
Δ	Variation
ρ	Density

Subscripts and superscripts

<i>BO</i>	Boiler
<i>c</i>	Cold
<i>cond</i>	Condenser
<i>d</i>	Design
<i>eff</i>	Effective
<i>env</i>	Environment
<i>evap</i>	Evaporator
<i>ex</i>	Exergetic
<i>f</i>	Fluid
<i>h</i>	Hot
<i>in</i>	Inlet
<i>is</i>	Isentropic
<i>max</i>	Maximum
<i>mecc</i>	Mechanical
<i>med</i>	Medium
<i>mean</i>	Average
<i>out</i>	Outlet
<i>off</i>	Off-design
<i>p</i>	Pump
<i>pp</i>	Pitch point
<i>PH</i>	Preheater
<i>pol</i>	Polytropic
<i>ref</i>	Reference
<i>s</i>	Solid
<i>SH</i>	Superheater
<i>source</i>	Coming from the source
<i>tes</i>	Thermal Energy storage
<i>Water</i>	Water, regarding the additional fluid used at the condenser
*	Design Conditions

Introduction

The world's energy scenario is affected by several numbers of complex phenomena that influence the quality of life and the economy of all the countries. All over the world, the most important target for researchers and manufacturers is to find out different sustainable energy supply which is competitive in terms of economic parameters but mainly can respect the requirements of the industrial process keeping low the environmental impact. If from one side, our planet gives us several signs that would lead to minimizing the consumption of energy, on the other hand, the global level of energy production is increasing in the last decades, mainly caused by the economic development of a lot of countries, predominantly China and India.

From 1992 with the Conference of Rio de Janeiro have been held at recurring intervals different international conferences and were aimed to reach a common agreement regarding reducing the level of emissions. They committed to keeping the increase in global average temperature to well below 2°C above pre-industrial levels. To do this CO_2 emissions must decrease significantly and renewable energies play an important role in the gradual replacement of fossil fuels, which are mostly responsible for global warming [1][2][3]. Options to tackle this huge problem can be simply summarized in a large use of renewable sources and/or reducing the energy demand.

The definition of a new energetic model that, on one hand, must satisfy the world's growing energy-demand and on the other side should protect and safeguard the environment containing CO_2 emissions.

1.1 Structure of the thesis

The structure of the thesis is illustrated in **Errore. L'origine riferimento non è stata trovata..**

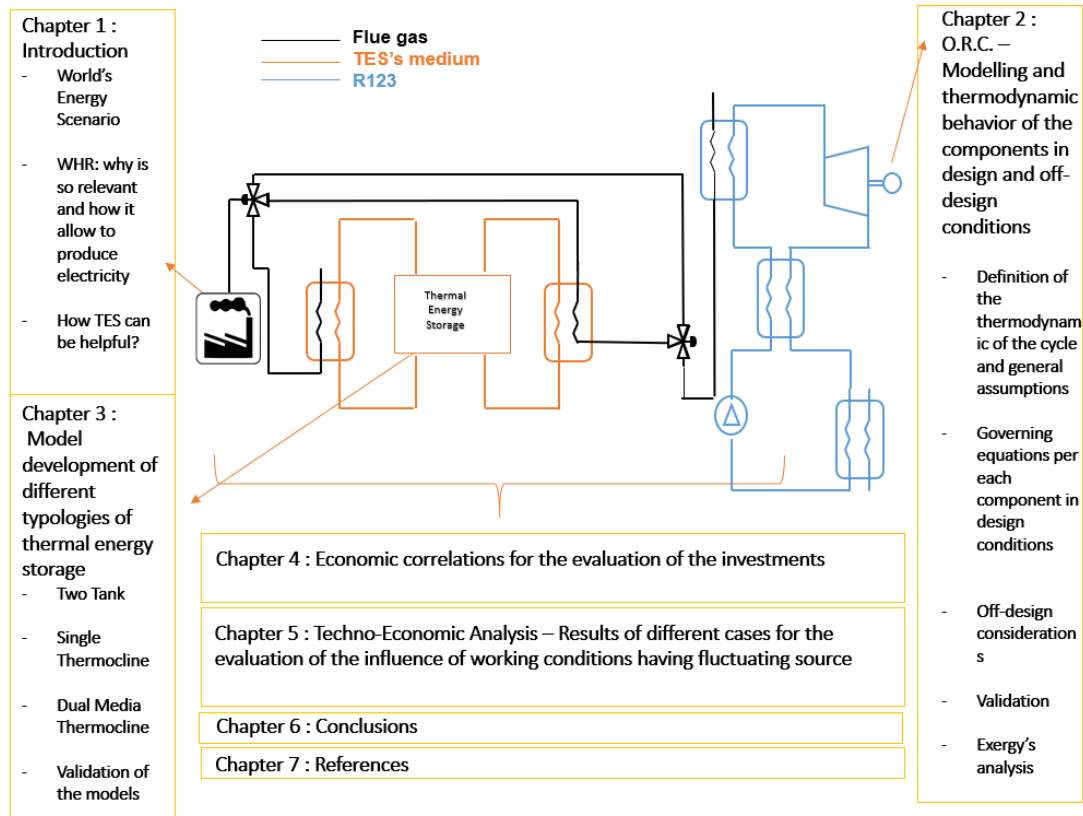


Figure 1 - Schematic representation of the chapter-by-chapter structure

The subdivision in chapters follows also the chronological order of the work. Chapter 1, is an introduction of the world's energetic scenario, focusing on the Waste Heat Recovery and its state of the art. In addition, a literature review of the world of the ORC and of TESs, precisely the manner in which they are able to improve the performance of the processes. Chapter 2 presents discussions and models related all the components of the ORC, validation of the thermodynamic process is present as well. Chapter 3 presents numerical models of the various typologies of TES under investigation, the model are already presented in literature, but the implementation has been carried out in a different environment (EES&MatLab) achieving positive results. Chapter 4 presents the correlations of the economic parameters needed to start the Techno-Economic analysis of the plant. Finally, Chapter 5 shows the results and comparisons between all the configurations after the integrations of all the tools

by combining the thermodynamic aspects (presents in Chapters 2/3) and the pure economic definitions (Chapter 4).

In the end, Chapter 6 summarise the conclusions and any possible developments of the work.

1.2 Energy's world scenario and the relevance of the WHR

For decades, the continuous increase in the consumption of fossil reserves caused several problems concerning the environment, like global warming, the ozone hole, and pollution. For those reasons, governments and institutions have an issue to tackle: energy saving. As direct consequences aim of several studies has been developed and performed various technologies to produce electricity avoiding bringing damage to the environment. The latter aim is tackled, in several different applications, with the following typologies of source:

- Solar
- Biomass
- Geothermal
- Waste-Heat-Recovery

Large studies are in the literature regarding the use of energy supply thanks to solar sources [4], biomass sources [5] or the use of geothermal plants [6].

Implementing a better energy management has an important role in several fields; recovering energy from the amount of waste-energy of process and as a consequences exploit low and medium temperature heat sources produce good results [7], there is a big effort in the deep analysis of sources at a low-medium scale of temperature. Thanks to that, it could be possible for the production of energy without using additional fossil fuels or decreasing the amount of them considerably.

Those listed are potential areas in which a good surplus of heat can be used; all of them are sources with a temperature range between 100/600 °C. Aim of this work is related to the Waste Heat Recovery from industrial processes. According to a study of the US Department of Energy [8], the total amount of energy considering as waste is 20/50% of the total primary energy consumption. With the term "waste heat" is meant the amount of heat which is not used, which comes from a combustion process or any other chemical reaction or thermal process and is discarded to the environment. Key-role is related to the technologies able to

recover heat, even partially, from those processes. Following the main advantages of recovery heat from an industrial process:

- The electricity production could be used in the same company as the source, avoiding problems of transmissions and connections with the grids.
- The encumbrance is not so relevant.
- High capacity factor compared with solar or wind sources.

Several sectors have a very energy-intensive industrial process, and there is a relevant amount of thermal energy at the end of it. The recovery of heat in those sectors have a huge impact not only for the reduction of the consumptions but also to increase the overall efficiency of the operational plant. The opportunity to recover heat from an industrial process is often related to a flux of hot gases, usually called flue gas. The heat exchange could be direct between the source and the heat transfer fluid or indirect. In this last case, an additional medium is used to allow the heat exchange.

Following a resume of the state of the art of the main sectors for WHR.

CEMENT INDUSTRY

The production of the cement has a huge amount of waste heat at a low-medium temperature. There are several studies on how to improve the efficiency of the cement production using those exhaust, but the only way to directly reduce the waste is adding another technology to produce electricity, so common is the use of the ORC. The main flux of heat exiting the plant are:

- Combustion Gas exiting the kiln with a range temperature of 250-400 °C.
- Cooling air from the clinked with a temperature range of 250-350 °C.

STEEL INDUSTRY

The heat from the steel production can be recovered from:

- Flue gas from the combustion of the natural gas, in kilns or for thermal treatments (usually clean and without special requirements for the heat exchange).
- Flues gas from the melts process (usually at a higher value of temperature but with more technical difficulties of treatment)

GLASS INDUSTRY

The production of glass could be a good candidate for recovering waste heat, especially related to its level of temperature (400-600 °C). In the same way of the steel industry, the technical issues are a factor in the way to use the WHR from the flue gas coming from the melts process of the glass.

1.3 How to produce electrical energy from WHR

The main problem of a renewable sources as waste heat from industrial processes is due to the low-medium grade of temperature of the flue gas which the traditional steam plants are not able to convert in electricity in efficient and proper manner: over recent years, several studies and applications on different thermodynamic cycles have been developed to use those kinds of sources. The main important are : Kalina's Cycle, Trilateral Flash Cycle (TFC) and the Organic Rankine Cycle (ORC).

The Kalina's Cycle performs thanks to two different fluids with different boiling point (usually water and ammonia). It is a complex cycle, in which the boiling point is not reached at a fixed temperature but the solution boils in a range of temperature related to the mixture of the fluids, the latter is able to extract more heat from the sources respects to a pure fluid. The main advantage of this cycle is that a proper tuning of the components allows a better match with the variability of the source.

The trilateral flash cycle has been proposed to perform with a low-medium grade of temperature. This system the expansion process starts when the fluid is in the condition of saturated liquid instead of vapor. Thanks to that, is possible to reduce the irreversibility of the heat exchange but is difficult the use of expanders able to work with a two-phase fluid.

The Organic Rankine Cycle, during the last years, has taken over for electricity production, probably related to its simplicity. Organic Rankine cycles (ORC) are a technology suitable to use efficiently low and medium temperature heat sources to produce electricity. ORCs have

the same components of a traditional steam Rankine cycle, but the working fluid is an organic compound characterized by a lower boiling temperature than water, thus it allows power generation from low heat source temperatures.

Obviously, the level of efficiency is lower than the traditional Rankine cycle. Several studies are in the literature regarding choosing a proper working fluid [9] or study of optimization of the process [10] and numerous considerations must be done. The thermophysical properties of the fluid need to be considered in relation to its intended application, as well as safety, environmental effects, availability, and costs. Regarding the features of an ideal working fluid in a subcritical ORC, the properties are suggested by [11].

The following table shows the most common working fluids used in commercial applications, arranged in terms of application [12].

Table 1 - Resume of working fluids

Model of ORC	
Application	Working Fluids
GEOTHERMAL	RE134,RE135,R245fa,R245ca,R600,R601,Ammonia,Propylene,n-pentane
WASTE HEAT RECOVERY	Benzene, Toluene,n-pentane,R123,R134a
SOLAR	R152a,R600,R290
BIOMASS	OMTS

However, the first application of the ORC was before the 20th century, but they have become more interested in this last few years when the problems related to the consumptions of fossil fuels are increasing. Compared with the previous two technologies, the ORC has a simpler structure, higher reliability and the same configuration of the traditional steam plant which allow using the know-how for those plants, especially in terms of maintenance. As we know, at the level of temperatures which the ORC wants to tackle, the traditional way to convert heat into electricity is inefficient and inconvenient; this is the main advantage of using the ORC and nowadays several studies have been performed in order to enhance that surplus of energy (prevalently with waste heat and renewable sources). In literature, there are different

ways to combine the ORC with other technologies to improve the total efficiency of the system as fuel-cells [13], engines[10], micro-turbine[14], Brayton cycles [15] and thermal storages [16].

Regarding the technical aspects of the ORC, the particular shape of the diagrams Temperature-Entropy (Figure 2) for the ORC's fluids allow a better expansion phase at a low-medium grade of temperature [17]. Is clear how using those, with respect to the water, as a working fluid give a better behavior for the transformations involved into the process at a lower temperature, especially, for the trend of the superior limit curve.

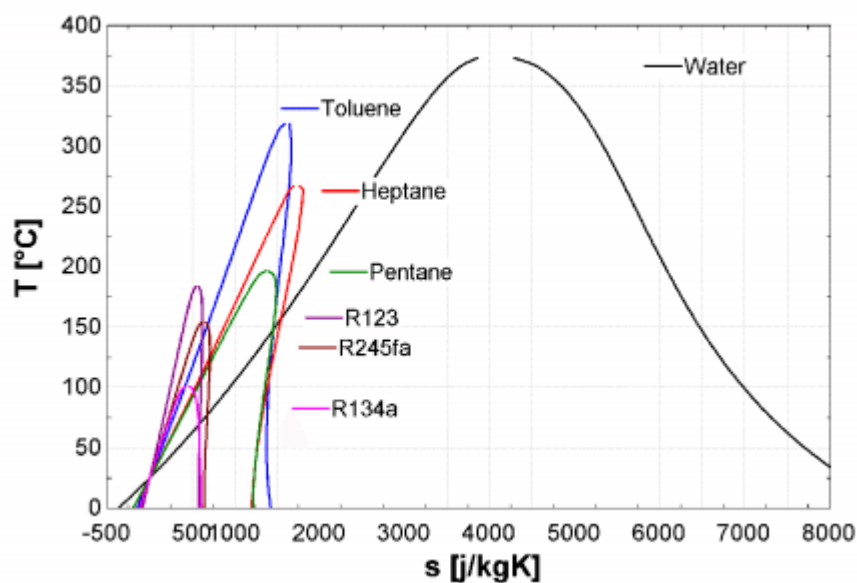


Figure 2 - Comparisons of the T-s diagram with some organic fluids and water

As said before, the ORC can exploit a different typology of the source. Its flexibility is combined with a different way to improve the efficiency of the cycle. This section is a little review of the different method existing to enhance the performances of the ORC.

ORC WITH RECUPERATOR or INTERNAL HEAT EXCHANGER

When the conditions of the working fluid at the outlet of the turbine are superheated steam, part of superheated heat could be used to preheat the fluid exiting from the pump before entering in the evaporator in which the source is exploited. To do that, an additional heat

exchanger must be involved, called recuperator or internal heat exchange (IXE); its operation will be better explained in the following chapters.

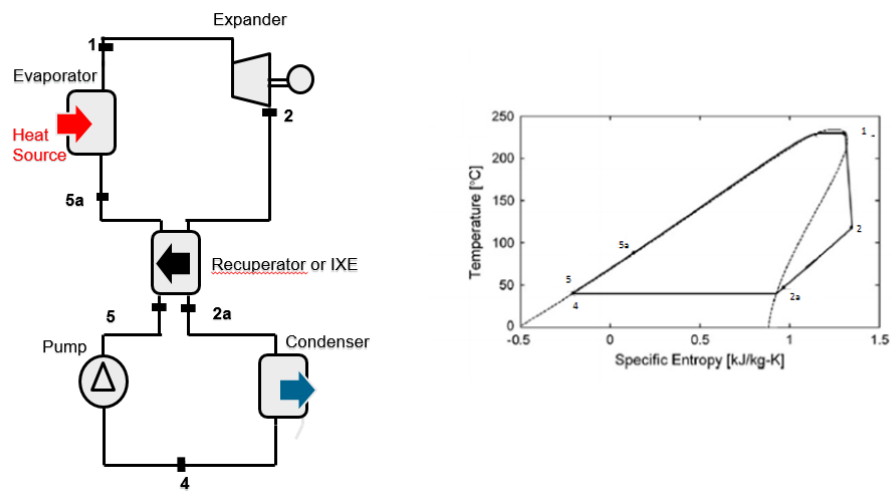


Figure 3 - Recuperator or Internal Heat Exchanger configuration with T-s diagram

ORC WITH MULTIPLE SUPERHEATING

It is possible to include in the traditional ORC a multistage expander with additional heat between two consecutive stages. After the heat exchange with the source, when the saturated vapor conditions of the steam are reached, the latter expands till an intermediate pressure. After that again it is re-heated by the source at constant pressure and eventually it re-expands. Has been demonstrated the advantage in terms of efficiency of the cycle with this approach but adding multiplies stages of re-heating means adding other heat exchangers. As a consequence not always is convenient use multiple superheating for the higher costs and technical complications (i.e. losses of pressure and temperature per each heat exchanger).

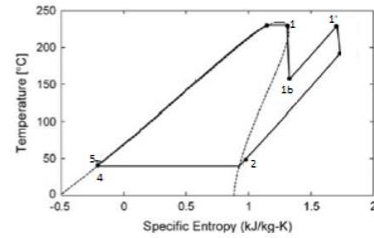
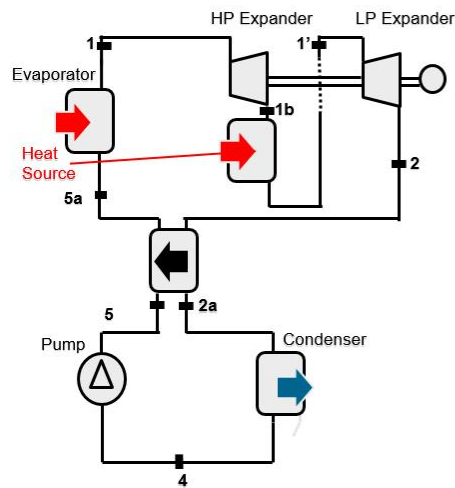


Figure 4 - Multiple superheating configuration with the T-s diagram

ORC WITH A DUAL-PRESSURE

In order to increase the efficiency of the plant, additional loops can be included to increase the level of heat at a lower temperature. The fluid exiting the condenser is splitting into two terms. One is pumped till the high pressure (HP) and the other till the low pressure (LP). The two different mass flow rates follow the process until the expansion. Here the fluids are at the same pressure but at two different temperature. The mass flow rate from the HP loop is used for the recuperator before bringing together the two terms and restart the process. The second level of pressure allows to exploit the source also at a lower temperature, but the complexity of the cycle increases, adding a lot of components. Without a proper economic analysis, these kind of changes to the cycle are not possible.

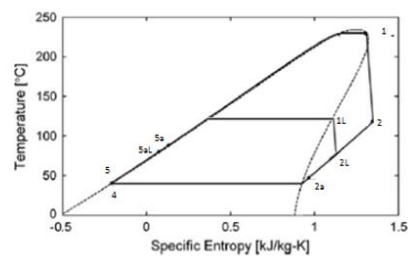
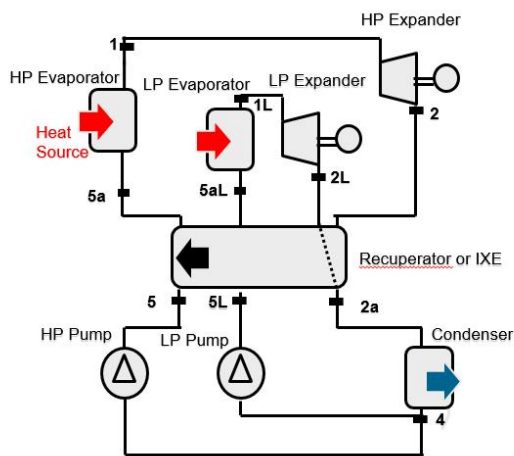


Figure 5 - Dual Pressure configuration with the T-s diagram

1.4 Thermal energy storage and how is possible to improve the processes with it

Developing new renewable sources and improve the use of the present technologies is one of the main issues of the energy sector, which has a big impact on the economic field of all the countries. One of the most interesting options, where a lot of investments have been performed, are the studies related to the devices called Thermal Energy Storage (TES). Storing energy, in various forms, means making it available in a different temporal scale in order to improve the adaptability of mismatch between the demand with the source. The most common example which explains the importance of those devices is for solar energy. Only via TES is possible to use electricity provided by the solar energy during the hours of darkness, the hours in which there are peaks of demand. Several applications have a discrepancy between demand and supply related to the intermittency of the source and the variation of the demand as well. Although, the presence of storage in a system is not only relevant for the improvements of the differences between demand and supply, but also for increasing the efficiency and reliability of the energetic plant. As a direct consequence, there will be the plant reduction in consumptions of fossil fuels and improvements of the competitiveness of the investments recovering energy that, in absence of the TES, will be discharged without any gaining, both economic and energetic. There are a lot of typologies of TES, with different values of efficiency and/or the response time of the changes in the operational conditions. The choice of the best solution depends on a lot of techno-economic aspects, and the aim of this work is to investigate on the field of WHR at a low-grade scale of temperature. A first way to classify the TES is for the form of energy stored.

- Mechanical energy: could be related to potential or kinetic energy. The most common are the PHPS (Pumped Hydro-Power Storage) and the CAES (Compressed Air Energy Storage)
- Electrical energy: could be related to the electromagnetic or chemical both via batteries.
- Thermal energy: could be related to the sensible heat, latent heat or thermos-chemical heat. The range of temperature of the TES is from 100/+1000 °C and their

presence in the market is relevant. The third chapter will explain them properly (Model development of different typologies of Thermal Energy Storage (TES)).

1.5 Aims and objectives

Since most of the works present in literature have focused on the best design and optimization of the various technologies of TES as itself, aims of this thesis is check and shows techno-economic benefits of this important device focusing on all the results of use it in the system. This thesis follows the Techno-Economic Approach (TEA). The target is to have a good representation of the system, the details must be enough satisfactory to describe the “engineering phenomena” in a proper manner but also taking account the economic aspects. How the technologies under investigation (TES) is able to save money, energy and also reducing the environmental impact of the process? Under the same operational conditions, different technologies of TES will be evaluated (Two-tank (TT), Single Thermocline (ST) and Dual-Media Thermocline (DMT)) to address the research questions and to highlight the research ideas from which the work began.

In literature, the status of the research for the TESs is high and it is still developing but there are results which are not possible to discover without a proper integration of those components in the energetic system in which they will be embed; hence, to find out the real techno-economic potential of the thermal energy storages, they must be analysed as a integrated component of the plant [18].

The WHR could be used with different technologies (as ORC, Kalina Cycle, etc) and possible additions of TES can be different in terms of components and costs, like it is the same outside this scenarios, like in solar plant or other form of energetic systems. Fixing a process (ORC with internal heat exchanger) and its operational data, a comparative study of it could give interesting results. What is the most feasible, reliable or viable TES which could operate in a determinate process with the fluctuating trend of the source? What are the techno-economically benefits of the system?

The power of the TEA, which is linked with quasi-steady model, allows understanding the best configuration of the plant exploiting different joint-simulations of the components. The

valence and the relevance of the results are closely related to the reliability of the model's thermodynamic.

Using the quasi-steady approach to evaluating the behavior of the ORC over time has been already used by several authors. For instance, Lecompte et al. [19] used it in a combined heat and power system for a 1- year period to model the ORC. Heberle and Brüggemann [20] studied the year power production of an ORC used in a geothermal combined heat and power plant. Moreover, Orbie [21] used this method to study the yearly performance of an ORC for waste heat recovery.

2. O.R.C. – Modelling and thermodynamic behavior of the components in design and off-design conditions

The modeling has been developed by the author in EES&MATLAB environment. The key role of the simulation is the ORC model which allows the plant to produce electricity. Following has been added at the simulation, in different configurations, the Thermal Energy Storages (TES) which are relevant for the best utilization of the ORC as said in the previous chapter(Thermal energy storage and how is possible to improve the processes with it).

The aim of this chapter is to explain the model of an Organic Regenerative Rankine Cycle able to perform thanks to the Waste heat recovery. The research of the optimum design point of an ORC system is a much-analyzed topic in literature [22].

Although, producing an optimization of the ORC is not the aim of the work, but implement a model of it as a tool for the techno-economic analysis is a necessary step.

In the first paragraph will be presented the general assumptions and the operational variables fixed which ensure characterizing the thermodynamic cycle. Following the governing equations of all the components to resume in which way they have been modeled. Lastly, has been reported the way in which the model is able to tune when the ORC has in input a value of heat entering the evaporator which is different respect to the design conditions.

2.1 Definition of the thermodynamic cycle and general assumptions

In this paragraph, the thermodynamic cycle of the ORC is presented. In a design process, thermodynamic cycle design is the initial step, and to develop the model some features must be fixed.

The first fundamental choice is the selection of the working fluid. In literature, several works aim to investigate what is the best fluid (How to produce electrical energy from WHR). The choice is influenced by different factor but the most relevant could be the properties of source under investigation. According to Wang [23], for the range of temperature of this work, R123 has been chosen.

After that, it must be clear what is the configuration of the ORC; this choice has a big influence on the results in terms of efficiency and electrical production. Superheated Regenerative Organic Rankine Cycle has been chosen in this work, according to [24] and [25].

All the simulations obtained from the model are thermodynamically based only and do not include heat transfer and pressure drop effects in the heat exchangers and in the pipes/lines. The model does not include also transport properties such as thermal conductivity and viscosity.

The first step of the design procedure is to fix specifications of the hot source e define the temperatures of the auxiliary fluid at the condenser, that is water for the present work.

Aim of this work is to exploit a surplus of energy from an industrial process. Usually, the latter comes from flue gas. A proper definition of the fluid is avoided to maintain a broad approach to the model and for the lack of the specific chemical configuration of it; for the scenarios implemented in the next paragraphs concerning the evaluation of the properties of the source has been used the fluid "AIR_HA" from the intern library of the software "Engineering Equations Solver" (EES). This last provides thermodynamic properties for the gas mixture composing air using the fundamental equation of state developed by Jacobsen [26].

Due to the temperatures under investigation, the heat capacity could be considered constant and the value is $cp_{source} = 1085 \text{ [J/kgK]}$.

The water at the condenser undergoes heating of 10 K varying from 290 to 300 K . The amount of the mass flow rate is computed, and so it is an output of the model.

Regarding the thermodynamic conditions of the source, the amount of heat entering at the evaporator is the fundamental input of the system; its properties will be defined in next chapters in terms of temperatures and mass flow rate.

As an ORC regenerative and subcritical cycle there are: evaporator, turbine, an internal heat exchanger (IXE), condenser, and pump. The traditional Rankine cycle uses the same components, but the working fluid is water. Using water with a low-medium level of temperature as a source at the evaporator has several issues. The possibility of use operational fluid with different properties, as the organic fluids, allows solving some problems of the water exploiting efficiently sources for the electricity production which is totally

inconvenient with it.

Here are summed the main advantages of using an ORC:

- Higher efficiency for cycles with a low-temperature grade as a source.
- Lower stresses at the turbine
- Higher compactness of the components due to the higher density of the organic fluids
- The lower level of evaporation pressure even close to the critical point and possibility to have a condensation pressure higher than the environmental pressure
- Not necessary to have superheating due to the shape of the T-s which allows always an expansion in the vapor zone, less technical problem at the turbine.
- Safe working conditions related to lower pressures and temperatures.

Following the schematic representation of the components of the ORC; its basic T-s graph will be presented in the next paragraph, with the operational parameters as well.

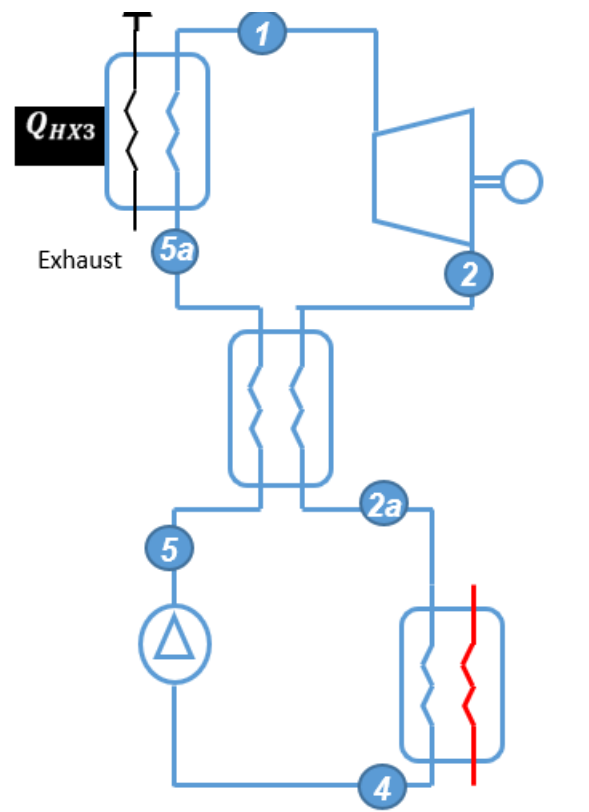


Figure 6 - Scheme of the plant with the denomination of state point

Assumptions:

Definition of intensive variables is needed (temperature and pressure) for the state-points of the cycle. Additional points are needed for the evaluation of properties, are evaluated saturated point as Point 3 which is the point at the condenser level with quality equal to 1, the point 6 and 7 which are at quality respectively 0 and 1 but at the evaporator level.

The mass flow rate of the working fluid is computed imposing the thermal coupling with the hot source and knowing the properties along the cycle; at the end also the mass flow rate of water at the condenser could be calculated.

Following the value of the independent variables needed to complete all the calculation:

- The temperature of the environment T_{env}
- The temperature of condensation which defines the low level of pressure of the cycle T_{cond}
- Temperature of evaporation T_{evap}
- Isentropic efficiency of the pump $\eta_{is\ pump}$
- Isentropic efficiency of the turbine $\eta_{is\ turbine}$
- The pitch point difference for evaporator $\Delta T_{pp\ evap}$
- The pitch point difference for the condenser $\Delta T_{pp\ cond}$
- The pitch point difference for the IXE $\Delta T_{pp\ IXE}$

Following a resume of the value of those variables in design-conditions.

Table 2 - Values of the independent variables for the design conditions

T_{amb}	298	[K]
T_{cond}	303	[K]
T_{evap}	408	[K]
$\eta_{is\ pump}$	0,85	[-]
$\eta_{is\ turbine}$	0,8	[-]
$\Delta T_{pp\ evap}$	8	[K]
$\Delta T_{pp\ cond}$	8	[K]
$\Delta T_{pp\ IXE}$	2	[K]

The isentropic efficiencies for the pump and the turbine are, respectively, 0.85 and 0.8, in design conditions. For the calculation has been fixed and the temperature of the environment is 20 °C.

Starting from those is easy to evaluate also the pressure ratio of the cycle, in the hypothesis of a cycle without super-heated vapor or fixing the level of the superheating that is calculated as $SH_{factor} = (T_{evap} - T_{evap_{sat}})/T_{evap_{sat}}$. The lower pressure is the saturated pressure of T_3 , that is known because is equal to T_{cond} . The higher pressure is the pressure in which at the T_{evap} the fluid is with a quality of $x = 1$, pressure which respect the conditions of the fixed SH_{factor} . Having a saturated vapor at the inlet turbine is a risk linked with the problem of droplets at the components of the turbine, although is often used in ORC because the organic fluids at high temperature could be decomposed.

2.2 Governing equations of the components in design-conditions

2.2.1 Evaporator

The evaporator is a shell-and-tube heat exchanger. It includes three different areas, for preheating, evaporation and superheating, respectively. The flue gas flows inside the tubes, while the organic medium fills the shell side. It has been considered as three different components, to take in account the different heat transfer coefficients for preheating and boiling that must be evaluated separately, due to the difference of the heat transfer processes (phase-changing) (pre-heater, boiler, and superheater). The total area is considered for the calculation. This approach is widely used for modeling that kind of component [27]. The governing equations of the component are the following:

$$Q_{ev} = \dot{m}_{ORC}(h_1 - h_{5a}) \quad 2.1$$

$$Q_{source} = \dot{m}_{source}c_{p,source}(T_{in_{eff}} - T_{out}) \quad 2.2$$

Those two terms, neglecting leakages, are equals.

However, in the evaporator, is relevant to evaluate the exchange-surface. Has been implemented the logarithmic mean temperature difference (LMTD). LMTD is used to

determine the temperature driving force for heat transfer in flow systems, most notably in heat exchangers. The LMTD is a logarithmic average of the temperature difference between the hot and cold fluids at each end of the double pipe exchanger. For a given heat exchanger with constant area and heat transfer coefficient, the larger the LMTD, the more heat is transferred. The use of the LMTD arises straightforwardly from the analysis of a heat exchanger with a constant flow rate and fluid thermal properties. The specific heat for the working fluid is evaluated by the average value of it at the two temperatures present in the heat exchange. $cp_{orc} = \frac{cp(T_{hot})+cp(T_{cold})}{2}$. For the source (the flue gas) is fixed at a value of $cp_{source} = 1085 J/kgK$, due to the not big range of temperature drop.

The next figure shows a schematization of the evaporator. Applying the balances per each sub-area has been possible to evaluate the unknown intermediate temperature of the flue gas and apply properly the LMTD method.

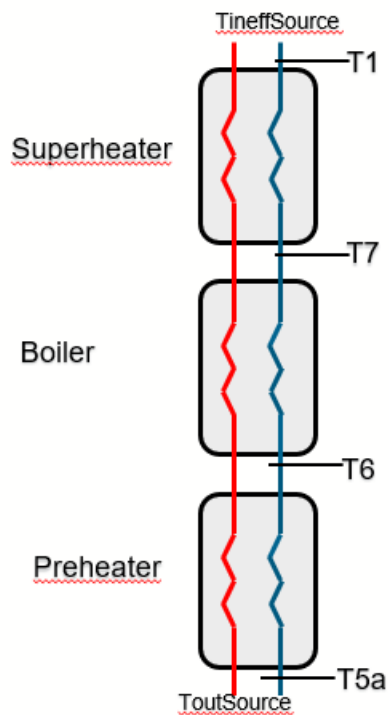


Figure 7 - Scheme of the evaporator

Super-Heater

$$\dot{m}_{source} c p_{source} (T_{in_{eff_{source}}} - T_{out_{SH}}) = \dot{m}_{ORC} (h_1 - h_7) \quad 2.3$$

$$\Delta_{LMTD_{SH}} = \frac{(T_{out_{SH}} - T_7) - (T_{in_{source}} - T_1)}{\ln \left(\frac{(T_{out_{SH}} - T_7)}{(T_{in_{source}} - T_1)} \right)} \quad 2.4$$

$$Area_{SH} = \frac{\dot{m}_{ORC} (h_1 - h_7)}{U_{SH} F_{t_{SH}} \Delta_{LMTD_{SH}}} \quad 2.5$$

Where U_{SH} is fixed to $120 \frac{W}{m^2 K}$ and F_t is a parameter evaluated as the ratio between the average of the two temperature drop inside the heat exchanger divided by the Δ_{LMTD} .

Boiler:

$$\dot{m}_{source} c p_{source} (T_{out_{SH}} - T_{out_{BO}}) = \dot{m}_{ORC} (h_7 - h_6) \quad 2.6$$

$$\Delta_{LMTD_{BO}} = \frac{(T_{out_{BO}} - T_6) - (T_{out_{SH}} - T_7)}{\ln \left(\frac{(T_{out_{BO}} - T_6)}{(T_{out_{SH}} - T_7)} \right)} \quad 2.7$$

$$Area_{SH} = \frac{\dot{m}_{ORC} (h_7 - h_6)}{U_{BO} F_{t_{BO}} \Delta_{LMTD_{BO}}} \quad 2.8$$

Where U_{BO} is fixed to $80 \frac{W}{m^2 K}$

Pre-Heater:

$$\Delta_{LMTD_{PH}} = \frac{(T_{out_{source}} - T_{5a}) - (T_{out_{BO}} - T_6)}{\ln \left(\frac{(T_{out_{source}} - T_{5a})}{(T_{out_{BO}} - T_6)} \right)} \quad 2.9$$

$$Area_{PH} = \frac{\dot{m}_{ORC} (h_6 - h_{5a})}{U_{PH} F_{t_{PH}} \Delta_{LMTD_{PH}}} \quad 2.10$$

All the values of the global coefficient of heat transfer are in the range suggested by Cavallini [28]. The size of the evaporator is fixed and calculated during the design conditions. However, the heat transfer area is calculated also during the off-design conditions only to do comparisons and be sure of a lower value required in those conditions.

2.2.2 Turbine

The component which allows an electricity production is an expander, classic turbine in this case. The main equation is the next one to evaluate the amount of production:

$$W_{turbine} = \eta_{mecc} \dot{m}_{ORC} (h_1 - h_2) \quad 2.11$$

In which $\eta_{mecc} = 0.9$ has been fixed.

The thermodynamic point 1, the turbine's inlet, is evaluated after having imposed the evaporating pressure. The latter is fixed under design conditions but changes in off-design conditions, how it will be explained in the next paragraph. The outlet conditions of the turbine, point 2, are computed by outlet enthalpy for an isentropic expansion process respecting:

$$\eta_{is,turb} = \frac{(h_1 - h_2)}{(h_1 - h_{2s})} \quad 2.12$$

State equations lead to calculate the value of other intensive variables of the state point by knowing two different of them for the specific state, using tools present in EES.

2.2.3 Intermediate Heat Exchanger

To improve the efficiency of the process has been integrated into the cycle, and its model, a regenerative heat exchanger (IXE) to increase the level of enthalpy of the working fluid before entering in the evaporator (Figure 6 - Scheme of the plant with the denomination of state point Point 5a) thanks the high level of the fluid at the outlet of the turbine (Point 2). To do that It's needed a value of drop temperature between the temperature inside of the recovery heat exchanger.

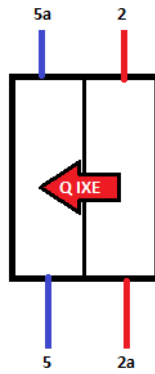


Figure 8 - Recovery Heat Exchanger (IXE)

Neglecting all the leakages in terms of pressure and temperature the equation that resume the relevance of this component is:

$$Q_{IXE} = \dot{m}_{ORC}(h_2 - h_{2a}) = \dot{m}_{ORC}(h_{5a} - h_5) \quad 2.13$$

To allow the software to achieve all the properties has been fixed a drop temperature which links the two sides of the component.

$$T_{2a} = T_5 + \Delta T_{pp_{IXE}} \quad 2.14$$

2.2.4 Condenser

$$Q_{cond} = \dot{m}_{ORC}(h_{2a} - h_4) \quad 2.15$$

$$Q_{cond} = \dot{m}_{water}cp_{water}(T_{out_Water} - T_{in_water}) \quad 2.16$$

Equation 2.16 allows the model to evaluate also the water's mass flow rate required at the condenser.

2.2.5 Pump

State point of the pump, n°4, has been evaluated fixing the condensing pressure and saturated liquid conditions. The same approach of the turbine has been followed for the evaluation of the outlet conditions.

$$W_{pump} = \dot{m}_{ORC}(h_5 - h_4) \quad 2.17$$

To allow a correct calculation of the properties along with the pump, it's necessary the use of the definition of isentropic efficiency:

$$\eta_{is,pump} = \frac{(h_{5s} - h_4)}{(h_5 - h_4)} \quad 2.18$$

2.3 Off-design considerations

The purpose of this paragraph is to explain how the models of single components have been developed for the analysis of the system in different working conditions.

For the study of this kind of problem there are two possibilities to follow:

- Dynamic approach:
- Quasi-steady state approach:

A dynamic approach is used for modeling components in which the concept of storage occurs (both for mass or energy). The evaluation of the results is closely linked to the input of the time-step under investigation but becomes crucial also the “history” of the system. Conditions in the time-steps before, called “state-variables”, affect the solution of the set of equations, clearly when at the beginning of the values of the simulation of them must be defined by the user.

Modeling the problem with this approach gives detailed results of the real behavior of the system, but it is the most complex in terms of code and, as a direct consequence, has a higher computational-time.

The quasi-steady-state approach means considering the behavior over time of the systems as a succession of steady-states, with a continuous changing of the boundary conditions and neglecting the energy or mass accumulation in all the components (transient effects)[29]. For each time step the output of the model depend only on the instantaneous input and boundary conditions under investigation, the “state-variables” are not relevant, anymore. Even so, this approach still means evaluate dynamic conditions but in a faster way compared to the previous approach reducing meaningfully the required computational time but keeping

a good approximation of the plant-behavior along the time, which perfectly fit with the Techno-Economic approach.

For the present work, a Quasi-steady approach has been used. The results of this model are not an accurate representation of the reality, but a good approximation of the trend for the integration of ORC in waste heat recovery.

Off-design considerations turbine

During the phase of modeling not always the characteristic curves are available, in those conditions usually the behavior of the vapor turbine can be assimilated to the behavior of a group of nozzles [30]. Full stage of the turbine is studied as nozzles; this analogy is called “Stodola’s Law” or “Stodola’s Eclipse” and allow us to develop general criteria in order to determine the pressure of the steam along the expansion line of a multi-stage turbine varying with the mass flow rate that is flowing in it. [31]

The expander selection is very important in an ORC design. The selection of such component depends on the thermodynamic properties of the working fluid, the mass and volume flow rate, the mechanical power required and the volumetric expansion ratio. A turbine is used in this model. Turbine isentropic efficiency in off-design conditions was evaluated using the polytropic efficiency while the expansion inlet pressure and the mass flow rate were evaluated through the Stodola’s ellipse approach [32].

$$\frac{\dot{m}_{off}}{\dot{m}_d} \frac{P_{ind}}{P_{inoff}} = \sqrt{\frac{1 - \beta_{off}^2}{1 - \beta_d^2}} \quad 2.19$$

$$\eta_{pol_d} = \frac{m - 1}{m} \frac{k}{k - 1} \quad 2.20$$

$$\eta_{pol_{off}} = \eta_{pol_d} \left(1 - 0.5 \left(\sqrt{\frac{\Delta h_{is_d}}{\Delta h_{is_{off}}}} - 1 \right) \right) \quad 2.21$$

$$\eta_{is_{off}} = \frac{1 - \left(\frac{1}{\beta_{off}} \right)^{\frac{k-1}{k}} \eta_{pol_{off}}}{1 - \left(\frac{1}{\beta_{off}} \right)^{\frac{k-1}{k}}} \quad 2.22$$

The inlet pressure of the turbine has been varied indirectly; it must change with the number of revolutions (rpm) of the pump. Indeed, changing this velocity changes the characteristic curve of the pump which means that with the same mass flow rate the head of the pump and the evaporation pressure will change. As shown with the 2.22, when the pressure ratio changes (β_{off}), the isentropic efficiency ($\eta_{is_{off}}$) of the turbine changes as well. All the equations are implemented in the code EES which allow the off-design simulations.

Eventually, inside the code, a choice has been made to block the outlet pressure of the turbine (P_{min}) even though the changes of the source. It was possible by modifying the mass flow rate of the cooling fluid to keep constant the outlet temperature at the condenser. This is related to practical considerations and problems in the codification as well; problems related with the possibility to let both the pressures free to vary.

2.4 Validation, the feasibility of the results, and assessment of the working conditions

2.4.1 Validation of the thermodynamic model

The accuracy of this model was assessed based on validating the output from the data outputs present of the work of Khaljdani [33]. In particular, has been used the same model that He used for its validation [34]. The model's inputs for this case are:

- $T_{Evap} = 137 \text{ }^{\circ}\text{C}$

- $T_{Cond} = 30 \text{ }^{\circ}\text{C}$

- $T_{Env} = 25 \text{ }^{\circ}\text{C}$

- $\eta_{is_{pump}} = 0.85$

- $\eta_{is_{turb}} = 0.80$

- $T_{2a} - T_5 = 2 \text{ }^{\circ}\text{C}$

The conditions of the two auxiliary's fluids, at the evaporator and condenser, are:

- $T_{ineff} = 425 \text{ K}$

- $T_{out} = 381.5 \text{ K}$

- $m_{source} = 96.45 \text{ kg/s}$
- $cp_{source} = 1085 \text{ J/(kgK)}$
- $T_{inwater} = 298 \text{ K}$
- $T_{outwater} = 308 \text{ K}$

In Table 3 – Comparisons for Validation the results of the Validation.

Table 3 – Comparisons for Validation of the ORC model

Fluid		Point		Temperature [°C]		Pressure [Mpa]		Enthalpy [kJ/kg]		Entropy [kJ/kgK]	
Khaljdani's [11]	MyWork										
R123	R123	15	1	137,00	137,00	1,6660	1,6610	460,80	460,80	1,708	1,709
R123	R123	16	2	60,09	60,30	0,1097	0,1097	423,10	423,20	1,737	1,737
R123	R123	17	2a	35,08	32,90	0,1097	0,1097	404,70	403,00	1,680	1,675
Water	Water	18	Out_w	25,00	25,00	0,1000	0,1010	104,80	104,20	0,367	0,365
Water	Water	19	In_w	35,00	35,00	0,1000	0,1010	146,60	146,10	0,505	0,503
R123	R123	12	4	30,00	30,20	0,1907	0,1097	231,40	231,40	1,109	1,109
R123	R123	13	5	30,67	30,20	1,6660	1,6610	232,60	232,70	1,109	1,109
R123	R123	14	5a	48,15	50,00	1,6660	1,6610	251,00	252,80	1,168	1,173

The latter table allows to understand the feasibility of the thermodynamics of the model, it has been tuned with the same input of the author to validate its reliability.

2.4.2 Definition of the Design conditions

The design of the ORC is a complex issue, especially related to the waste heat recovery because the sources are very varied in chemicals compositions and temperature, the choice of the fluid is influenced and with it also the main parameters of the cycle. Usually, it does not exist just one optimal solution. The target of the designer is to understand which parameters need to maximize and reach a better solution for the specific case.

The present work is focused on the analysis of the ORC with a flux of waste heat recovery from an industrial process as a source. Due to the huge variability of the industrial processes, it is not possible to define the conditions of the flue gas. A trend has been assumed for explanatory purposes only in the following paragraphs.

In the next table are summed the main information of the flue gas for the industrial process, according to the real Case-study present in literature [35].

Table 4 - Information of the source of the plant: flue gas exiting an industrial process (Cement Industry)

Other input parameters		
Higher temperature	395.00	[C°]
Lower temperature	310.00	[C°]
Heat capacity	1085	[J/kgK]
Mass flow rate	53.8	[kg/s]

Starting with this operational data has been fixed a sinusoidal trend and consequently also the design conditions. Starting from those operational conditions has been tuned the ORC and all the components, achieving overall efficiency of the cycle close to 0.15, which goes perfectly with the range present in literature. The production of electrical energy from the turbine is of almost **800 kW**. Following the representation of the source and its trend and the operational parameters of the cycle (design conditions).

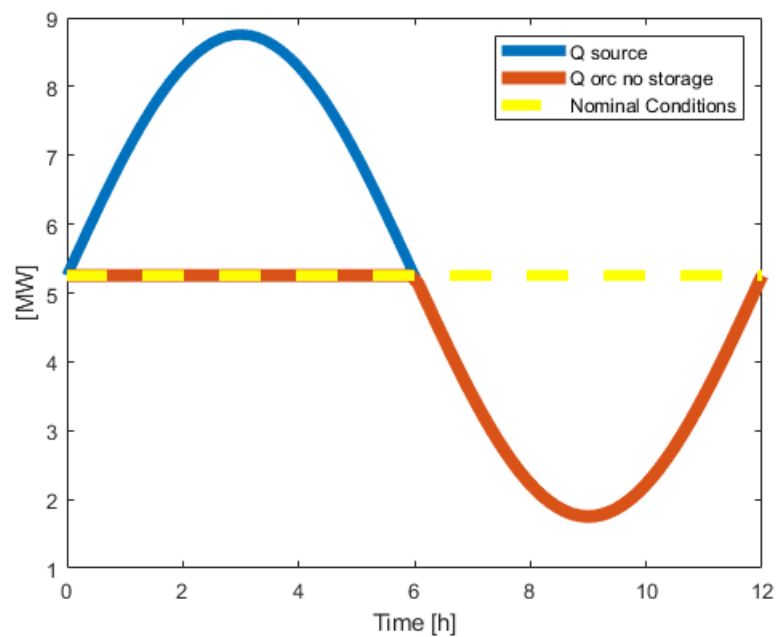


Figure 9 - Theoretical trend of the source

Table 5 - Operational Design Parameters of the Organic Rankine Cycle

Q_{evap}	Heat exchanged at the evaporator	5254.00	[kW]
Q_{cond}	Heat exchanged at the condenser	4365.00	[kW]
W_{turb}	Power at the turbine	820.33	[kW]
W_{pump}	Power at the pump	22.67	[kW]
W_{net}	Net electrical Power	797.66	[kW]
β	Pressure ratio	11.01	[-]
η_{orc}	The overall efficiency of the ORC	15.18	[%]
$T_{in\,turbine}$	Inlet temperature at the turbine	134.85	[C°]
$\eta_{isturbine}$	Isentropic efficiency of the turbine	0.80	[-]
m_{orc}	Working fluid mass flow rate	23.83	[kg/s]
m_{water}	Cooling fluid mass flow rate	104.30	[kg/s]

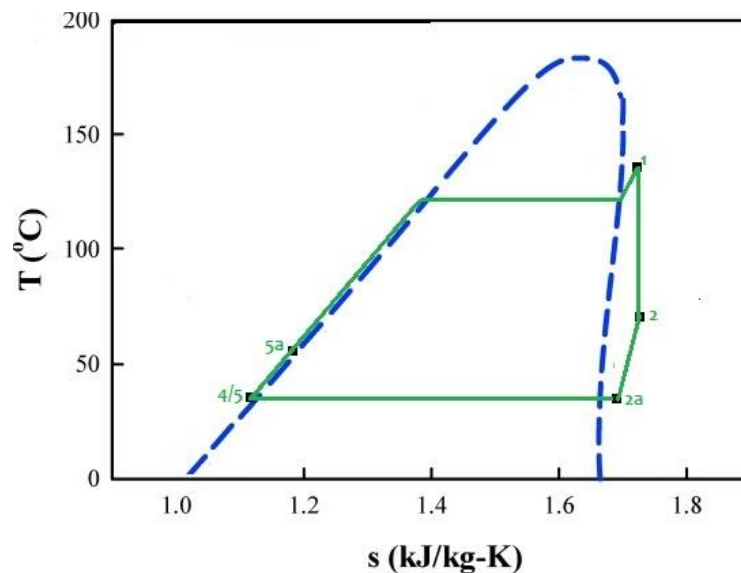


Figure 10 - Temperature/Entropy diagram of the R123 at the design conditions

Figure 10 - Temperature/Entropy diagram of the R123 at the design conditions, shows the shape of the ORC with the IXE, as mentioned in chapter 2 (ORC WITH RECUPERATOR or INTERNAL HEAT EXCHANGER)

2.4.3 The response of the system at the variability of the source

A sinusoidal trend allows explaining the idea which is behind the concept to introduce storage to keep higher possible the performances of the plant, analyzing the techno-economical benefits of the investment of the TES. As can be seen from, Figure 9 - Theoretical trend of the source, when the heat which is entering in the evaporator is higher, nominal conditions are reached at the ORC wasting the amount difference of energy between the blue line and

the red ones. When the source is lower, the cycle works following its trend in off-design conditions and with lower performances.

Before introducing the results obtained with the thermal energy storage, the conditions without it are presented. Next table shows a first comparison between the nominal conditions and the worst point of Figure 9 (2.627 MW at the evaporator, 50% of reduction respect to the nominal conditions).

Table 6 – Operational Parameters - Comparison between nominal and off-design conditions (50% of the source at the evaporator)

Operational Parameters		Source at Nominal Conditions	50% of Source at Nominal Conditions		%Variation
Heat exchanged at the evaporator	Q_{evap}	5254,00	2627,00	[kW]	-50,00
Heat exchanged at the condenser	Q_{cond}	4365,00	2282,00	[kW]	-47,72
Power at the turbine	W_{turb}	820,00	315,78	[kW]	-61,49
Power at the pump	W_{pump}	22,67	6,18	[kW]	-72,73
Net electrical Power	W_{net}	797,66	309,60	[kW]	-61,19
Pressure ratio	β	11,01	6,21	[-]	-43,62
The overall efficiency of the ORC	η_{orc}	15,18	11,79	[%]	-22,33
Inlet temperature at the turbine	$T_{in\,turbine}$	134,85	134,85	[C°]	0,00
Isentropic efficiency of the turbine	$\eta_{is\,turbine}$	0,80	0,73	[-]	-8,63
Working fluid mass flow rate	m_{orc}	23,83	13,32	[kg/s]	-44,10
Cooling fluid mass flow rate	m_{water}	104,30	54,55	[kg/s]	-47,70

The table above shows the main parameters of the cycle and their variation when the source is halved. As can be seen, the value of the net electrical power has a reduction of more than 60%. Usually, especially when the topic is recovery energy from a free power source like in this context, many designers attempt to maximize it even working with not necessarily great efficiency of the process. In this case, the overall efficiency of the ORC decreases to 11.79 % with a reduction of almost 22.5 %. Particularly important is also the variation of the isentropic efficiency of the turbine which goes to 0.80 to 0.73. This deviation must be decreased as much as possible to optimize the performance of all the investments.

The pressure ratio which may be changed thanks to the regulation of revolutions per minute of the pump (Off-design considerations turbine) reaches a value of 6.21 with a 43.62% of reduction. During the developments of the work was assessed also the lower bound of the reduction of the maximum pressure of the cycle. The limit is caused by the pressure

calculated with the 2.19. When the heat at the source is lower than the 37% of the nominal conditions ($\sim 1900 \text{ kW}$), the pressure calculated reaches the two-phase zone and it doesn't allow the resolution of the set of the equations. The software returns a message which explains that the properties cannot be calculated. So for the continuation of the work a limitations is fixed, when the heat at the evaporator is lower than the 37% of the nominal conditions the ORC is set in NO-work phase, without a production of electric power.

Following the results of the simulations also for the heat transfer surfaces of the ORC. As a reminder, the value of the row "evaporator" is the sum of the values for preheater, boiler, and superheater, according to the governing equations (Evaporator)

Table 7 - Heat transfer surfaces - Comparison between nominal and off-design conditions (50% of the source at the evaporator)

Heat transfer Surface		Source at Nominal Conditions	50% of Source at Nominal Conditions		%Variation
Preheater	A_{PH}	272,6	37,01	[m ²]	-86,42
Boiler	A_{BOIL}	373,3	171	[m ²]	-54,19
SuperHeater	A_{SH}	60,03	45,47	[m ²]	-24,25
Evaporator	A_{EVAP}	705,9	253,5	[m ²]	-64,09
Condenser	A_{COND}	773	409,6	[m ²]	-47,01
Ixe	A_{IXE}	459,6	274,9	[m ²]	-40,19

2.5 Exergy's analysis

Per each thermodynamic state point of the plant shown in Figure 6 can be defined exergy like:

$$E_i = \dot{m}[(h_i - h_0) - T_0(s_i - s_0)] \quad 2.23$$

In which with the 0 state is the reference of the environmental conditions.

The equations of the exergy balances are summed in the following table. Has been possible to evaluate the term of the destruction of exergy and the efficiency as well.

Table 8 – Resume of Exergy balances

Component	Destruction [J/s]	Efficiency [-]
Evaporator	$E_{D,ev} = E_{in,eff} * - E_{out} * + E_{5a} - E_1$	$\varepsilon_{ev} = \frac{E_1 - E_{5a}}{E_{in,eff} - E_{out}}$
Turbine	$E_{D,turb} = E_1 - E_2 - W_{turb}$	$\varepsilon_{turb} = \frac{W_{turb}}{E_1 - E_2}$
IXE	$E_{D,IXE} = E_5 - E_{5a} + E_2 - E_{2a}$	$\varepsilon_{IXE} = \frac{E_{5a} - E_5}{E_2 - E_{2a}}$
Condenser	$E_{D,cond} = E_{2a} - E_4 + E_{in,water} - E_{out,water}$	$\varepsilon_{cond} = \frac{E_{out,w} - E_{in,w}}{E_{2a} - E_4}$
Pump	$E_{D,pump} = E_4 + W_{pump} - E_5$	$\varepsilon_{pump} = \frac{E_5 - E_4}{W_{pump}}$

* Regarding the thermodynamic properties of the flue gas has been used Air_ha present the library of the EES. The latter has two different fluids for Air, in this report is used Air as non-ideal gas.

Following the comparison between nominal and off-design conditions (50% of the source). The destruction of exergy and the exergetic efficiency are calculated as shown in Table 8 – Resume of Exergy balances.

Table 9 - Exergy's parameters in the comparison between nominal and off-design conditions (50% source at the evaporator)

Exergetic parameters	Source at Nominal Conditions	50% of Source at Nominal Conditions		%Variation
EVAPORATOR				
Destruction of exergy	693,32	1366,00	[kJ/kg]	97,02
Exergetic efficiency	63,03	27,16	[-]	-56,91
CONDENSER				
Destruction of exergy	25,70	13,40	[kJ/kg]	-47,86
Exergetic efficiency	64,66	64,61	[-]	-0,08
IXE				
Destruction of exergy	16,59	19,81	[kJ/kg]	19,41
Exergetic efficiency	72,86	72,76	[-]	-0,14
PUMP				
Destruction of exergy	3,30	0,98	[kJ/kg]	-70,30
Exergetic efficiency	85,32	85,31	[-]	-0,01
TURBINE				
Destruction of exergy	291,50	140,96	[kJ/kg]	-51,64
Exergetic efficiency	73,78	69,14	[-]	-6,29
ORC				
<u>Destruction of exergy</u>	<u>1030,41</u>	<u>1541,15</u>	<u>[kJ/kg]</u>	<u>49,57</u>

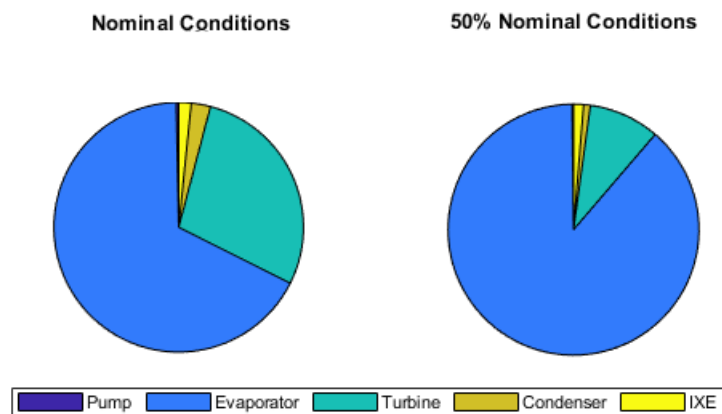


Figure 11 - Pie graphs of the Exergy's Destruction

As seen above, most of the destruction of exergy refers to the evaporator. In nominal conditions, in the evaporator there is almost 75% of the total destruction (693 kJ/kg), during the off-design the impact of the evaporator which is forced to work in an unefficient manner is close to 90% and in particular its destruction is 1366 kJ/kg which is even bigger than the total destruction of the plant in nominal conditions (1030 kJ/kg). Those results highlight the need of improve the conditions of work at the evaporator and stay as close as possible to the nominal conditions, not only for the direct improvement regarding the production of electric power, but also under the exergetic point of view.

3. Model development of different typologies of Thermal Energy Storage (TES).

To perform a proper TEA, in the system under investigation, mathematical models of the TES systems are required. Aim of the present chapter is to discuss assumptions and present also the validations. The different kinds of TES modeled are the scenario of ideal thermal storage (two-tank), and the thermocline thermal storage systems, one using heat transfer fluid alone (Single thermocline) and the other with an additional solid medium (called filler) with the heat transfer fluid (Dual-Media Thermocline).

TES systems can be shared in two big families: Direct or Indirect.

The Direct TES are defined as the ones in which the HTF performs also as the storage medium, instead of the Indirect TES have a different medium for storing the heat [36]. Alva et al. in [37] show different representations of the TES systems in the CSP plant. The same subdivision could be used to explain the typologies of this work, obviously instead of the sun as source here there is the flue gas from the waste heat, and the electricity production is due to the ORC and not only the boiler and the turbine as in Figure 12 - TES systems subdivision: a) Two tank direct b) two tank indirect c) Thermocline system d) Concrete block system.

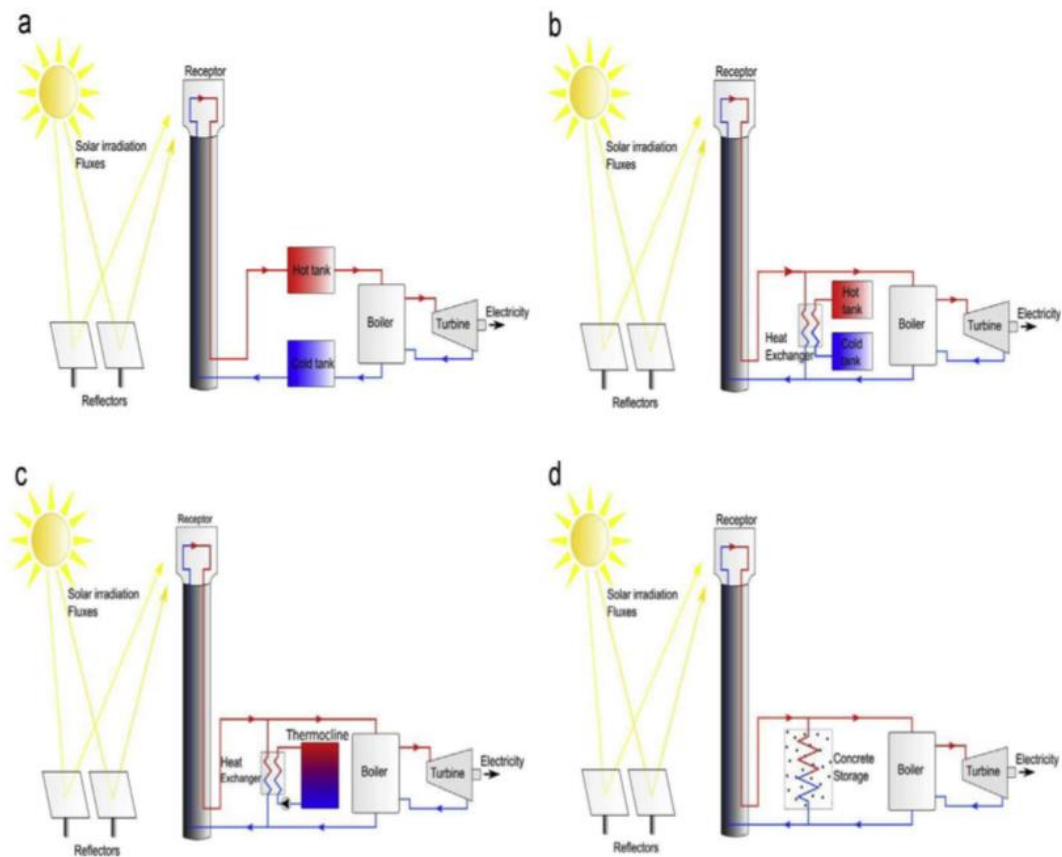


Figure 12 - TES systems subdivision: a) Two tank direct b) two tank indirect c)Thermocline system d) Concrete block system - [37]

In this work, the plant's configuration of TES is the Indirect one, where the HTF is flue gas coming from the industrial process and, giving/receiving heat to/from the storage, is the source of the evaporator of the ORC.

The difference between the three will be described. In all the systems, during the charging process, the hot HTF flows from the top to the bottom of the tanks. Regarding the discharging phase, the fluid flows in the opposite manner. This is a stated theory in the world of the TES [38]. As general assumptions, the HTF was considered incompressible and for the DMT configuration, the materials used as filler were considered homogeneous. Additional simplification, the heat losses through the walls of the tank were neglected as well.

3.1.1 Two-Tank

For the simulation of the two-tank molten salt, has been necessary only proper use of the thermodynamic laws. By defining the amount of heat as the capacity of the tank, the Volume of the fluid which the latter is able to contain could be calculated as in 3.1:

$$V = \frac{Q_{tes}}{c_{p_{medium}} \rho_{medium} (T_h - T_c)} \quad 3.1$$

Where Q_{tes} is the heat capacity of the tank, T_h and T_c are the temperatures of the hot and cold tanks; the properties of the fluid were evaluated at a mean value of temperature between them. This kind of TES expected two different tanks, the hot one which is filled after the heat exchange with the source and the cold one that includes the entire HTF at the lower temperature. The simulation consists in the calculation of the amount of mass flow rate cold which achieves the higher temperature, obviously, the latter is affected by the amount of heat entering the plant, under the variability of the industrial process. The model is able to capture the volume required each time-step of the simulation and also to stop the process when the maximum capacity is achieved.

TWO TANK

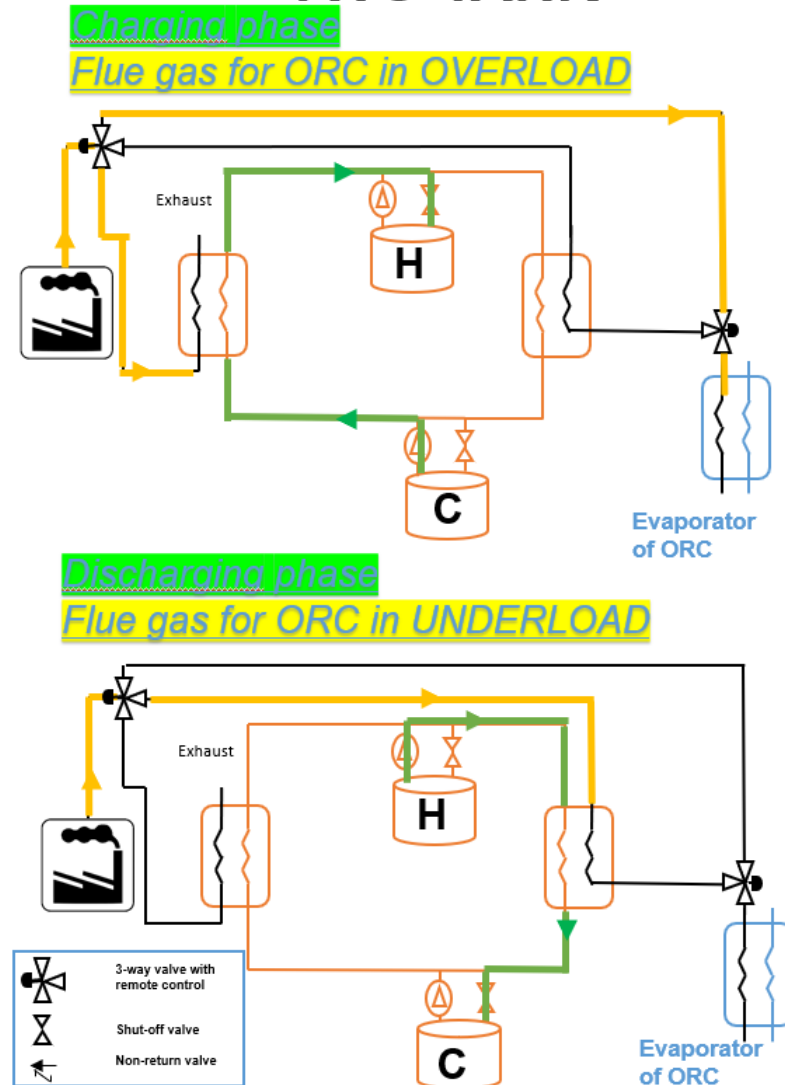


Figure 13 - Two tank TES - Operating principle of the integration between components of the plant

Figure 13 - Two tank TES - Operating principle of the integration between components of the plant, explains the way of working of this TES in the scenario under investigation. On the left, there is the flue gas exiting the industrial process, when it is in OVERLOAD conditions (*CHARGING PHASE* – $Q_{source} > Q_{source*}$), as shown on the top of the Figure 13, the mass flow rate is split in order to have : $Q_{source*}$ at the evaporator of ORC and the remaining part flows to TES's block (in orange) to charge the TES (the subscript * means design conditions). When the monitoring control warns the presence of a surplus of heat, HTF starts from the cold tank and advances its temperature until it reaches the hot tank's temperature (the dependent variable is the mass flow rate of the HTF). The ideal hypothesis of this systems is

that the stored “heat” or “cold” be delivered with no degradation of temperature. A possible reduction of temperature means a directly reduction of efficiency and also of electrical output. On the bottom the UNDERLOAD conditions shall be depicted (*DISCHARGING PHASE – $Q_{source} < Q_{source*}$*), in this case the source is not able to serve heat equals to the design conditions so the ORC works in off-design receiving less heat. If the hot tank of the TES contains enough HTF to reach the working conditions thanks the flue gas, another heat exchange is necessary. Although the main target of the plant is to produce electricity from a waste-energy, so producing as close as possible to the design conditions means improve parameters and as a consequence the entire investment.

For the additional heat exchangers connecting the TES’s block to the source and the ORC the LMTD process has been followed, as for those present in the ORC (Governing equations of the components in design-conditions).

The governing equations of the molten salt pump and the analysis of the results are presented in following paraghaps (Governing equations and considerations of Molten Salt Pump).

3.1.2 Single Thermocline

Two-tank thermal energy even though is an ideal TES, shows always a tank space which is empty (when the hot tank is fully charged, for instance, the cold one is empty). Throughout the years, this not cost-effective aspect of the technology has been improved until the thermocline concept has been implemented with the thermocline thermal storage using only a single tank. The thermocline phenomena develops when layers of fluid separate into several layers and at the bottom of the region there is the one at the lower temperature than either of the surrounding layers; the thermocline is subject of several scientific studies in the world of oceanography as well. As in the ocean the stratification goes from the warmer water on the top due to the sunlight to the deeper and colder temperature, also in the TES’s tank the hot fluid must be charged into it always from the top to facilitate the development of the thermocline, while during the hot fluid delivery, the flow direction is reversed so that cold fluid flows into the tank from the bottom and thus hot fluid is discharged out from the top [39]. As a result of this process there is always hot fluid on the top, and cold on the bottom. It could remind the process of the two-tank TES explained in the previous paragraph(Two-Tank). The concept of separating the hot and cold could be even more ideal, as suggested in

[40], with a thermal insulation baffle presented in Figure 14 - Thermocline thermal storage using a heat transfer fluid only (A) Thermocline; (B) hot and cold fluid separated with a baffle. [39] (B). The real thermocline is the one described in Figure 14 (A) and the conditions to have a proper stratification are related to the dimensions and the temperature range of the tank under investigation.

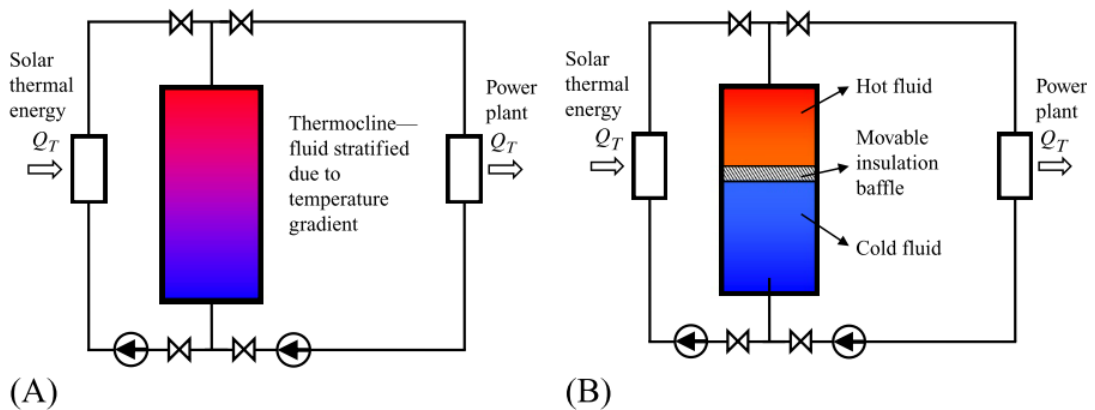


Figure 14 - Thermocline thermal storage using a heat transfer fluid only (A) Thermocline; (B) hot and cold fluid separated with a baffle. [39]

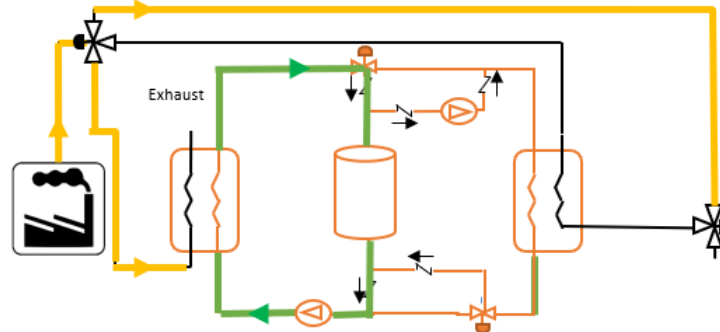
Regarding this work, the simulation of the Single Thermocline has been carried out as the configuration (B), so the thermodynamics of the model is the same as the Two-Tank model. Although the benefit of the cost reduction will be evaluated in Chapter 5. A study of the proper layering has been developed for the Dual Media Thermocline.

The single thermocline in ideal conditions is the same as the two-tank. The equations behind the process are the same but only with the use of one single tank. The hypothesis of the configuration (B) is that thanks to the thermocline stratification the pump can withdraw always medium fluid at the maximum and minimum temperature, in discharging and charging process respectively.

SINGLE THERMOCLINE

Charging phase

Flue gas for ORC in OVERLOAD



Discharging phase

Flue gas for ORC in UNDERLOAD

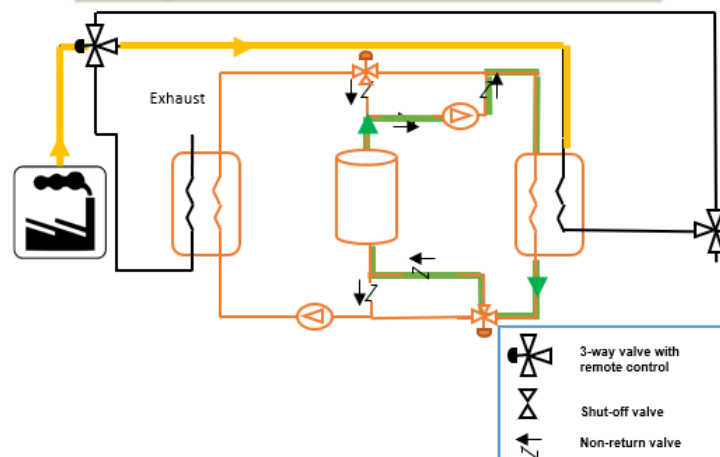


Figure 15 - Single Thermocline TES - Operating principle of the integration between components of the plant

Figure 15 - Single Thermocline TES - Operating principle of the integration between components of the plant shows the way in which this typology of TES works. As is clear from the figure, the pump and the valves-system has a relevant role. Thermodynamic and economic values of the system will be described in the following paragraphs.

3.1.3 Dual-Media Thermocline

It should be noted that usually, the HTF alone may not be enough to achieve the target which thermal energy storage requires. Problems can be caused by not large enough energy storage capacity (ρC_p) or related to the prices of the HTF which is heavy and make even more expensive the investment of introducing a TES technology in a energetic system, especially

when the pressures of it are high and the stresses of the tank may have a relevant impact on the evaluation of the economic expenditure. That's why the Dual-Media Thermocline (DMT) is a well-established technology. The idea behind the DMT is to have a HTF flowing through a tank which contains a different storage material. This second material must have a much higher energy storage capacity. The amount of HTF which receives heat from the source flowing through the DMT could release heat to the filler of the tank (in literature this tank is usually called also : packed-bed). This means to store energy in another medium, so an additional heat exchange which makes impossible the ideality of the process (due to an unavoidable degradation of temperature), but the latter allow a big reduction of HTF required, so reduced volume, costs, and an improvement of the total performances as well. The DMT may be with a sensible thermal storage material or phase change material (PCM) [41]. The following Table shows a resume of all the materials most widespread for sensible heat TESs and their main properties, as shown the energy storage capacity is higher for the fillers.

Table 10 - Main HTF and Filler material for Sensible Heat TESs

	ρ [kg/m ³]	C_p [J/kgK]	ρC_p [MJ/m ³ K]
HTF for Active Sensible Heat TESs			
Sodium	745-884	1270-1310	~1,04
HITEC	1680-1980	950-1400	~2,10
Synthetic Oil	673-815	2370-2730	~1,75
Filler for Sensible TESs			
Concrete	2750	916	2,52
Rocks and Sand	2500	830	2,08
Cast Iron	7200	560	4,03
Ceramics	2400	850	2,04
Graphite	1700,00	1900,00	3,23

The idea of saving costs introducing the single thermocline despite the classic two tank configurations is strength also with this type of technology. Furthermore, the dual media thermocline store the thermal energy from HTF (at the hotter temperature) in another material present in the tank in solid form. (Next step can be introducing the Phase change material (PCM) capsules). The heat transfer involved is the convection within the HTF and

conduction in the storage solid medium. The set of equations is the same as the model used by Van Lew [42] and Pei-Wen Li [39], the core of the problem is to solve both typologies of heat exchange simultaneously. In the present work, the equations were discretized by applying the explicit-forward difference scheme in time and the upwind difference scheme in space. The one-dimensional model is presented, following a representation of the tank with the fillers and a the definition of the geometrical variables of the control volume for analysis.

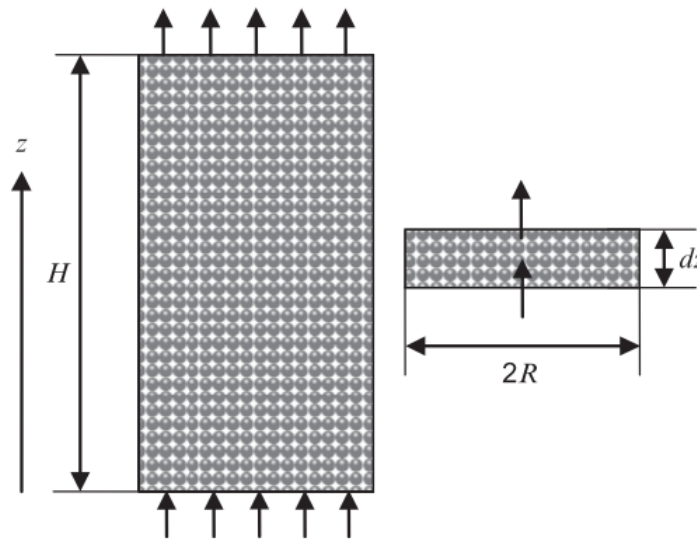


Figure 16 - Scheme of the packed bed TES and a control volume for analysis

It has been developed with the following assumptions with a target of saving computational time and still reach relevant results:

- Uniform radial distribution of the fluid flow and filler material along with the storage tank (MONODIMENSIONAL MODEL along the main length of the tank).
- No conduction between filler material.
- The heat conduction in the axial direction in the fluid is negligible compared to the convective one.
- No heat loss from the storage tank to the surroundings.

Particularly, the last assumption allows to use the results from a heat charge process as the initial conditions of the following discharge process, and vice-versa. Other assumptions related to the calculation of the heat transfer coefficient will be presented in the next sections.

Under those assumptions, the balance equations for the fluid in a control volume dz :

$$\varepsilon(\rho C_p)_f \pi R^2 u \frac{\partial T_f}{\partial z} dz + h S_s (T_s - T_f) dz = \varepsilon(\rho C_p)_f \pi R^2 \frac{\partial T_f}{\partial t} dz \quad 3.2$$

Where ε is the % of fluid present in the total volume of the tank, R is the radius of the tank, u is the velocity of the fluid which is easy to calculate knowing the mass flow rate and f and s are the subscripts respectively for fluid (HTF) and solid (storage medium). The term S_s denotes the heat transfer surface between the filler material and the HTF per unit length of the tank. The heat transfer coefficient, h , for the fluid with the packed material has been evaluated with the 3.3:

$$h = 0.191 \frac{m \dot{C}_p f}{\varepsilon \pi R^2} (Re)^{-0.278} (Pr)^{-2/3} \quad 3.3$$

Fixing the geometrical parameter of the tank and of the filler can easily evaluate the heat transfer area solid/fluid:

$$S_s = 3\pi R^2 (1 - \varepsilon) / r \quad 3.4$$

Where r is the radius of the filler when the shape of the rock is a sphere.

The properties of the fluid influencing the governing equations of the model (ρ , C_p , and k) follow the laws of variation provides by [39].

To solve the problem in which the unknown variables are the two temperature the energy balance of the filler material in a control volume dz is needed:

$$(1 - \varepsilon)(\rho C_p)_s \pi R^2 \frac{\partial T_s}{\partial t} dz = h S_s (T_f - T_s) dz \quad 3.5$$

Boundaries conditions and initial time temperature (provides by codification in Matlab) are needed to solve with an EES simultaneously the equations 3.2 and 3.5 to reach the resolution of the problem. Of course, the solution is possible per each layer of volume in consideration.

The hypothesis used to proceed with the simulation of all the tank along the time are:

- The inlet fluid temperature is the maximum available of the HTF during the charging process and minimum during the discharging process.

- For the first layer, during the calculation of the term regarding the discretization along the dz , has been fixed the previous temperature. For all the other layer along with the tank, the inlet temperature is the unknown T_f evaluated at the previous layer.
- Initial conditions of the filler and the fluid inside the tank are totally charged when the discharging phase starts and the other way around.

According to the assumption of no heat loss from the storage tank, it can be seen that the equilibrium temperature at the end of one process (charge or discharge) will necessarily be the initial condition of the next process in the cycle which permits a connection between processes so the possibility of overall periodic analysis.

The process of charging and discharging is considered complete when the last layer of the tank (the most far from the hot/cold source, respectively) has a 5 C° drop respect to the limit conditions.

3.1.4 Governing equations and considerations of Molten Salt Pumps

Concerning the evaluation of the properties of the molten salt pumps the following approach has been used (all those considerations have been applied in the worst-case scenario, so when the mass flow rate is higher):

- 1) Definition of the diameter of the pipe considering a maximum value of velocity inside the system of $v_{max} = 4 \frac{m}{s}$

$$\dot{m}_{tes_{medium}} = \rho_{mean} v_{max} A(d) \quad 3.6$$

The value which comes from the 3.6 has been increased until the closest value of the nominal diameter existing in commerce.

- 2) The hypothesis of the length of the pipes-path along the TES-loop. As a first approximation, has been considered a length which can include also all the equivalent length for all the concentrated losses along the loop.

- 3) Evaluation of the pressure losses along the pipe with the following equations:

Cole-brook-White Equation (for a conduit flowing completely full of fluid at Reynolds number greater than 4000):

$$\frac{1}{\sqrt{f}} = -2\log\left(\frac{\varepsilon}{3.7d} + \frac{2.51}{Re\sqrt{f}}\right) \quad 3.7$$

$$\Delta p = f \frac{L}{d} \rho \frac{v^2}{2} \quad 3.8$$

$$H = \frac{\Delta p}{\rho g} \quad 3.9$$

4) Evaluation of the Power's Pump:

$$W_p = \frac{mHg}{\eta_p} \quad 3.10$$

Eventually, the results obtained under the next assumptions:

- Length of the pipes for charging-phase: 50 m
- Length of the pipes for discharging-phase: 50 m
- The diameter of all the pipes (TT, SMT): 0.05 (evaluated as explained above)
- The diameter of all the pipes (DMT): 0.15 (evaluated as explained above)
- Rugosity: 1 μm
- $\eta_p = 0.8$

Table 11 - Results of the pump in the TES-Loop

Worst-case Scenario		\dot{m}	Δp	H	Power	d
		[kg/s]	[bar]	[m]	[kW]	[cm]
Two-Tank/Single Thermocline	Charge	10,44	0,176	2,23	0,285	50
	Discharge	10,44	0,176	2,23	0,285	50
Dual-Media Thermocline	Charge	52,68	0,052	0,62	0,669	150
	Discharge	51,78	0,051	0,62	0,691	150

3.2 Validation

The validation has been carried out with the simulation work of Van Lew [42]. The hypothesis of the model are the same. Following the data present in the paper used for the validation. The author considers constant the properties with the variation of the temperature.

Table 12 - Material properties (HTF and filler) present in the tank

Fluid : Therminhol VP-1			Solid :Granite rocks		
ρ	753.75	[kg/m ³]	ρ	2630.00	[kg/m ³]
c_p	2474.50	[J/kgK]	c_p	775.00	[J/kgK]
k	0.086	[W/mK]	k	2.80	[W/mK]

Table 13 - Data used for the validation

Other input parameters		
Higher temperature	395.00	[Celsius]
Lower temperature	310.00	[Celsius]
Radius Tank	7.30	[m]
High tank	14.60	[m]
Void Factor	0.25	[-]
Radius rock	0.02	[m]
Operational time	4.00	[hours]
Mass flow rate	128.740	[kg/s]

The problem has been solved as shown in paragraph Dual-Media Thermocline. Next figure compares the dimensionless fluid temperature inside the tank every 30 minutes during the heat exchange. The governing equations 3.2 and 3.5 after the discretization could be written as follow :

$$\varepsilon(\rho C_p)_f \pi R^2 u \frac{T_{fi}^n - T_{fi-1}^n}{\Delta z} dz + h S_s (T_{si}^n - T_{fi}^n) dz = \varepsilon(\rho C_p)_f \pi R^2 \frac{T_{fi}^{n+1} - T_{fi}^n}{\Delta t} dz \quad 3.11$$

$$(1 - \varepsilon)(\rho C_p)_s \pi R^2 \frac{T_{si}^{n+1} - T_{si}^n}{\Delta t} dz = h S_s (T_{si}^n - T_{fi}^n) dz \quad 3.12$$

Where the subscripts “n” and “i” are respectively for the discretization in time and space. Next equations show the way chosen for the definition of the dimensionless variables.

$$\theta_i = \frac{T_i - T_c}{T_h - T_c} \quad 3.13$$

$$z = \frac{h_i}{H} \quad 3.14$$

Where h represents the spatial coordinate along the tank and H is the high of the tank. The work used for the validation provides the boundary conditions and the initial conditions as well, as is clear from the Figure, the trend of the temperature is not constant (the yellow line). This is a well-established approximation used for the periodic analysis [43]. At the beginning of the process, the HTF obviously is cold and at the lower temperature but after a considerable number of cycles, the profile take a particular shape which remains constant along the time.

The dashed lines show the results of the paper, the continue lines show the result of the current simulation model.

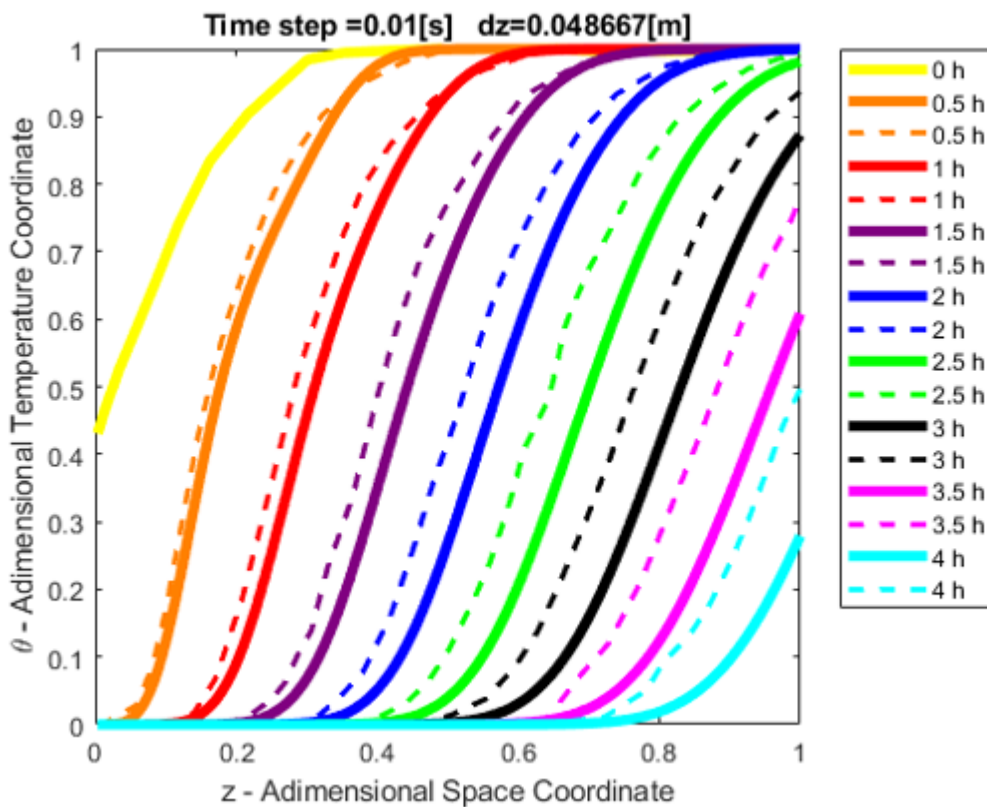


Figure 17 - Comparisons between thw Van Lew's work (dashed line) and the results obtained with the model

Once the geometry was fixed and the discretization along the height of the tank was chosen equal to the latter divided by 300, an independent-time study has been carried out. Multiple

simulations have been implemented, decreasing every time the time-discretization until the changes between two consecutive simulations were not so relevant. Furthermore, an evaluation of the error of the temperature has been evaluated along the time and the spatial distribution of the tank :

$$err\% = \frac{T_{model} - T_{ref}}{T_{ref}} \quad 3.15$$

Then the results obtained with time-step of 1,0.1 and 0.01 seconds:

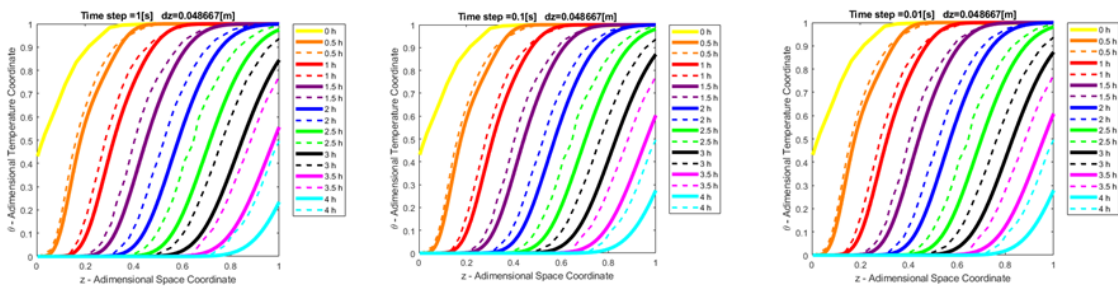


Figure 18 - Time-independent study, Adimensional coordinates (Time and space)

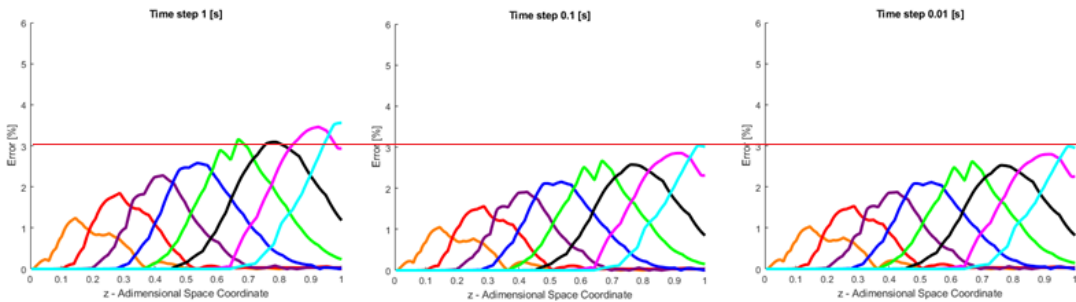


Figure 19 - Time-independent study, Trend of the percentage error

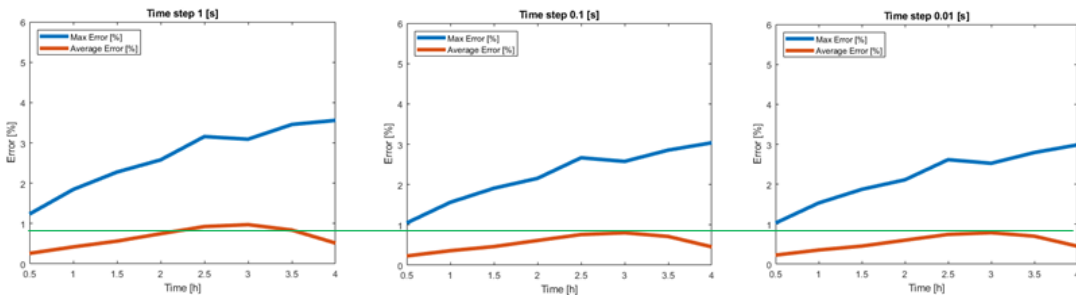


Figure 20 - Time-independent study, Trend of the maximum and average percentage error

The difference between the results obtained with the time-step of 0.01 and 0.1 are negligible so will be used the highest time-discretization, in order to reduce the computational-time still

reaching good results. An average percentage error of less than 1% is achieved regarding the temperatures of the tank which ensure the reliability of the model and of its assumptions. The validation can be relevant indistinctly from a charge or discharge thanks to the assumptions made in the previous section.

4. Economics correlations for the evaluation of the investment

The estimation of cost is a relevant step to perform a good evaluation of the investment. How the costs of the plant's components are evaluated is summed in this chapter. The structure of the chapter consists of three parts to resume the comprehensive cost model developed using assumptions and correlations present in literature. First part shows an estimation cost of each component of the ORC. Second, all the considerations and correlations for the TES's block. The last paragraph shows the main techno-parameters present in literature that may be useful in this context. The target of them is to capture relevant results as far as possible from the specific case and obtain considerations of the process always according to the systematic approach. All costs are evaluated in € (April 2019).

4.1 Organic Rankine Cycle

An estimation of the costs of the ORC has been possible thanks to the work of Gabbrielli [44]. Following the correlations per each component of the cycle.

Heat Recovery Steam Generator

$$C_{HRSG} = 9090 \left(\frac{Q}{\Delta_{TML}} \right)^{0.8} + 23115 * m_{cold} + 1286 * (m_{hot})^{1.2} \quad 4.1$$

Where m are the mass flow rates are in $\frac{kg}{s}$, Q is power exchanged in it measured in kW and the Δ_{TML} the logarithmic temperature drop inside the HRSG.

Pump

$$C_{pump} = 2076(P)^{0.71} * 1.41 * \left(1 + \frac{(1 - 0.8)^3}{(1 - \eta_{ex\,pump})^3} \right) \quad 4.2$$

Where P is the power of the pump in kW and $\eta_{ex\,pump}$ is the exergy efficiency of the pump.

Heat Exchanger

$$C_{HE} = 2111 * (S)^{0.69} * (p)^{0.28} \quad 4.3$$

Where S is the heat exchange surface in Sm^2 and p is the highest pressure (bar) in the heat exchanger.

Electric Generator

$$C_{Electricgenerator} = 70 * (P)^{0.95} \quad 4.4$$

Where P is the power kW .

Condenser

$$C_{cond} = 168 * S + 1346 * m \quad 4.5$$

Where S is the heat exchange surface in m^2 and m is the mass flow rate in the condenser.

Turbine

$$C_{turbine} = \frac{927}{1 - \eta_{is}} * m * \ln(\beta) \quad 4.6$$

Where η_{is} is the isentropic efficiency of the turbine and β is the pressure ratio.

The estimation of the total cost of the ORC has been used a supplement of 30% respect to the values of the components to consider:

- Price of the organic fluid
- Installation costs
- Other miscellaneous costs

$$C_{ORC} = 1.3 * (C_{HRSG} + C_{pump} + C_{HE} + C_{Electricgenerator} + C_{cond} + C_{turbine}) \quad 4.7$$

The installations costs for the ORC are quite relevant, especially for an application of waste heat recovery. The costs for the integration of the ORC module into an existing plant cannot be neglected.

Several works are in the literature regarding the estimation of the costs of an organic Rankine cycle. Lemmens has been developed a review of the studies present in literature and gives an overview of them [45]. The latter has been used to understand the viability of the values obtained under the assumptions of this work.

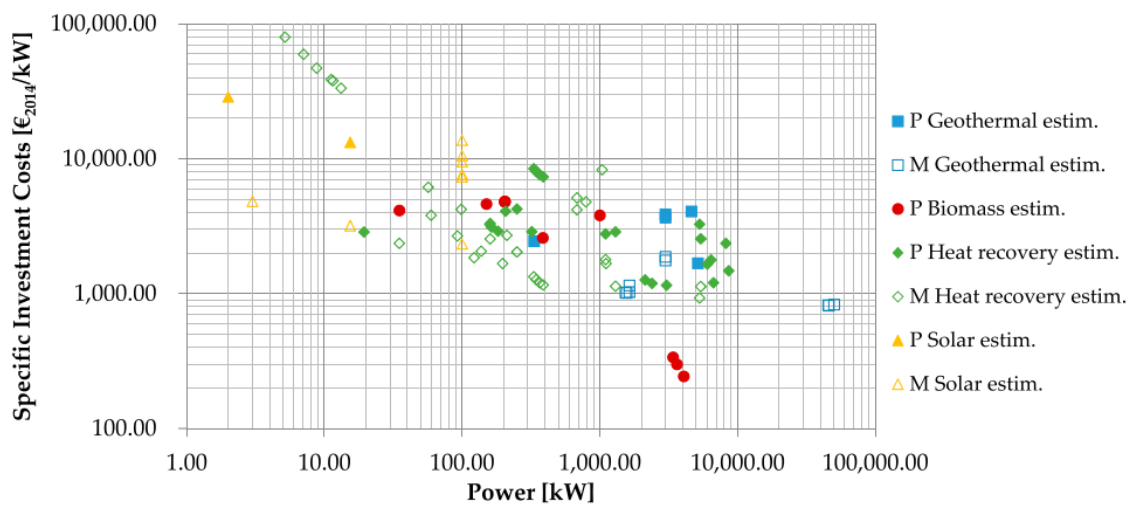


Figure 21 - From [9], Overview of the specific investment costs of ORGANIC RANKINE CYCLE

The figure shows the values present in the literature which have the following requirements:

- the paper performs a bottom-up estimate of ORC costs, using various techniques
- the power output of the ORC system is given
- the paper presents the resulting specific investment cost (SIC) or the total investment costs of the ORC system

With the color-scale of Figure 21 - From [9], Overview of the specific investment costs of ORGANIC RANKINE CYCLE is possible to recognize different technologies linked with the ORC and the “P” stands for Project and “M” for the module. The projects are the work with the considerations of all the costs of the plant, including the installations costs and miscellaneous. The modules are only the costs of the components.

Regarding this work, an ORC of **797 kW** as nominal power, coupled with a heat recovery

system with a total investment cost of **2.2 M€** has been considered appropriate (**3013 €/kW**). The post process analysis of the overview explains an estimated module costs of **2781€/kW** and regarding the project costs of **3414 €/kW**.

The values of the costs of all the components will be presented in the next chapters.

4.2 Thermal energy storage

For the thermal energy storage has been considering the cost of the fluid, tank (or tanks) and of the additional components needed for the work of it as pump and heat exchangers.

For the heat exchangers, in the TES's block, has been used the equation 4.3.

The next table shows the unit cost of the medium (fluid/HTF and solid) used for the analysis in the TESs. The last row shows the reference of the data source.

Table 14 - The unit cost of the storage medium

Unit cost [€/kg]	Ref.
Therminol VP-1	1.60 [16]
HITEC	0.74 [16]
Concrete	0.05 [46]
Rock and sands	0.150 [46]
Cast Iron	1 [46]

For the estimated cost of the tank in each configuration has been followed the work of Jacob, Bruno, and Saman present in literature [47].

Table 15 - Formulations for tank estimation cost

Tank cost estimation	
Insulation tank	200/m ² [€]
Foundation tank	1000/m ² [€]
Material tank	1.26 [€/kg]
Pipes&Valves	850/MWh _t [€]
Instrumental Control	200/MWh _t [€]
Pump Molten Salt	1500/MWh _t [€]

4.3 Techno-Economic Parameters

4.3.1 LCOE

It's the most common parameters used in literature to make comparisons with different technology in different configurations.

The LCOE (Levelized cost of electricity) is, as defined by[16]:

$$LCOE = \frac{\sum_{t=1}^n \frac{M_i}{(1+r)^t} + C_i}{\sum_{t=1}^n \frac{E_t}{(1+r)^t}} \quad 4.8$$

Where C is the depreciation charge of the total cost of the plant for the i-th year, M is the maintenance assumed 2% of C, r is the interest rate considered to be 4% and n is the lifetime of the system(20 years). E is the energy produced in the year t.

4.3.2 NCOTES

The NCOTES (Normalized cost of thermal energy storage) is a parameter introduced by Mostafavi and Tehrani [46], which takes into account both the cost and performance of the systems. This is the ratio between the cost of the storage unit divided by the annual gross electricity generation of the plant. He suggests this term in order to capture the overall techno-economic comparisons of the TES systems.

$$NCOTES = \frac{\text{Total cost of TES system [€]}}{\text{Annual electricity generation of the plant [MWh}_e\text{]}} \quad 4.9$$

4.3.3 NET PRESENT VALUE

Net Present Value (NPV) is the most common criterion in the economic assessment of investment projects. The NPV of the investment is the algebraic sum of all the discounted cash flows generated by the project in question, net by the initial cost of the investment.

$$NPV = \sum_{i=1}^n \frac{\text{Cash Flow}_i}{(1+r)^t} - I_0 \quad 4.10$$

Where r is the interest rate considered to be 4 %, n is the lifetime of the system and I_0 represents the initial investment cost of the plant as a whole.

The Cash Flow during the various years has been calculated, per each configuration, considering the UK electricity price [<https://powercompare.co.uk/electricity-prices/>]. Usually, a company which decided to build up a system to obtain energy from its industrial waste heat use for itself the amount of electricity for other issues needed inside the own building, that's why the income has been evaluated with the cost of the electricity in the UK. It's not a proper income, but a missed outcome which anyway is relevant for an estimation of the investment.

4.3.4 CAPACITY FACTOR

The Capacity Factor (CF) is a ratio between the real electricity production which the organic Rankine cycle is able to perform divided by the amount of energy that the plant would provide if it works at its nominal conditions all along with the timescale analysis. The latter for this work has been considerate a day.

$$CF = \frac{\text{Production of electricity } \left[\frac{Wh_{el}}{\text{day}} \right]}{\text{Nominal Production of electricity } \left[\frac{Wh_{el}}{\text{day}} \right]} \quad 4.11$$

5. Techno-Economic Analysis – Results of different Cases for the evaluation of the influence of working conditions having a fluctuating source.

Very challenging for the Waste Heat Recovery is the large fluctuations in temperature and/or mass flow rate of the source and how to adapt the plant to this variability. Being strongly linked to the conditions of the industrial process a proper study of the off-design conditions is relevant. Off-Design considerations can influence also design choices. The adaptability of the plant at the variation of the source is important and, nowadays, its optimization is one of the main problems in this sector.

5.1 Presentation of Scenarios

Three scenarios are presented and the following results are discussed in different configurations. A brief resume of the scenarios :

- Scenario 1): the variation of the heat source is simulated with a parameter which follows the sinusoidal trend and tuning the temperature changes the value of the heat entering in the system from the industrial process. The time analysis is 12hours.
- Scenario 2): using the data of a real process of the cement industry present in literature, an extrapolation of 12hours of working conditions has been made.
- Scenario 3): a study of the whole process present in literature (Time analysis 48h)

5.1.1 Scenario 1: Hypothetic sinusoidal trend of source

For academic purpose has been developed a profile of source with a sinusoidal trend which is useful to easily understand some parameters present in this chapter and also to make good comparisons with the real processes under investigation.

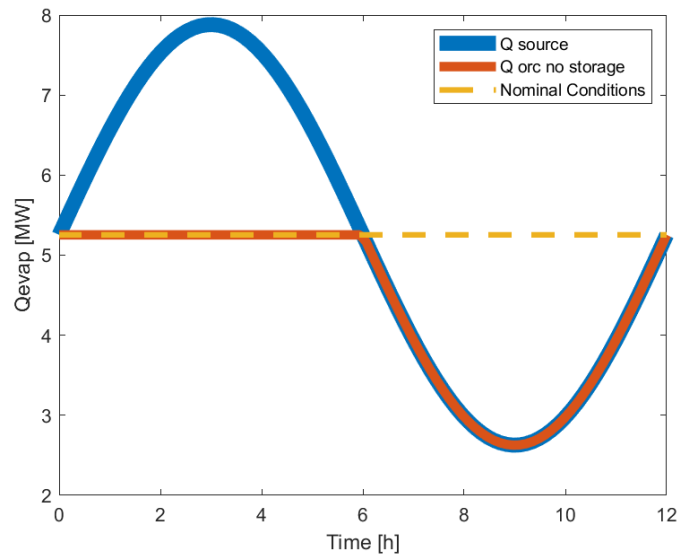


Figure 22 - Scenario 1) Source-profile representation

5.1.2 Scenario 2: Clinker cooling

From the work of Legmann [35], an extrapolation of 12 hours has been made. The process regards the cement production, particularly the phase of it which is related to the waste air that cools down the produced clinker. The latter is usually found in the range of 150-350°C. As shown in Fig. 23, the temperature of the clinker cooling air can fluctuate, leading to large fluctuations in heat rate available. The mass flow rate can instead be considered approximately constant.

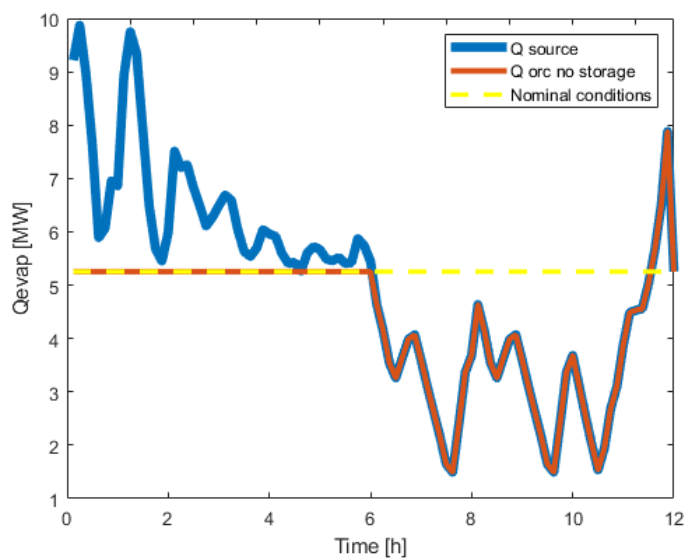


Figure 23 - Scenario 2) Source-profile representation

5.1.3 Scenario 3: Periodic analysis

The periodic analysis of this scenario comes from the whole process present in the work of Legmann [35].

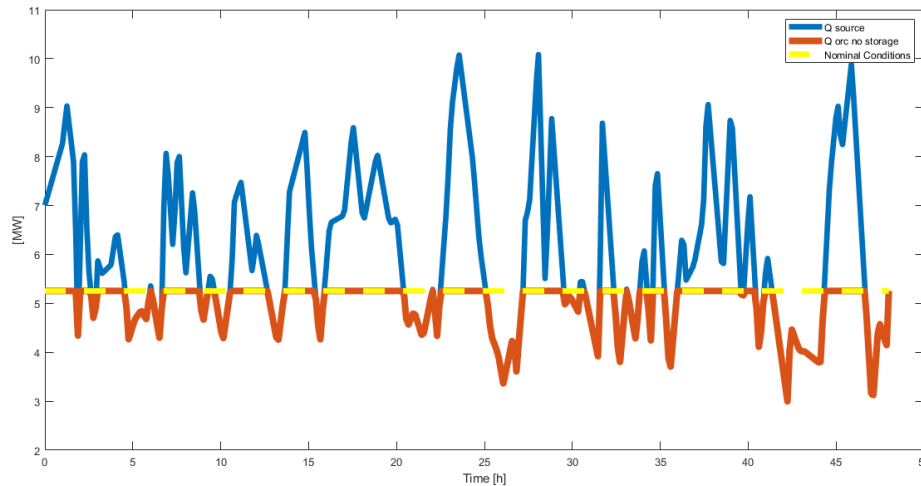


Figure 24 - Scenario 3) Source-profile representation

5.2 Sizing of Thermal Energy Storages

This paragraph includes methods for calculating the volume of the thermal storage tank to better couple the system with the several configurations of TESs (TT-ST-DMT).

The main role of those devices is to provide a hot HTF and releases the heat at the destination. When this process occurs, a change of temperature from a high to a lower value is necessary ($T_h \rightarrow T_l$). On the other side, during the discharging phase, the temperature has to reach the upper value of temperature ($T_l \rightarrow T_h$). The HTF to satisfy those processes has to respect a certain amount of mass flow rate based on the amount of the required thermal energy demand (Q_{TES}).

$$Q_{TES} = \dot{m}c_{p_{HTF}}(T_h - T_l) \quad 5.1$$

The mass flow rate must respect the 5.1 without any relations with the typology of the TESs under investigation [39].

The evaluation of the mass flow rate in the context of this work becomes:

$$\dot{m}_{charge}(t) = \frac{Q_{source}(t) - Q_{orc_{nom}}}{C_{pHTF}(T_h - T_l)} \quad 5.2$$

$$\dot{m}_{discharge}(t) = \frac{Q_{orc_{nom}} - Q_{source}(t)}{C_{pHTF}(T_h - T_l)} \quad 5.3$$

Following will be explained other observations related to the different TES approach.

5.2.1 Only HTF as Thermal Storage Medium

When the thermal storage uses only an HTF as a single medium (TT and ST) an ideal energy storage efficiency could be used. After evaluating the mass flow rate as in 5.1, knowing the time-analysis (Δt) and the time-step discretization, the Volume could be easily calculated following the next equations :

$$M_{ideal} = \sum \dot{m}_{charge/discharge}(t) \quad 5.4$$

$$V_{ideal} = \Delta t \frac{M}{\rho_{HTF}} \quad 5.5$$

Where M and V are respectively the total mass flow rate and the volume required. According to the hypothesis of perfect insulation (Model development of different typologies of Thermal Energy Storage (TES).) of the tank, this approach may reach 100% of efficiency.

5.2.2 Dual Media Sensible Thermal Storage, Solid and HTF

In packed-bed solution, so a solid base with the HTF which flows through it, the thermal storage volume must satisfy the following equation [48]:

$$\{[(\rho C p)_s(1 - \varepsilon) + (\rho C p)_f \varepsilon] * V\} \geq (\rho C p)_f V_{ideal} \quad 5.6$$

On the left of the equations, there is the total heat capacity regarding the porous media (packed bed with the HTF filled in the void) and the right side is the ideal case shown in the previous paragraph.

Appears clear the strict dependence from the material properties and a reduction of the total mass of HTF required which means a good benefit in terms of cost of the storage as a whole.

5.2.3 Geometry definition and sizing of the tanks in different scenarios and configurations

In the next table are summed the main parameter fixed to define the geometry and consequently the thermal capacity of the TESs. The tanks have been modeled as a cylinder. All the simulations are carried out considering the same thermal capacity per each Scenario. The capacity has been fixed per each Scenario in order to make always comparisons between different configurations (in terms of materials used). Due to the variability of the processes, the choice of the maximum capacity is not easy to define. In this work, the total heat which the TESs are able to store has been fixed as the total amount of heat present in the OVERLOAD phase (so the sum of all the surplus respect the nominal conditions).

Table 16 - Input fixed for the determination of the geometry of the tank

Higher Temperature	232	[°C]
Lower Temperature	152	[°C]
Void Factor (only for DMT)	0,3	[]
Height of the Tank	5	[m]

Following a graph regarding the results in terms of the geometry of the tanks obtained for the different scenarios.

Scenario 1

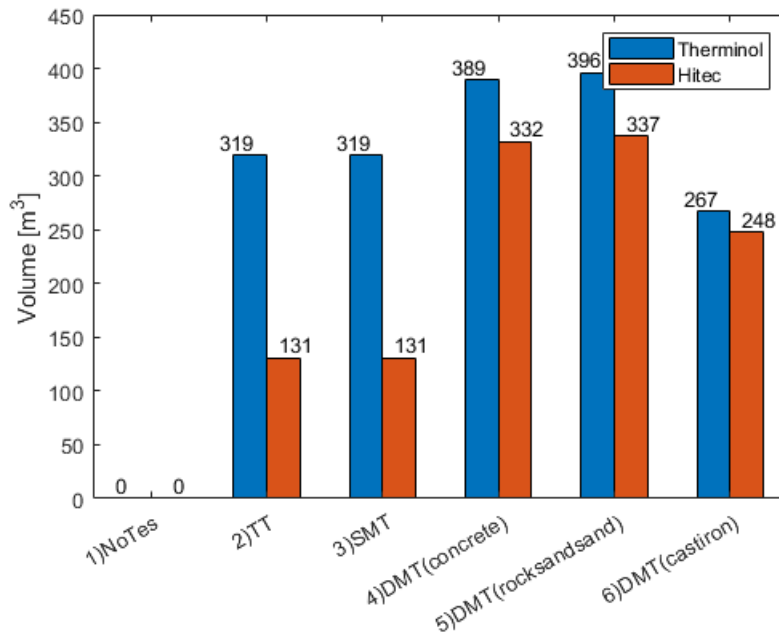


Figure 25 - Volumes of the different configurations regarding SCENARIO 1

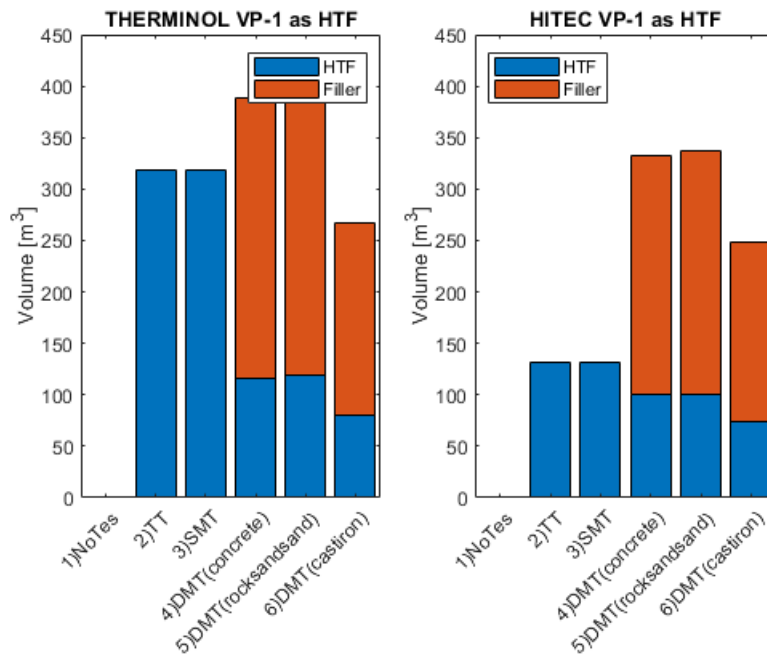


Figure 26 - Breakdown of the volume of the tank between HTF and Filler – SCENARIO 1

Scenario 2

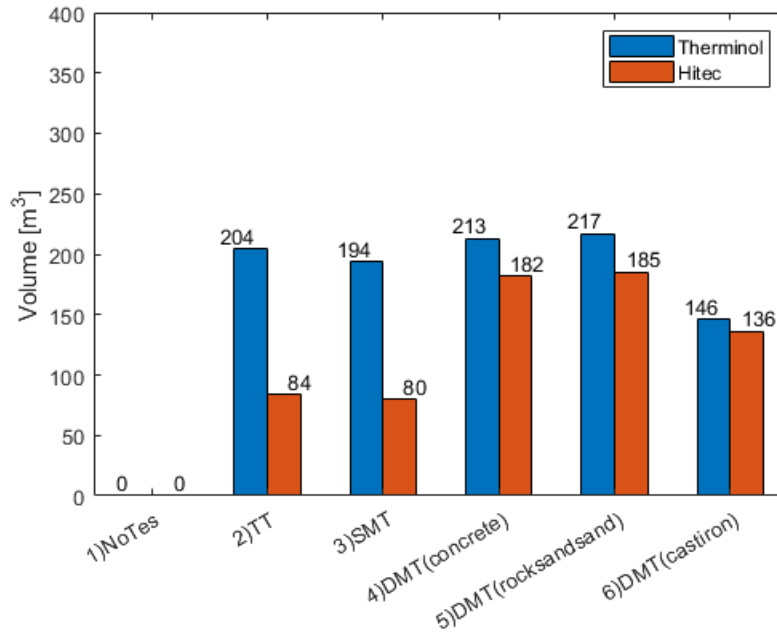


Figure 27 - Volumes of the different configurations regarding - SCENARIO 2

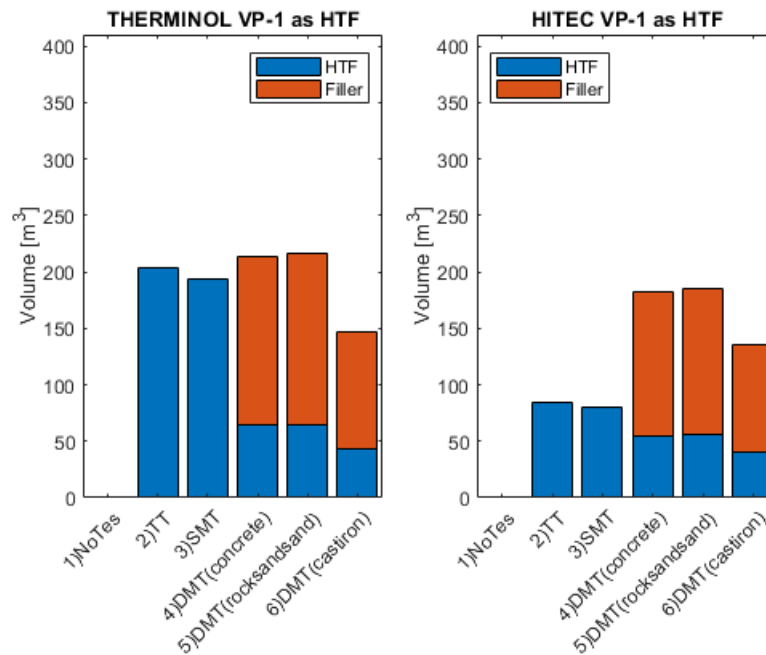


Figure 28 - Breakdown of the volume of the tank between HTF and Filler – SCENARIO 2

Scenario 3

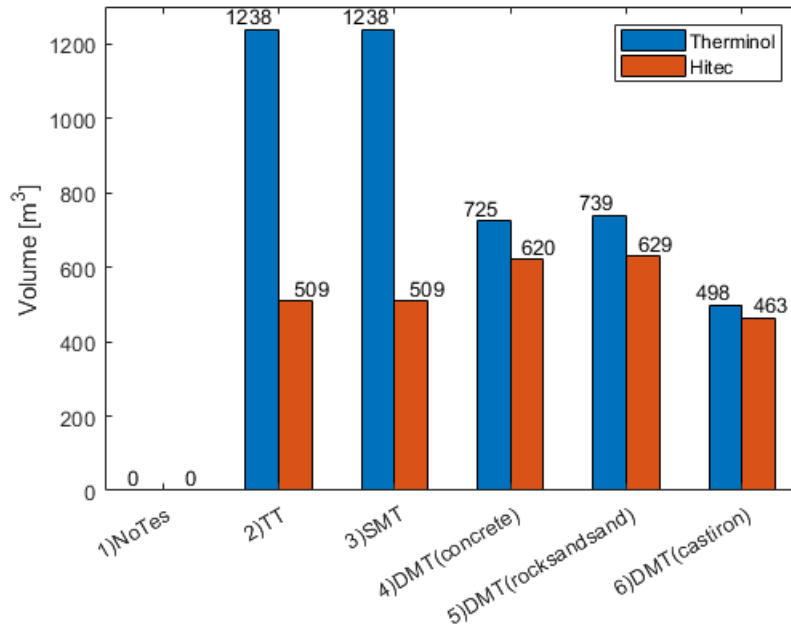


Figure 29 - Volumes of the different configurations regarding - SCENARIO 3

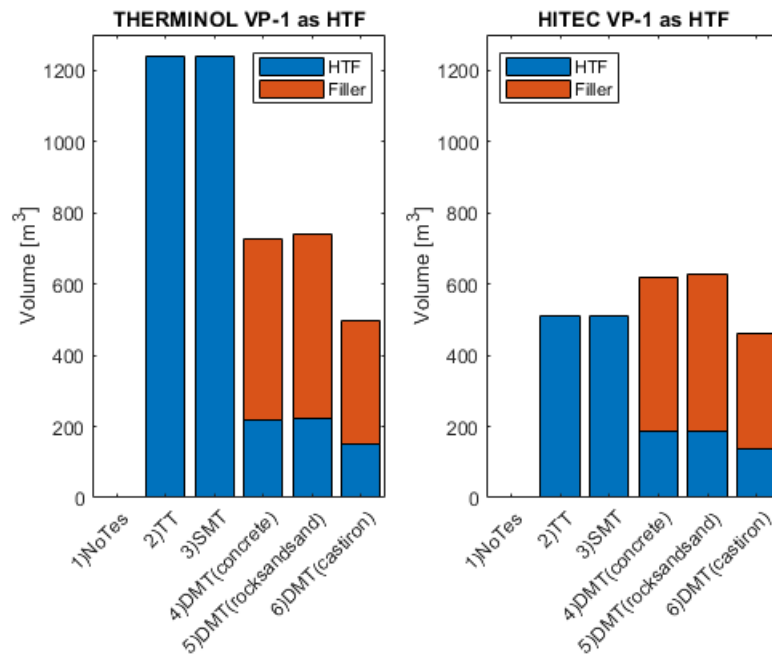


Figure 30 - Breakdown of the volume of the tank between HTF and Filler – SCENARIO 3

5.3 Comparisons between the scenarios with and without the storage focusing on the differences in terms of thermal load

During the design phase of a plant shall be taken into account several aspects which are strictly related to the scenario's characteristics under investigation. The decision-making regarding a system like the one considered in this work is to tune the heat entering the evaporator during the design conditions as much as possible to a value which allows better configurations based on the target fixed in the feasibility study. For this work, it was pioneered the idea of introducing a TES so the choice of the design conditions is influenced by the ability to charge and discharge it. By observing figures above, even is often possible receive much more heat from the "free-source", has been chosen to fix a proper value of design-conditions in order to store heat in the TESs and, thanks a timely discharging phase, obtain work conditions of the plant as close as possible to the design-conditions which follows relevant advantages from the economic and thermodynamic point of view as well.

In Off-Design conditions could be possible to have two different configurations:

- OVERLOAD ($Q_{source} > Q_{source}^*$)
- UNDERLOAD ($Q_{source} < Q_{source}^*$)

In **OVERLOAD** conditions the cycle, without the TES technologies, receives a higher amount of heat at the evaporator, respect the nominal conditions. To perform work with the best efficiency of all the components inside the plant this source is reduced until its value is equal to Q_{source}^* . The surplus of energy flowing from the industrial process can be used to charge the TES. At the end of the day, with a TES, there will be a lower value of Q_{evap} entering the system, that is equal to Q_{evap}^* .

Without adding a TES, in those conditions, all the components of the plant work with the efficiencies best possible chosen during the phase of design, but obviously there is a not best utilization of the surplus of energy of the industrial process. Following the equations of the η_{glob} which decrease, and of η_{ORC} which is constant during the overload phases.

$$\eta_{glob} = \frac{W_{net}}{Q_{source}} < \eta_{glob}^* \quad 5.7$$

$$\eta_{ORC} = \frac{W_{net}}{Q_{evap}} = \eta_{ORC} * \quad 5.8$$

Where W_{net} is the net production of electricity at the turbine.

During the **UNDERLOAD** conditions the cycle work with a lower value of heat entering at the evaporator. That usually means a reduced value of efficiencies of all the components. Using the discharge process of the TES, in this case, allows at the system to reach (when there is enough amount of energy stored) nominal conditions of energy entering the evaporator. The main scope of the use of TES is to improve the quantity of the production of electricity. Furthermore, the quality of the production increases, using all the plant's components as close as possible to their best conditions selected during the design phase.

The third case possible is the **NO WORK** conditions. Following the regulation of the turbine present in 2.2.2, could be possible reaches pressure at the inlet of the turbine, so the high pressure of the cycle, in which the working fluid of the cycle (R134) is not in the phase required for a proper function of it. By defining the dimensionless Thermal Load as :

$$T.L. = \frac{Q_{source}}{Q_{evap*}} \quad 5.9$$

$T.L.$ could be lower than 1 during the UNDERLOAD and during the OVERLOAD the upper limit is related to the amount of heat of the industrial process ($0 \leq T.L. \leq \infty$).

The NO-WORK conditions of this system have been identified with a $T.L. = 0.37$, thus a $Q_{evap} = 1.76 \text{ MJ/kg}$. Automatically, in the model when the heat of source is lower, the production of the turbine is stopped and the amount of heat is used to charge the TES if it is possible. Following the representation of the T-s diagram of the limit conditions compared with the design-conditions.

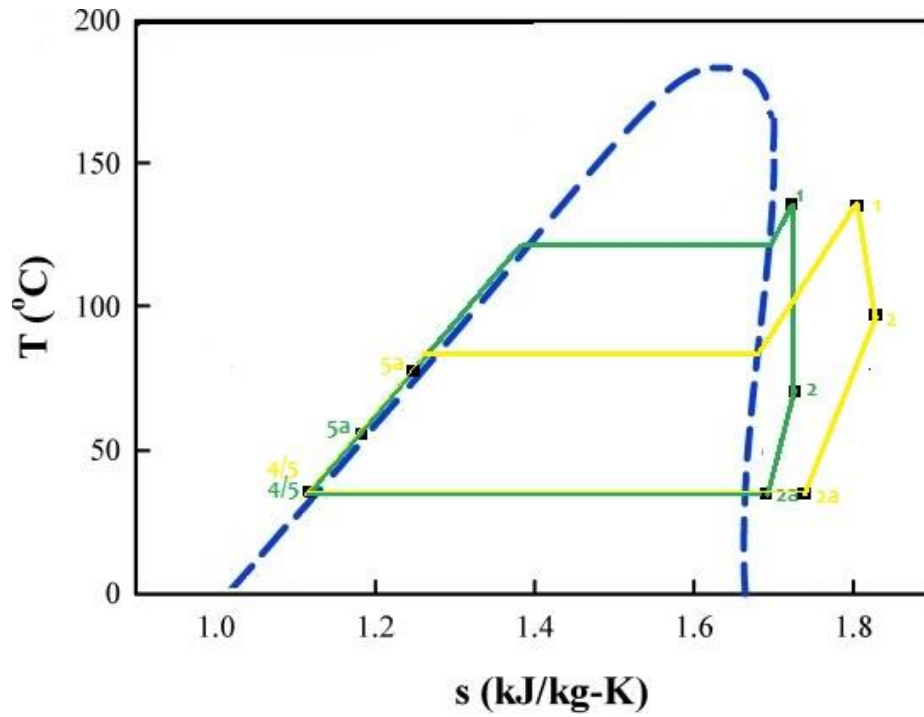


Figure 31 - T-s representation of Nominal conditions (GREEN) and limit conditions (YELLOW)

Following per each scenario a graph with a color-scale in order to easily understand the different phase of the system (Overload, Underload & No work conditions).

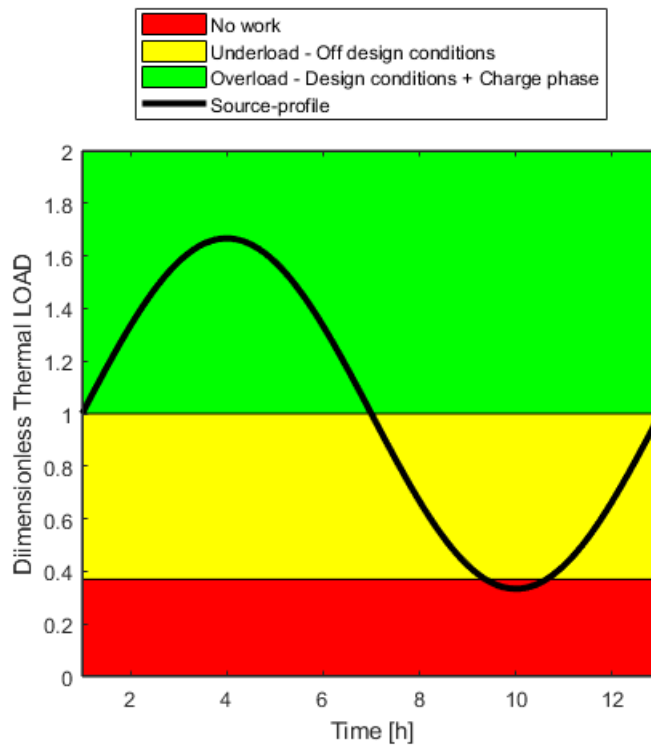


Figure 32 - Different phases of the source-profile: SCENARIO 1

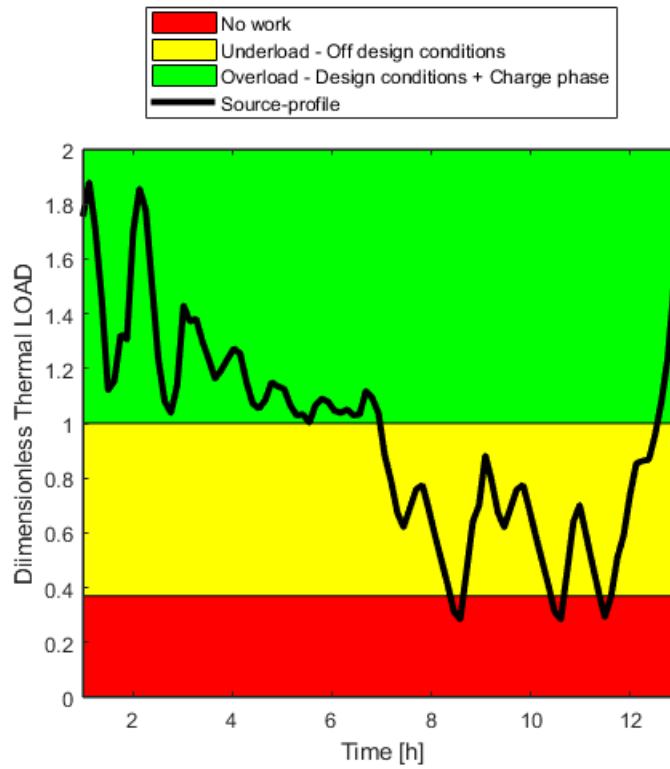


Figure 33 - Different phases of the source-profile: SCENARIO 2

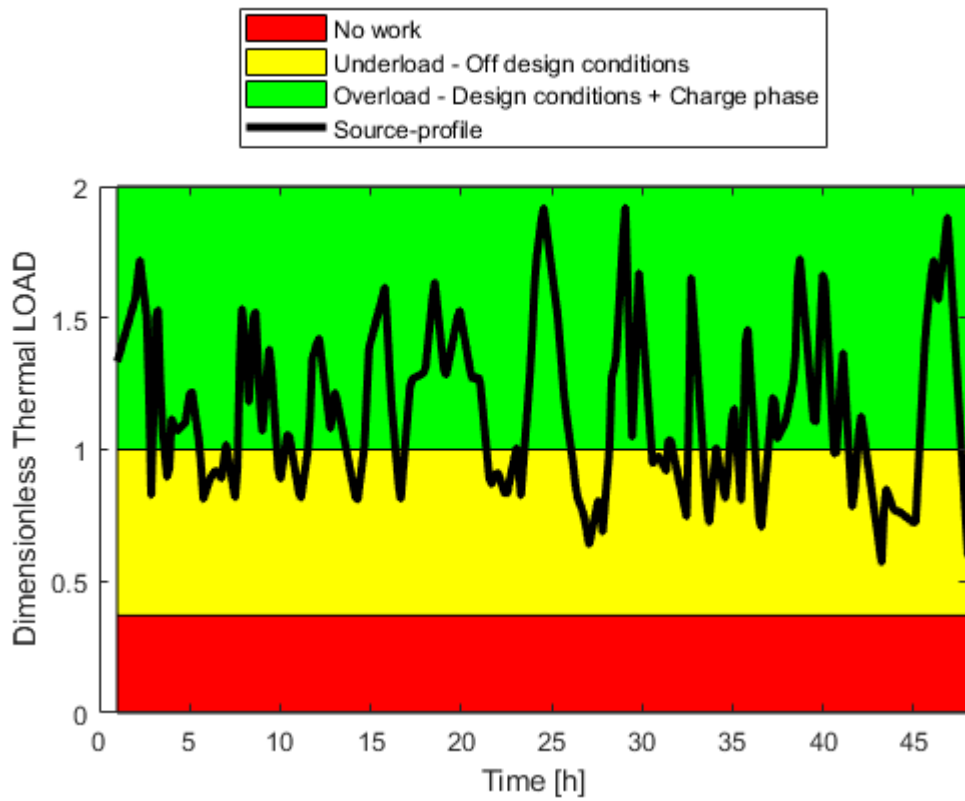


Figure 34 - Different phases of the source-profile: SCENARIO 3

Introducing the different configurations, in terms of materials, of TESs presented in Chapter 3, Table 14 - The unit cost of the storage medium, appears clear the reduction of the work conditions in the yellow zone (Off-design conditions) in favour of a production of electricity at the nominal conditions ($T.L. = 1$). Next graphs show the working conditions of all the configurations of this analysis, and subsequently the trend of the power net production.

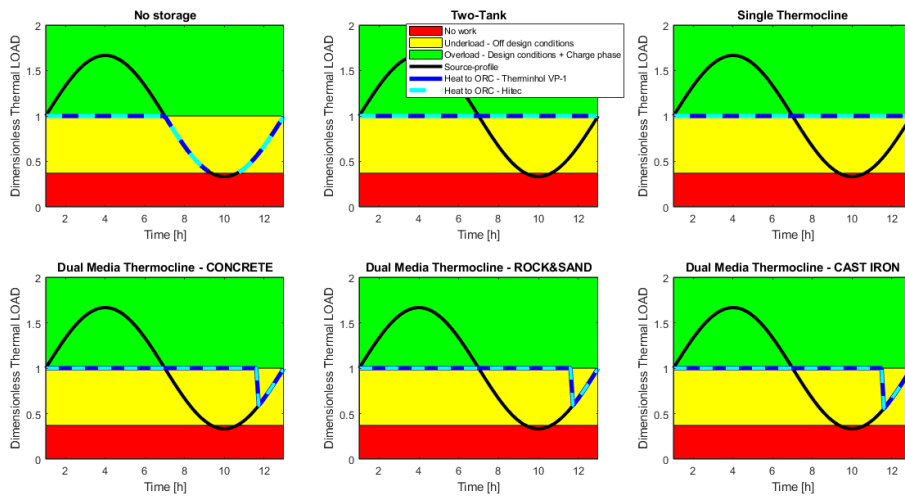


Figure 35 - Comparisons of the work conditions with/without storage in terms of Thermal Load in different configurations – SCENARIO 1

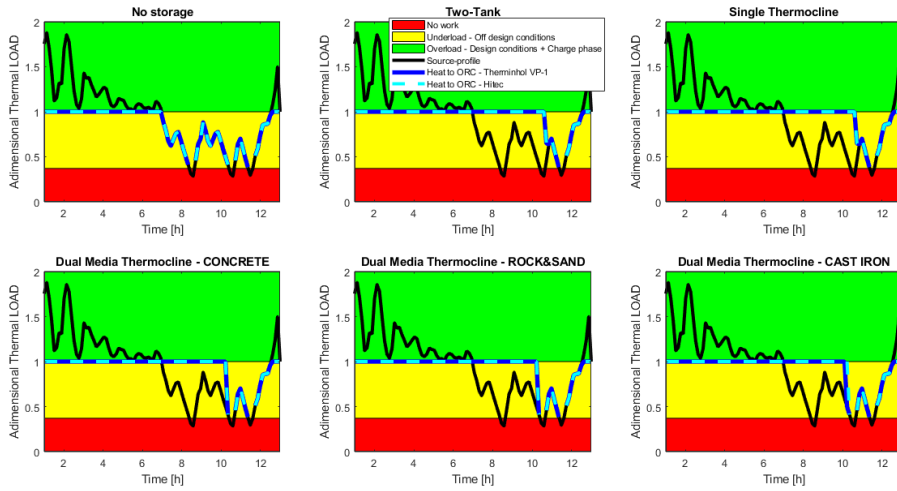


Figure 36 - Comparisons of the work conditions with/without storage in terms of Thermal Load in different configurations – SCENARIO 2

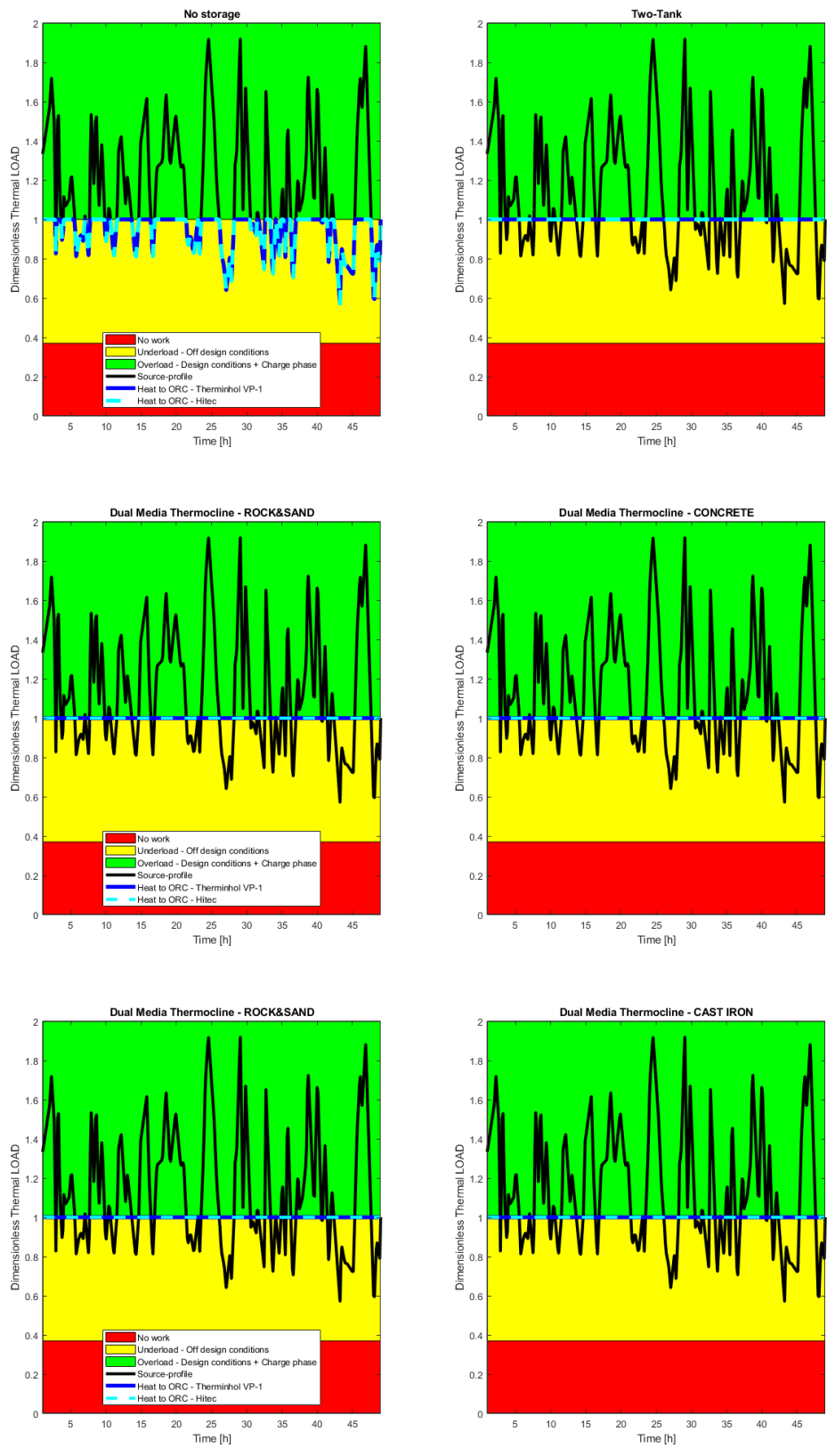


Figure 37 - Comparisons of the work conditions with/without storage in terms of Thermal Load in different configurations – SCENARIO 3

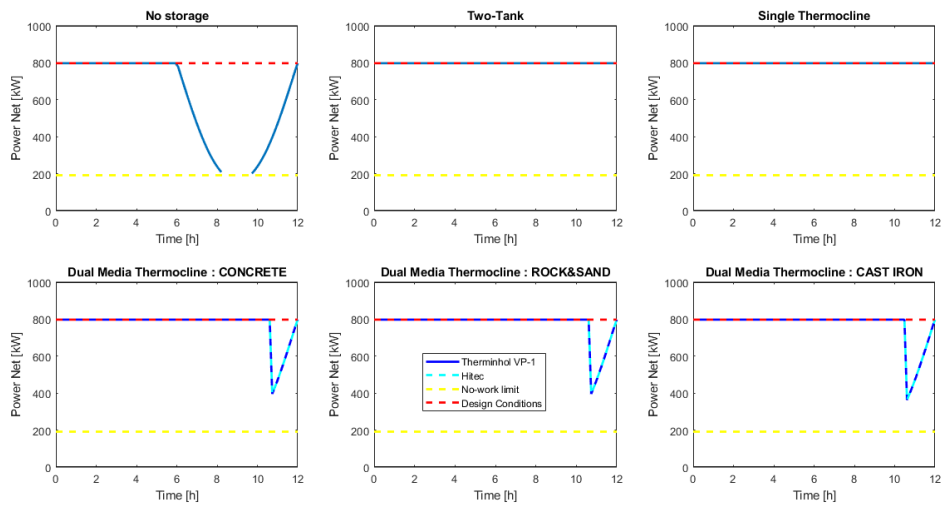


Figure 38 - Comparisons of POWER NET with/without storage in different configurations – SCENARIO 1

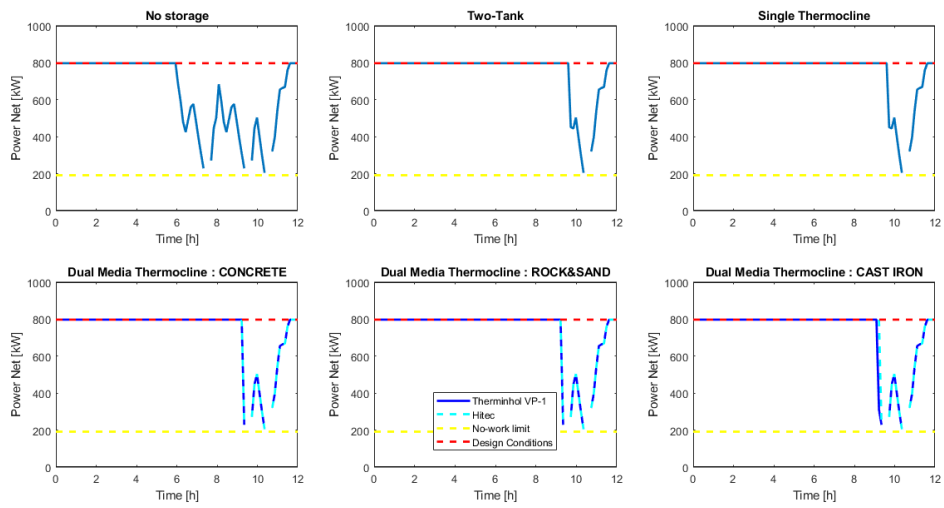


Figure 39 - Comparisons of POWER NET with/without storage in different configurations – SCENARIO 2

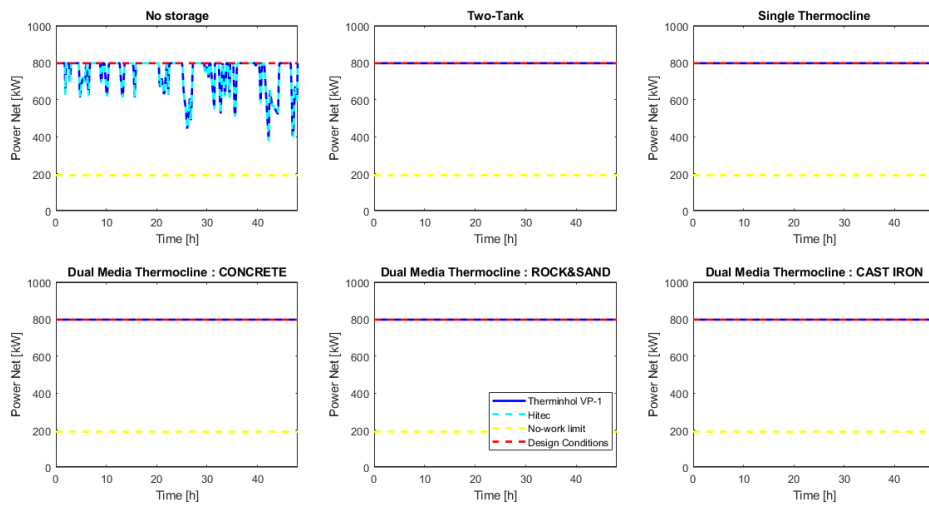


Figure 40 - Comparisons of POWER NET with/without storage in different configurations – SCENARIO 3

5.4 ORC's analysis

The core of the energetic system under investigation is the ORC. A proper explanation and analysis of the main parameters of it is necessary and could explain the achievements and improvements of introducing a TES in the plant. The first parameter to define the ORC performances is its efficiency defined as :

$$\eta_{ORC} = \frac{W_{net}}{Q_{evap}} \quad 5.10$$

Following the results obtained for the simulations of all the cases-studio.

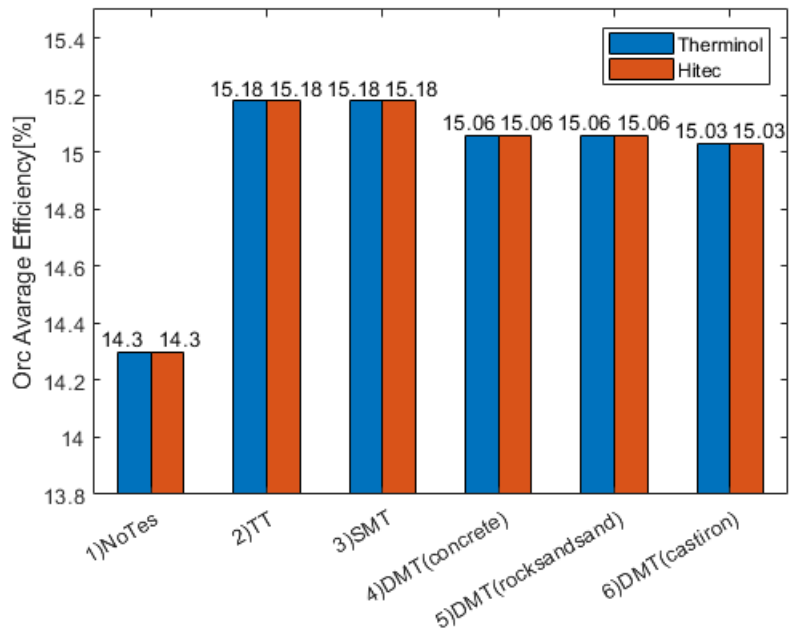


Figure 41 - Orc average efficiency for different configurations – SCENARIO 1

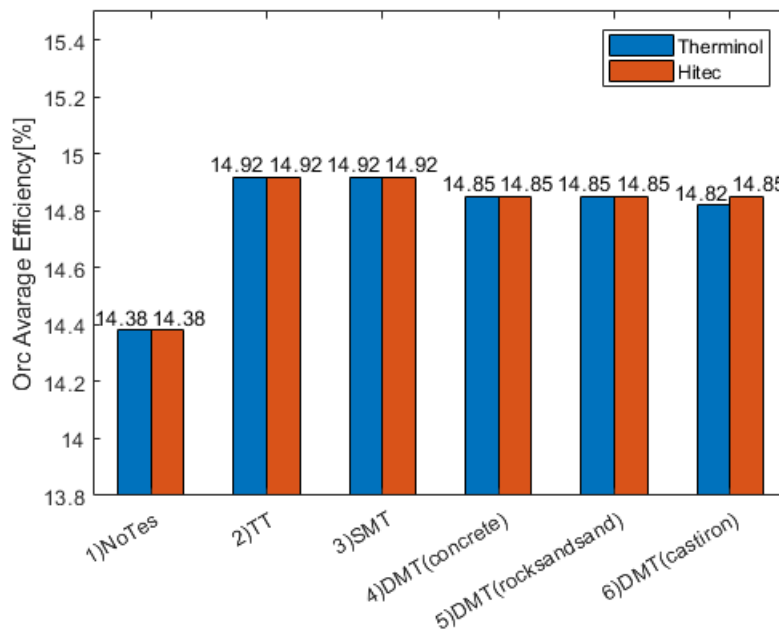


Figure 42 - Orc average efficiency for different configurations – SCENARIO 2

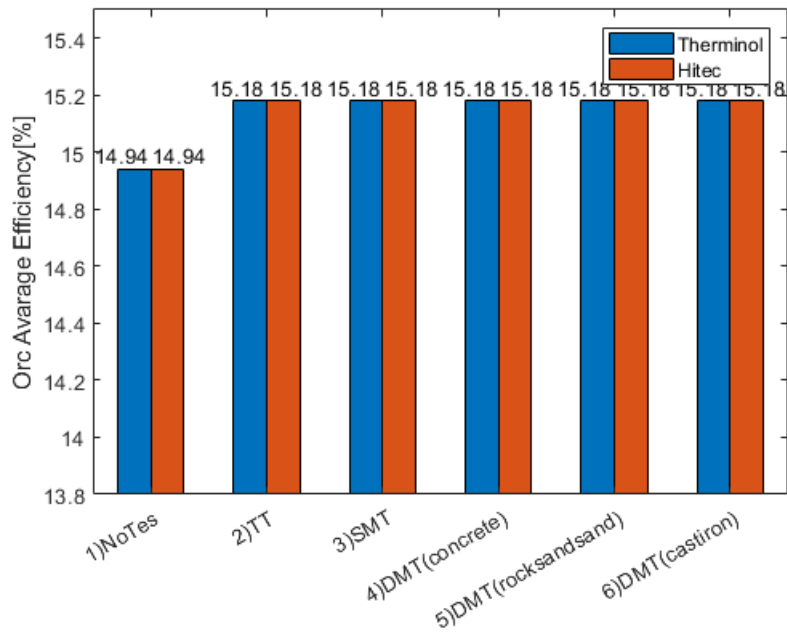


Figure 43 - Orc average efficiency for different configurations – SCENARIO 3

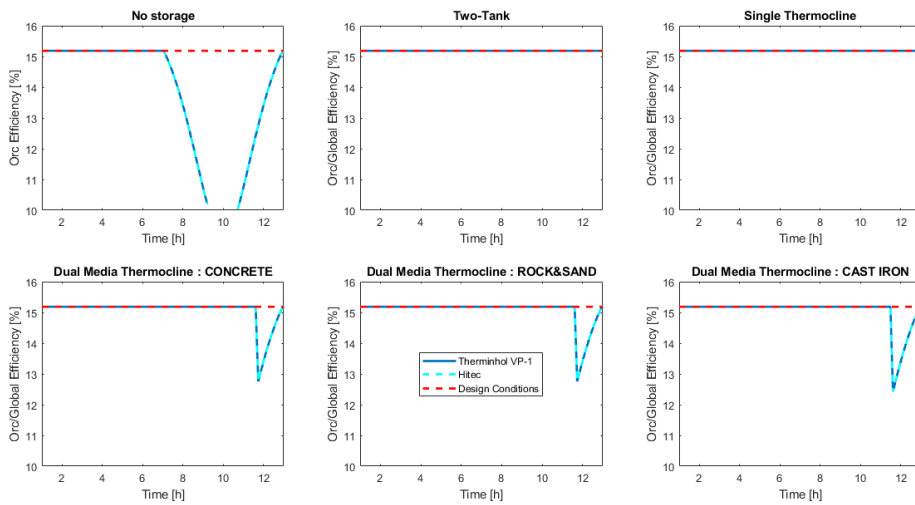


Figure 44 - Orc Efficiency trend along the time analysis – SCENARIO 1

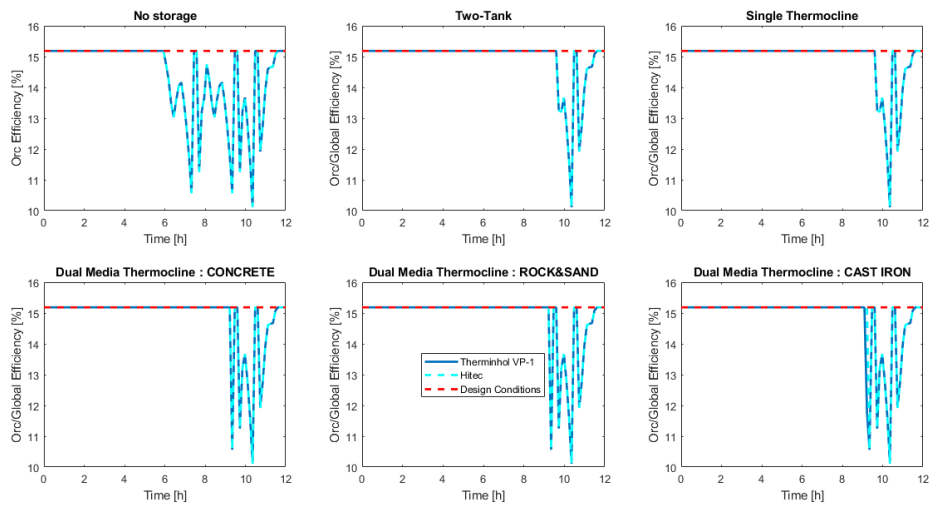


Figure 45 - Orc Efficiency trend along the time analysis – SCENARIO 2

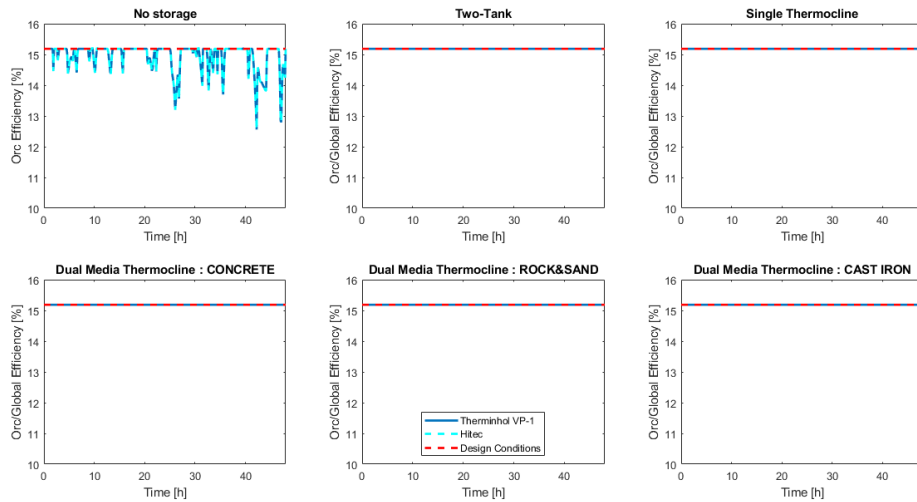


Figure 46 - Orc Efficiency trend along the time analysis – SCENARIO 3

Special mention is required for the different behavior of global efficiency, which is a factor of proper utilization of the source, defined as :

$$\eta_{glob} = \frac{W_{net}}{Q_{source}} \quad 5.11$$

As shown clearly from the trends along with the time analysis presented in the previous figures, the ORC and GLOBAL efficiencies for cases with the storages are the same values (because during the OVERLOAD phase the surplus of heat is charged in the storage so there is no waste of the source). To better understand the best utilization of the source the next

graph presents the trend of those parameters for the NO STORAGE CASE. The figure underlines the deviation of those values respect to the best conditions.

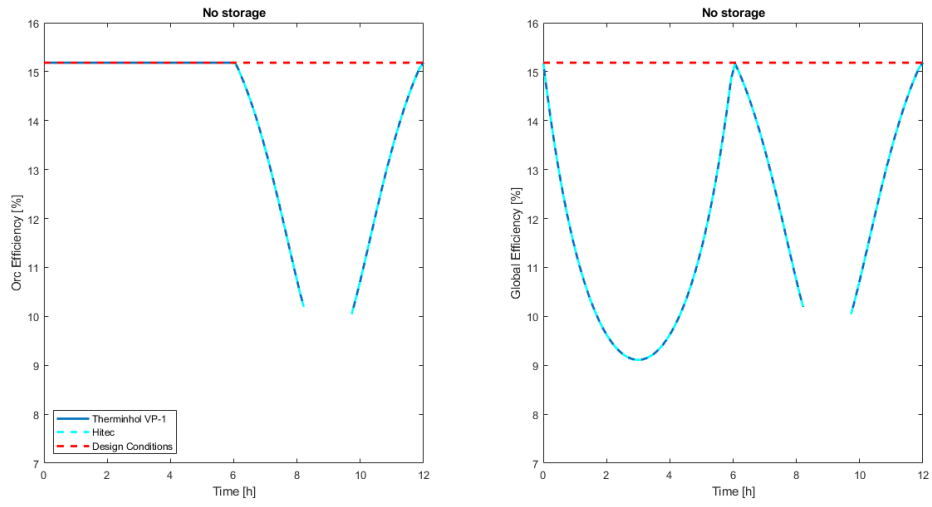


Figure 47 - No storage case, ORC and GLOBAL efficiency comparisons – SCENARIO 1

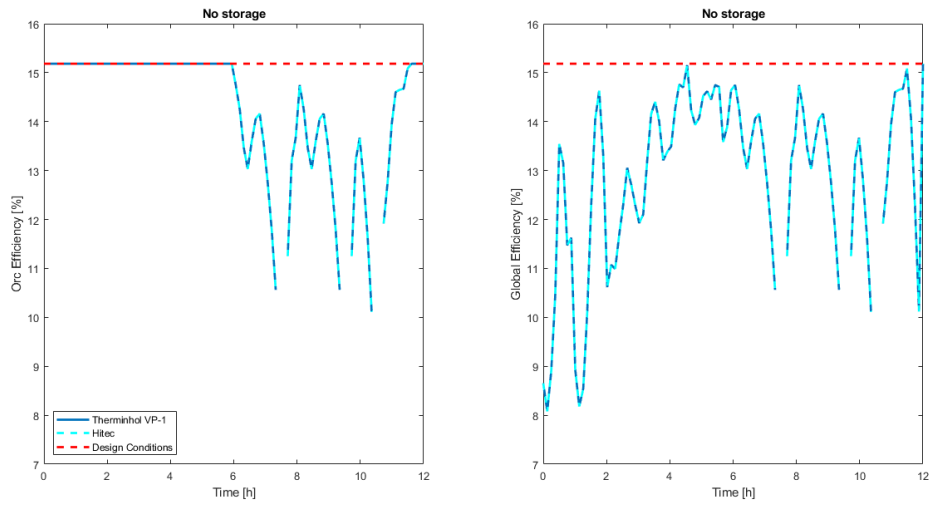


Figure 48 - No storage case, ORC and GLOBAL efficiency comparisons – SCENARIO 2

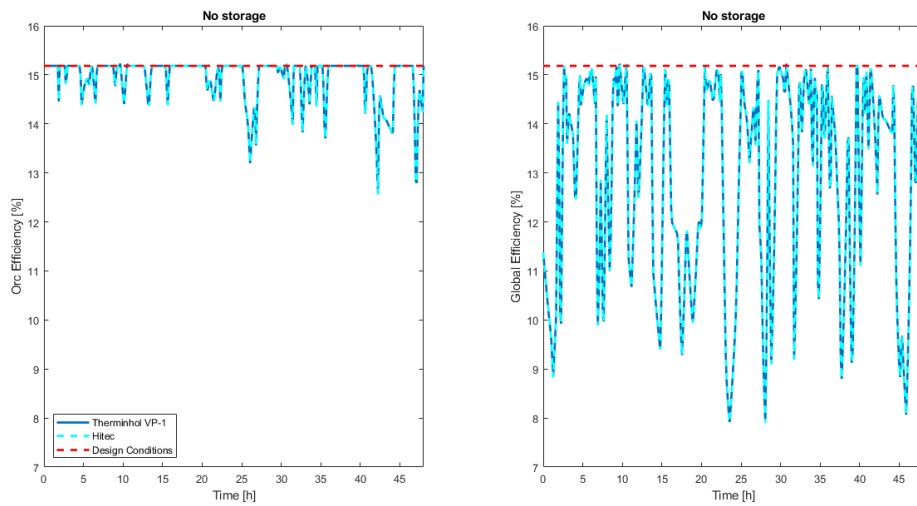


Figure 49 - No storage case, ORC and GLOBAL efficiency comparisons – SCENARIO 3

As direct consequences of the higher general value of the efficiencies of the cycle, good results have been achieved in terms of electrical output at the turbine. Following the presentation of the Power Net at the turbine (take in account the production of the turbine minus the amount of electricity required at the pump of the ORC, adding the losses due to the mechanical efficiency of the system). As appears clear from the graph there is a relevant gap in terms of electrical energy on daily time analysis, following representation of that surplus of production on yearly scale supposing the availability of 12hours per 360day/year for all Scenarios (So the Scenario 3 has been considered as a 3 days-analysis). Also, a trend of the Power Net production along the daily time analysis is provided.

Scenario 1

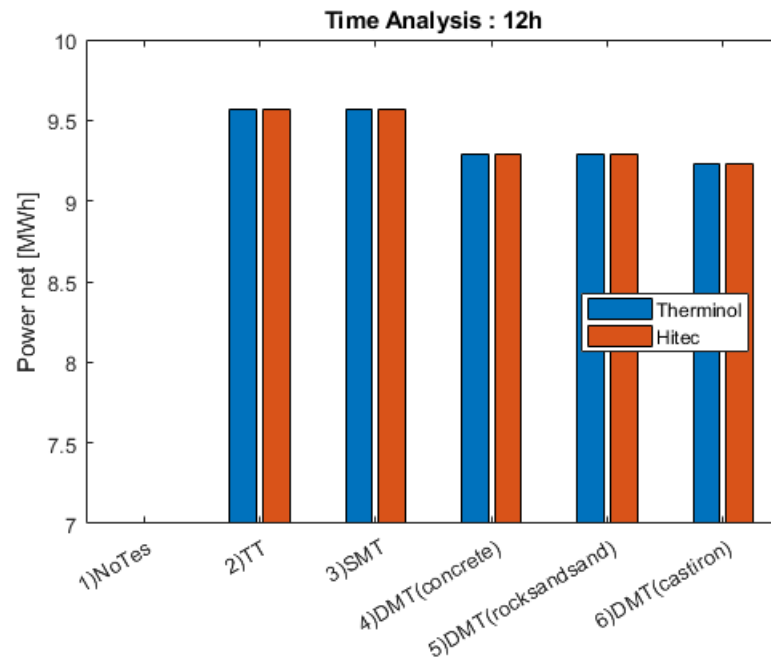


Figure 50 - Electrical energy production on daily time analysis – SCENARIO 1

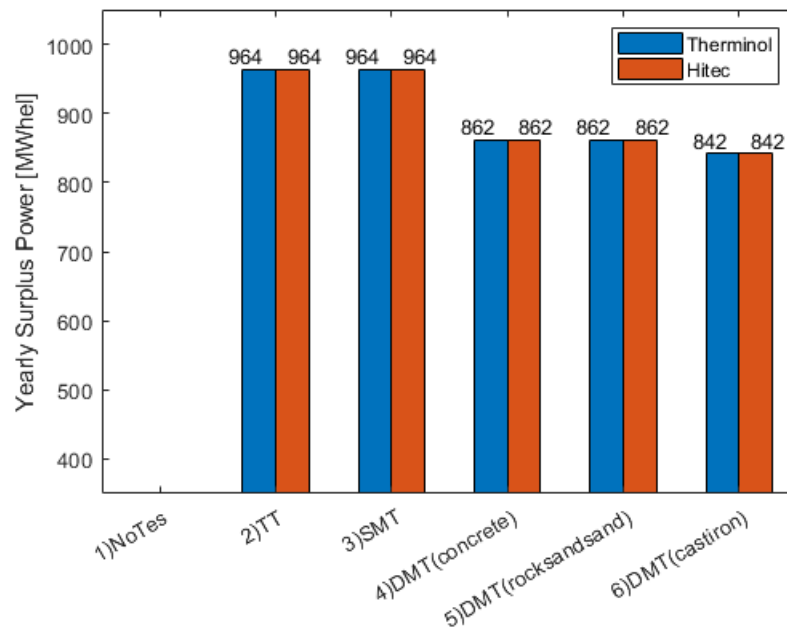


Figure 51 - Surplus of Electrical power production on yearly time-analysis - SCENARIO 1

Scenario 2

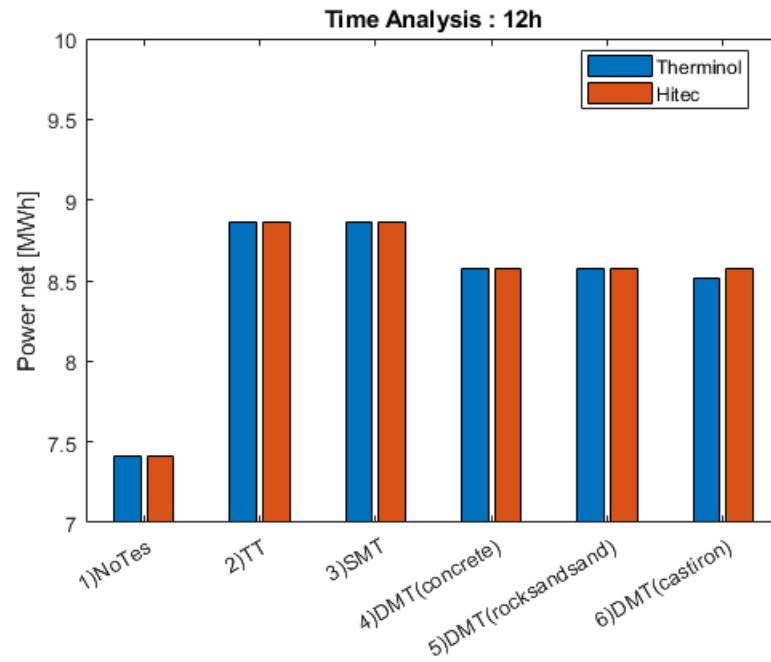


Figure 52- Electrical energy production on daily time analysis – SCENARIO 2

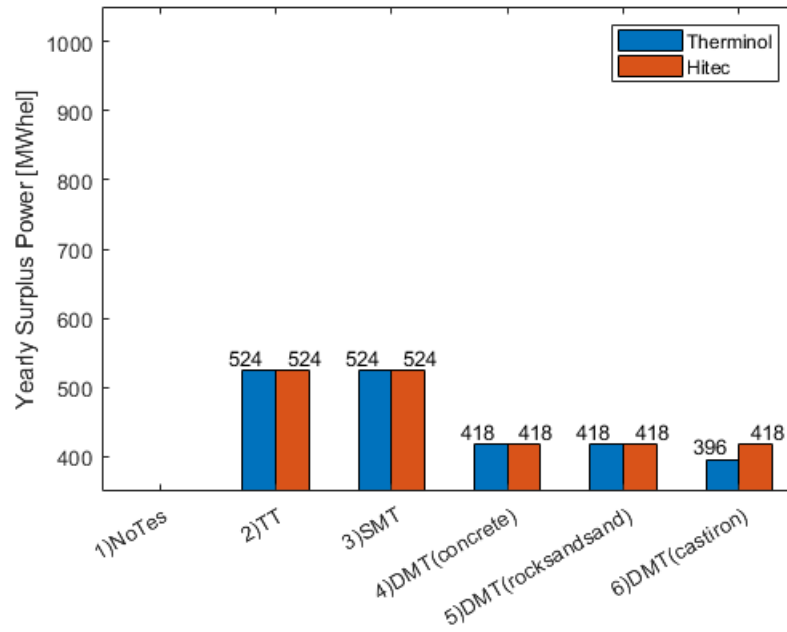


Figure 53 - Surplus of Electrical power production on yearly time-analysis - SCENARIO 2.

Scenario 3

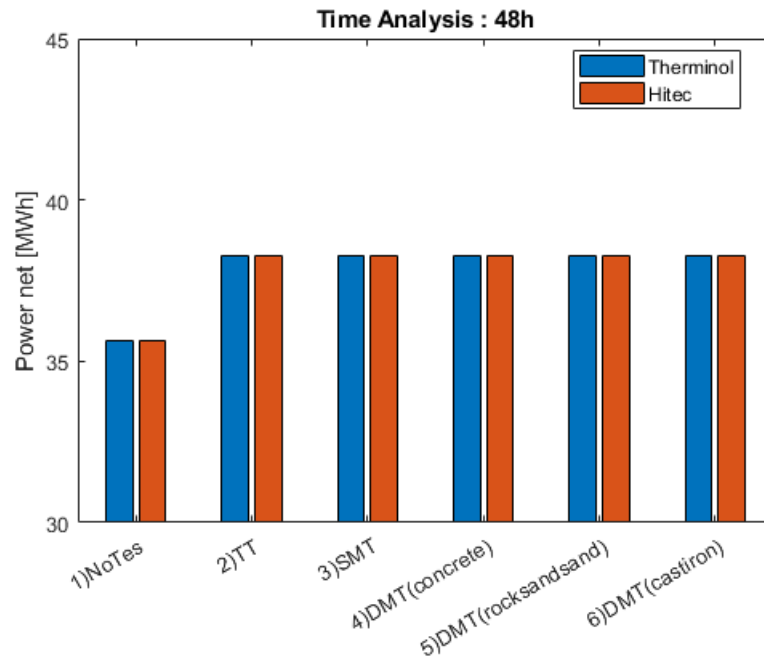


Figure 54 - Electrical energy production on daily time analysis – SCENARIO 3

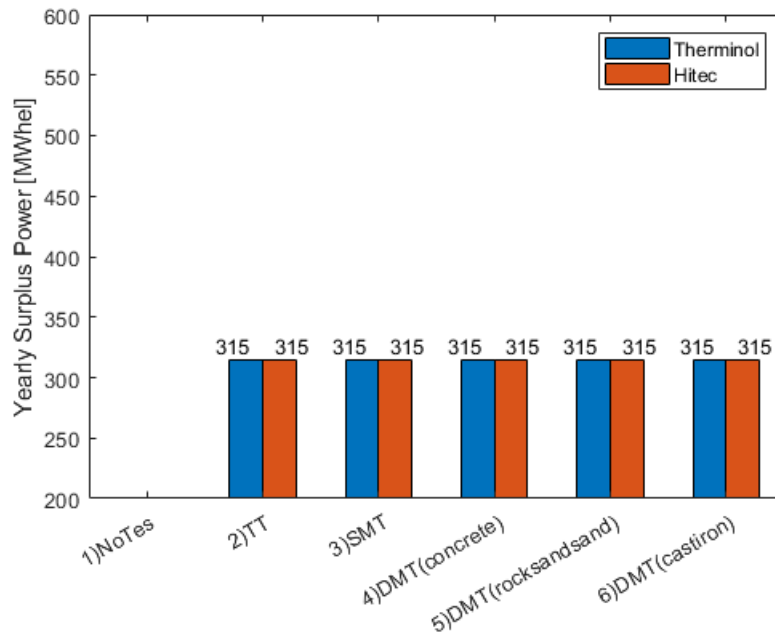


Figure 55 - Surplus of Electrical power production on yearly time-analysis - SCENARIO 3

The thermodynamic behavior of the plant is strictly related to the model of the turbine which can be considered as the key component of the cycle. The model has been developed in environment MatLab&EES as explained with the governing equations at 2.2.2 Turbine. A well-established way to model the turbine is through the deviation of the isentropic efficiency of it, that for this work has been modified also through the polytropic efficiency. Following the results obtained :

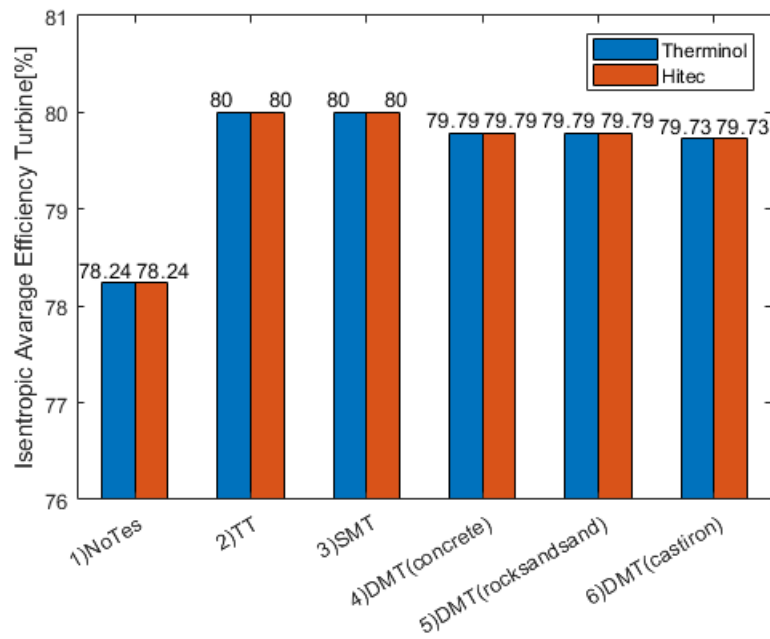


Figure 56 - Isentropic average efficiency Turbine – SCENARIO 1

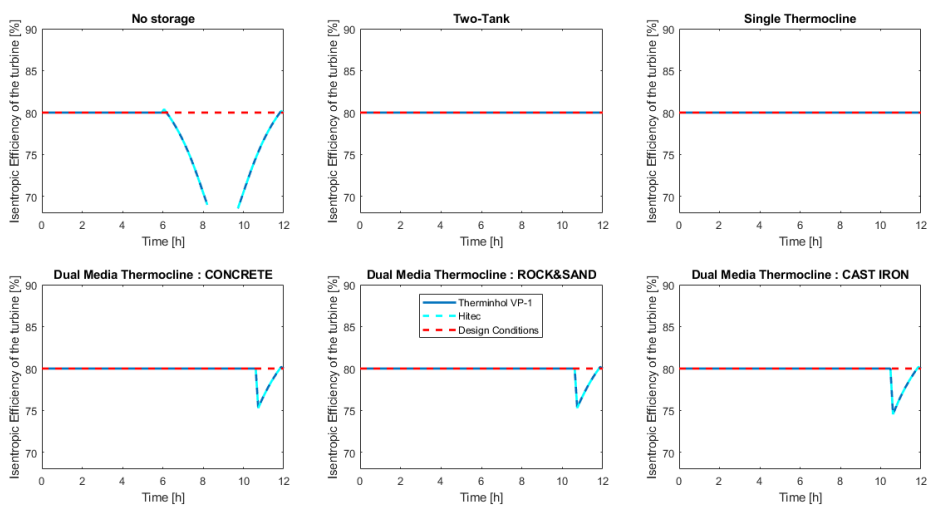


Figure 57 - Trend of isentropic efficiency of the turbine – SCENARIO 1

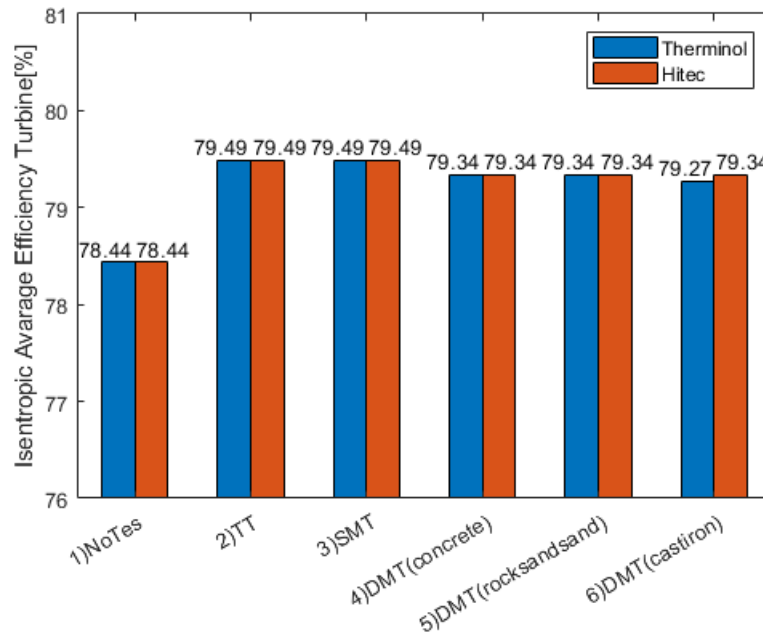


Figure 58 - Isentropic average efficiency Turbine – SCENARIO 2

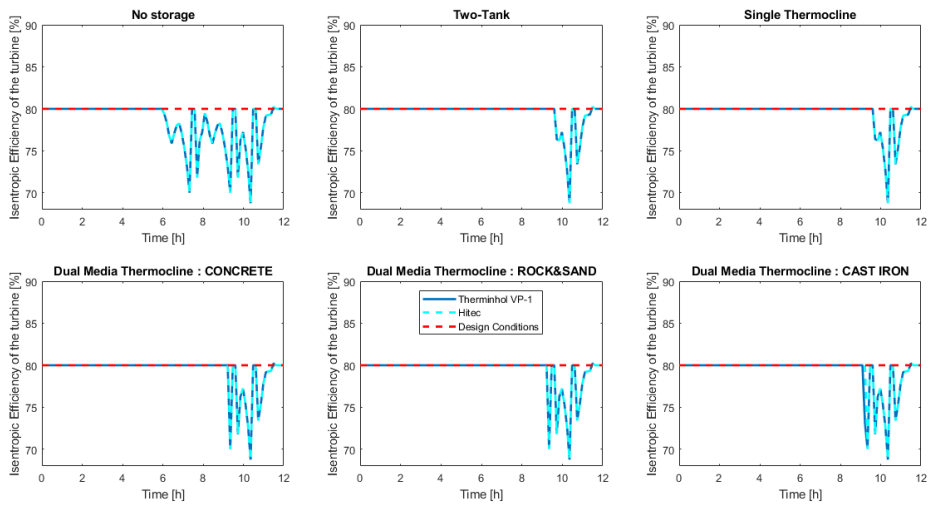


Figure 59 - Trend of isentropic efficiency of the turbine – SCENARIO 2

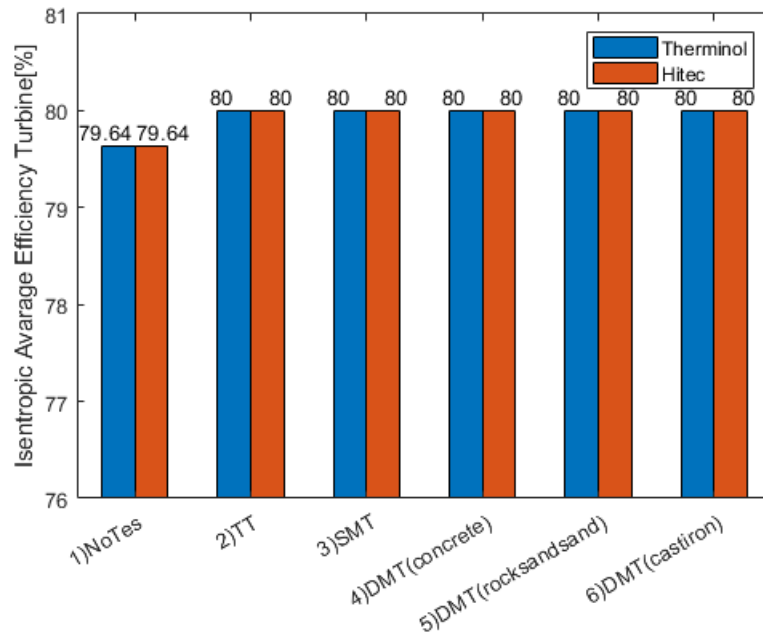


Figure 60 - Isentropic average efficiency Turbine – SCENARIO 3

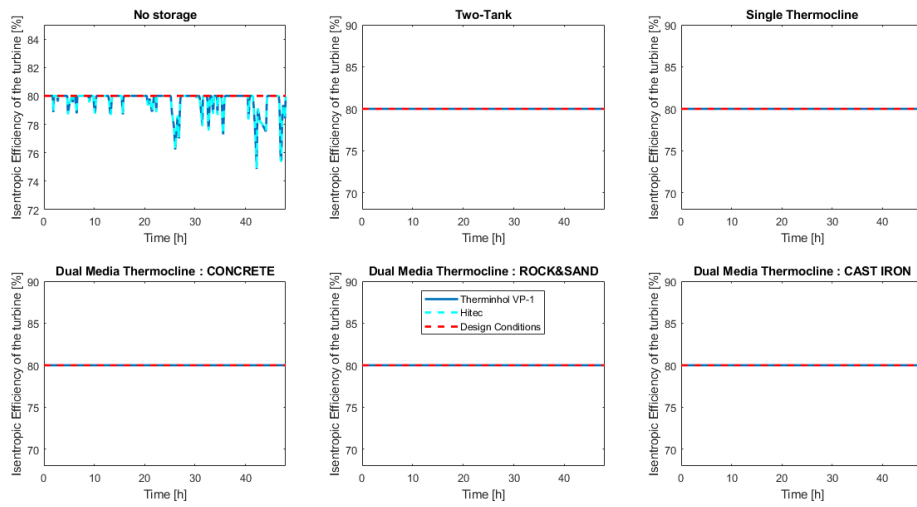


Figure 61 - Trend of isentropic efficiency of the turbine – SCENARIO 3

5.5 Exergy's results of the plant

Exergy analysis is a necessary tool to evaluate the performance of a thermal system. The governing equations are reported in Exergy's analysis. Following the breakdown of the destruction of exergy along with the component of the ORC, per each scenario.

Scenario 1

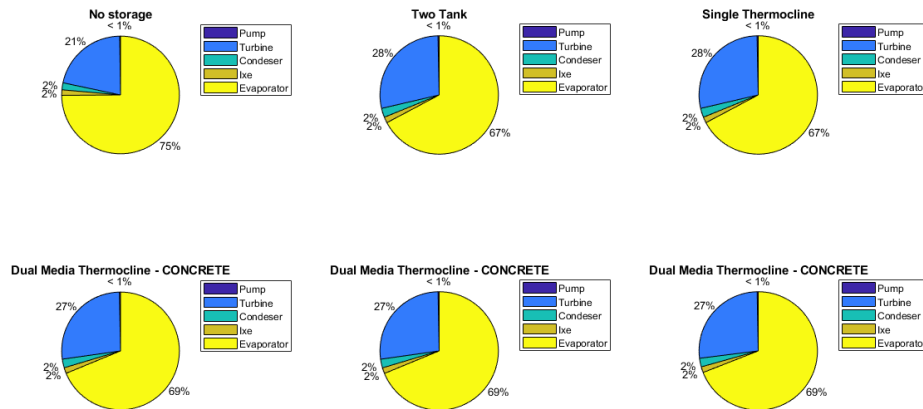


Figure 62 - Destruction of exergy breakdown - SCENARIO 1

Scenario 2

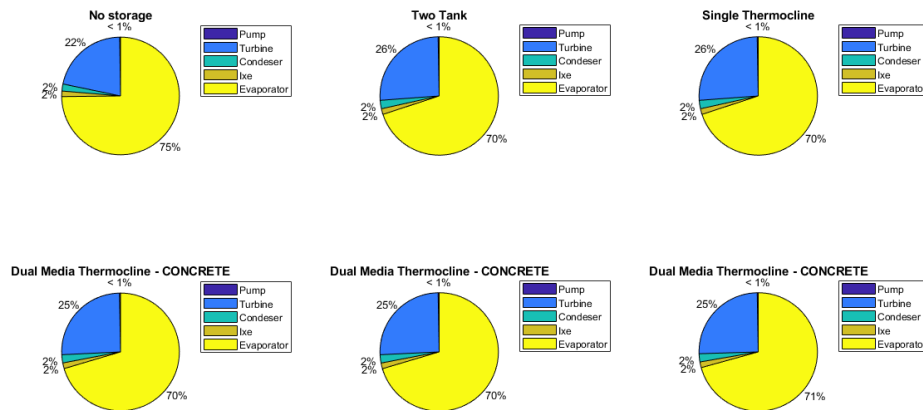


Figure 63 - Destruction of exergy breakdown - SCENARIO 2

Scenario 3

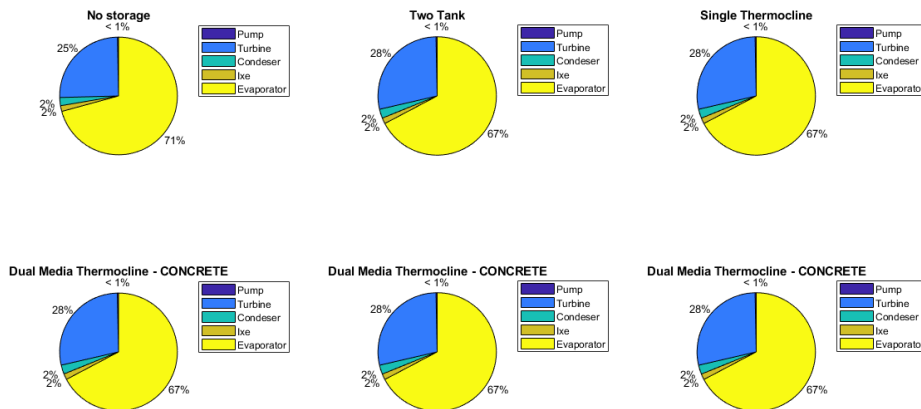


Figure 64 - Destruction of exergy breakdown - SCENARIO 3

The main results which come out from this analysis of the destruction of exergy in the plant are the dominant contribution of the evaporator. Emerge that if the target of the study is to tackle the exergy production of the plant, a most accurate model of the evaporator is required in order to understand the tuning of which parameters could reduce this aspect.

5.6 Techno-Economic Analysis

5.6.1 Cost analysis of the investment - LCOE & NCOTES evaluation

In a proper evaluation of an investment usually consider only the amount of the costs in €/€ is not enough; to obtain costs-results as much possible comparable the results are reported also divided by some thermodynamic variable in order to have results expandable to different energetic systems, in terms of field of application or size as well.

Here the breakdown of the costs for the production of the TESs. The equation used to evaluate them are reported in 4.2. Following tables referred to all the configurations considered in this work.

Scenario 1

Table 17 - Breakdown of the costs of TESs – THERMINOL VP1 - SCENARIO 1

Cost BreakDown of TES - THERMINOL VP-1 as HTF						
Type of System Factor)	(Void	Two-Tank (1)	SMT (1)	DMT(0.3)	DMT(0.3)	DMT(0.3)
Filler		-	-	CONCRETE	ROCKS&SAND	CAST IRON
Fluid material cost	[€]	469.667,57	469.667,57	171.606,63	174.846,21	117.876,04
Filler material cost	[€]	0,00	0,00	12.512,98	38.247,61	171.902,56
Insulation tank	[€]	18.229,19	9.114,60	11.100,94	11.310,50	7.625,20
Foundation tank	[€]	91.145,97	45.572,98	55.504,69	56.552,51	38.126,00
Pipes&Valves	[€]	22.503,83	11.251,91	11.251,91	11.251,91	11.251,91
Instrumental Control	[€]	2.382,76	2.382,76	2.382,76	2.382,76	2.382,76
Pump Molten Salt	[€]	19.856,32	19.856,32	19.856,32	19.856,32	19.856,32
HX1 moltensalt/steam	[€]	302.536,02	302.536,02	167.061,51	167.061,51	167.061,51
HX2 steam/moltensalt	[€]	388.080,90	388.080,90	180.059,07	180.059,04	180.060,25
Total cost	[€]	1.314.403	1.248.463	631.337	661.568	716.143
Specific Cost *	[€/kWth]	99,29	94,31	47,69	49,98	54,10

Table 18 - Breakdown of the costs of TESs –HITEC - SCENARIO 1

Cost BreakDown of TES - HITEC as HTF						
Type of System Factor)	(Void	Two-Tank (1)	SMT (1)	DMT(0.3)	DMT(0.3)	DMT(0.3)
Filler		-	-	CONCRETE	ROCKS&SAND	CAST IRON
Fluid material cost	[€]	188.848,36	188.848,36	143.461,82	145.465,56	107.150,66
Filler material cost	[€]	0,00	0,00	22.617,85	68.801,28	337.862,43
Insulation tank	[€]	7.497,67	3.748,83	9.492,88	9.625,47	7.090,17
Foundation tank	[€]	37.488,34	18.744,17	47.464,41	48.127,35	35.450,84
Pipes&Valves	[€]	22.503,83	11.251,91	11.251,91	11.251,91	11.251,91
Instrumental Control	[€]	2.382,76	2.382,76	2.382,76	2.382,76	2.382,76
Pump Molten Salt	[€]	19.856,32	19.856,32	19.856,32	19.856,32	19.856,32
HX1 moltensalt/steam	[€]	302.536,02	302.536,02	167.061,51	167.061,51	167.061,51
HX2 steam/moltensalt	[€]	388.080,90	388.080,90	180.058,82	180.058,81	180.059,55
Total cost	[€]	969.194	935.449	603.648	652.631	868.166
Specific Cost *	[€/kWth]	73,22	70,67	45,60	49,30	65,58

* Specific cost referred to the thermal capacity of the storage equal to 13238 kWth.

Scenario 2

Table 19 - Breakdown of the costs of TESs – THERMINOL VP1 - SCENARIO 2

Cost BreakDown of TES - THERMINOL VP-1 as HTF						
Type of System Factor)	(Void	Two-Tank (1)	SMT (1)	DMT(0.3)	DMT(0.3)	DMT(0.3)
Filler		-	-	CONCRETE	ROCKS&SAND	CAST IRON
Fluid material cost	[€]	299.806,12	285.524,84	94.027,87	95.802,92	64.587,44
Filler material cost	[€]	0,00	0,00	6.856,20	20.956,89	94.190,02
Insulation tank	[€]	11.636,37	5.541,03	6.082,50	6.197,33	4.178,05
Foundation tank	[€]	58.181,83	27.705,17	30.412,51	30.986,63	20.890,25
Pipes&Valves	[€]	13.680,74	6.840,37	6.840,37	6.840,37	6.840,37
Instrumental Control	[€]	1.448,55	1.448,55	1.448,55	1.448,55	1.448,55
Pump Molten Salt HX1	[€]	12.071,24	12.071,24	12.071,24	12.071,24	12.071,24
moltensalt/steam HX2	[€]	307.210,67	307.210,67	183.161,08	183.161,08	183.161,08
steam/moltensalt	[€]	407.518,03	407.518,03	185.076,13	185.076,09	185.077,43
Total cost	[€]	1.111.554	1.053.860	525.976	542.541	572.444
Specific Cost *	[€/kWth]	138,12	130,96	65,36	67,42	71,13

Table 20 - Breakdown of the costs of TESs – HITEC – SCENARIO 2

Cost BreakDown of TES - HITEC as HTF						
Type of System Factor)	(Void	Two-Tank (1)	SMT (1)	DMT(0.3)	DMT(0.3)	DMT(0.3)
Filler		-	-	CONCRETE	ROCKS&SAND	CAST IRON
Fluid material cost	[€]	120.548,86	114.806,51	78.606,57	79.704,47	58.710,71
Filler material cost	[€]	0,00	0,00	12.392,93	37.698,06	185.123,87
Insulation tank	[€]	4.786,04	2.279,03	5.201,40	5.274,05	3.884,89
Foundation tank	[€]	23.930,19	11.395,14	26.007,02	26.370,26	19.424,47
Pipes&Valves	[€]	13.680,74	6.840,37	6.840,37	6.840,37	6.840,37
Instrumental Control	[€]	1.448,55	1.448,55	1.448,55	1.448,55	1.448,55
Pump Molten Salt HX1	[€]	12.071,24	12.071,24	12.071,24	12.071,24	12.071,24
moltensalt/steam HX2	[€]	307.210,67	307.210,67	183.161,08	183.161,08	183.161,08
steam/moltensalt	[€]	407.518,03	407.518,03	185.075,80	185.075,79	185.076,62
Total cost	[€]	891.194	863.570	510.805	537.644	655.742
Specific Cost *	[€/kWth]	110,74	107,31	63,47	66,81	81,48

* Specific cost referred to the thermal capacity of the storage equal to 8047 kWth.

Scenario 3

Table 21 - Breakdown of the costs of TESs – THERMINOL VP-1 as HTF – SCENARIO 3

Cost BreakDown of TES - THERMINOL VP-1 as HTF						
Type of System Factor)	(Void	Two-Tank (1)	SMT (1)	DMT(0.3)	DMT(0.3)	DMT(0.3)
Filler		-	-	CONCRETE	ROCKS&SAND	CAST IRON
Fluid material cost	[€]	1.822.471,35	1.822.471,35	320.395,45	326.443,86	220.078,60
Filler material cost	[€]	0,00	0,00	23.362,17	71.409,59	320.947,96
Insulation tank	[€]	70.735,53	35.367,76	20.725,83	21.117,09	14.236,51
Foundation tank	[€]	353.677,64	176.838,82	103.629,16	105.585,47	71.182,54
Pipes&Valves	[€]	87.322,57	43.661,28	43.661,28	43.661,28	43.661,28
Instrumental Control	[€]	9.245,92	9.245,92	9.245,92	9.245,92	9.245,92
Pump Molten Salt HX1	[€]	77.049,32	77.049,32	77.049,32	77.049,32	77.049,32
moltensalt/steam HX2	[€]	307.871,24	307.871,24	188.663,58	188.663,58	188.663,58
steam/moltensalt	[€]	286.584,21	286.584,21	149.027,82	149.027,82	149.027,83
Total cost	[€]	3.014.958	2.759.090	935.761	992.204	1.094.094
Specific Cost *	[€/kWth]	26.45	24.21	8.21	8.71	9.60

Table 22 - Breakdown of the costs of TESs – HITEC – SCENARIO 3

Cost BreakDown of TES - HITEC as HTF						
Type of System Factor)	(Void	Two-Tank (1)	SMT (1)	DMT(0.3)	DMT(0.3)	DMT(0.3)
Filler		-	-	CONCRETE	ROCKS&SAND	CAST IRON
Fluid material cost	[€]	732.796,43	732.796,43	267.848,12	271.589,17	200.053,94
Filler material cost	[€]	0,00	0,00	42.228,31	128.454,34	630.800,70
Insulation tank	[€]	29.093,52	14.546,76	17.723,53	17.971,08	13.237,59
Foundation tank	[€]	145.467,62	72.733,81	88.617,67	89.855,40	66.187,93
Pipes&Valves	[€]	87.322,57	43.661,28	43.661,28	43.661,28	43.661,28
Instrumental Control	[€]	9.245,92	9.245,92	9.245,92	9.245,92	9.245,92
Pump Molten Salt HX1	[€]	77.049,32	77.049,32	77.049,32	77.049,32	77.049,32
moltensalt/steam HX2	[€]	307.871,24	307.871,24	188.663,58	188.663,58	188.663,58
steam/moltensalt	[€]	286.584,21	286.584,21	149.027,81	149.027,81	149.027,82
Total cost	[€]	1.675.431	1.544.489	884.066	975.518	1.377.928
Specific Cost *	[€/kWth]	14.70	13.55	7.76	8.56	12.09

* Specific cost referred to the thermal capacity of the storage equal to 113958 kWth.

- As we can see there is a great reduction in terms of specific cost regarding the DMT configuration (around 50%) respect the traditional TT in constant in all the scenarios.
- In the calculation of the costs has been included also the heat exchanger needed to the correct work of the TES-loop that is a consistent component of the total (30%).
- Installation costs are not present in this calculation.

Scenario 1

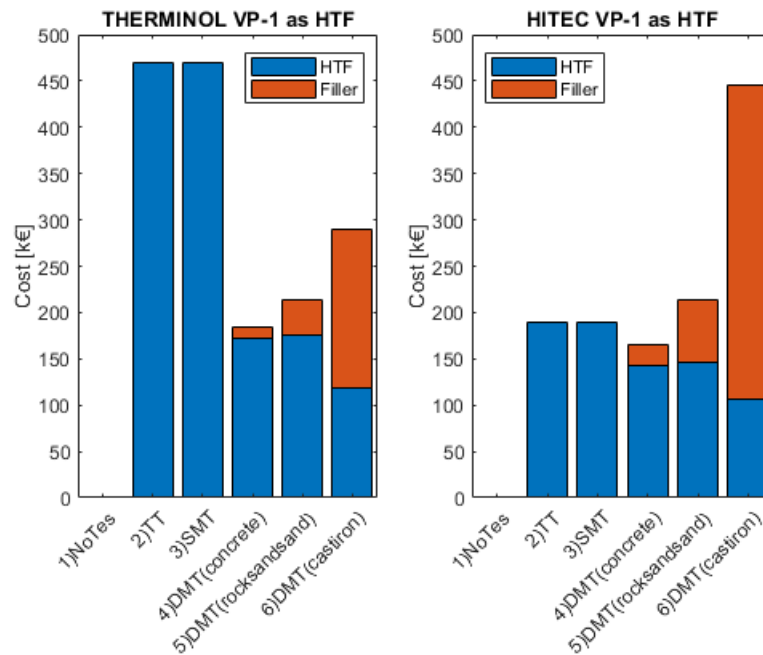


Figure 65 - Cost of the materials for the tank - Breakdown between HTF and Filler – SCENARIO 1

Next graph shows the cost of the storage divided by the thermal capacity of it, the result is a parameter [€/kWhth] which put in evidence a clear advantage of the DMT technology.

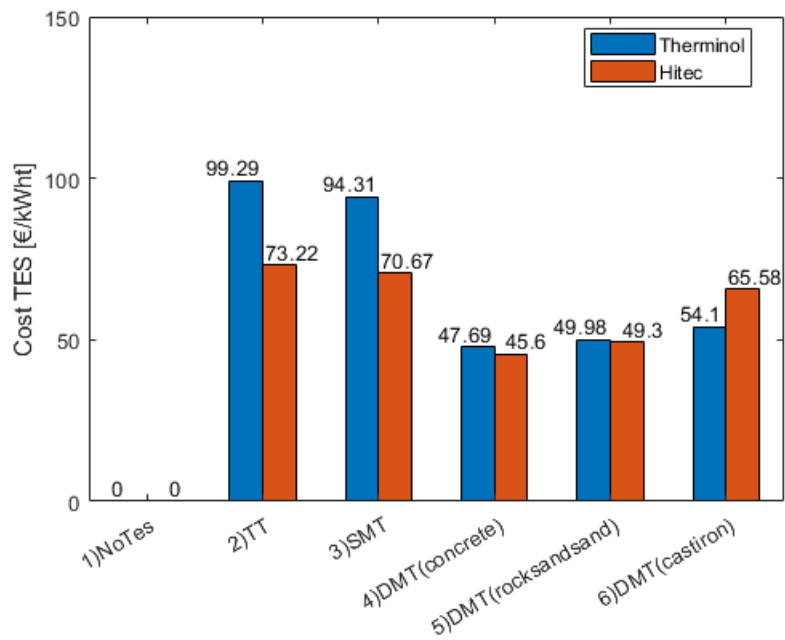


Figure 66 - Cost TES per kWhth of thermal energy storage capacity – SCENARIO 1

The LCOE and NCOTES obtained are now presented.

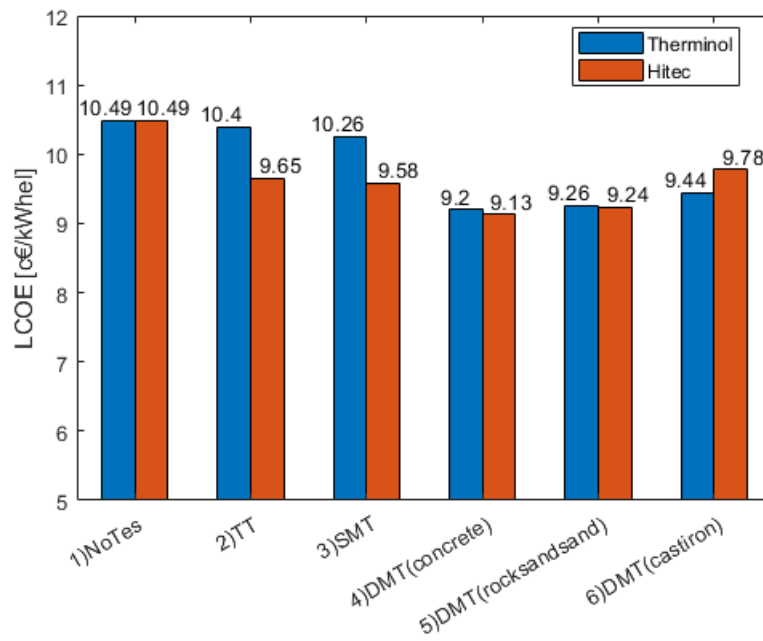


Figure 67 – LCOE results – SCENARIO 1

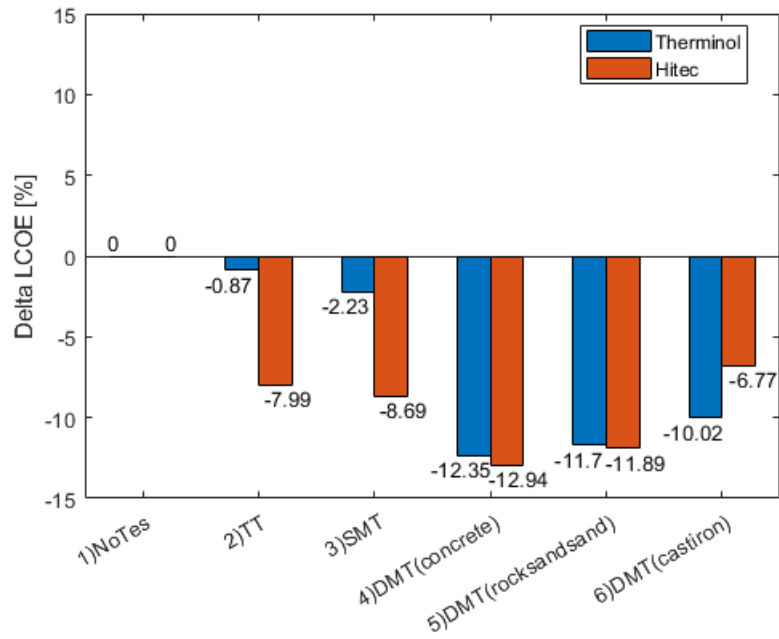


Figure 68 – Deviation of the LCOE respect the conditions without storage – SCENARIO 1

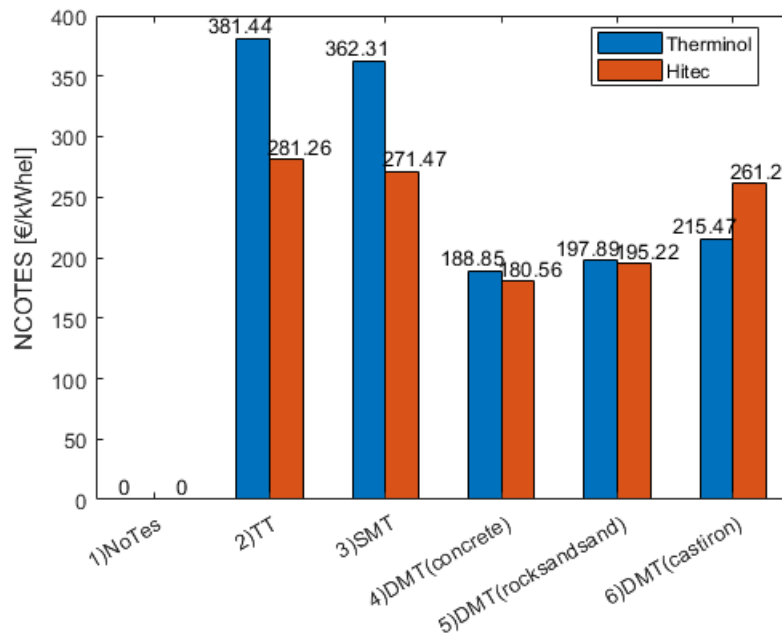


Figure 69 - NCOTES results – SCENARIO 1

Scenario 2

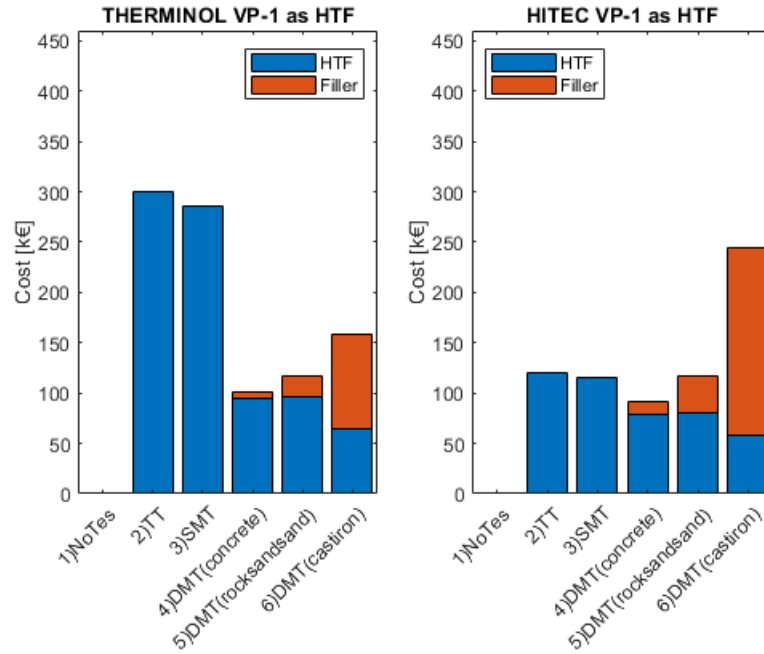


Figure 70 - Cost of the materials for the tank - Breakdown between HTF and Filler – SCENARIO 2

Next graph shows the cost of the storage divided by the thermal capacity of it, the result is a parameter [€/kWhth] which put in evidence a clear advantage of the DMT technology.

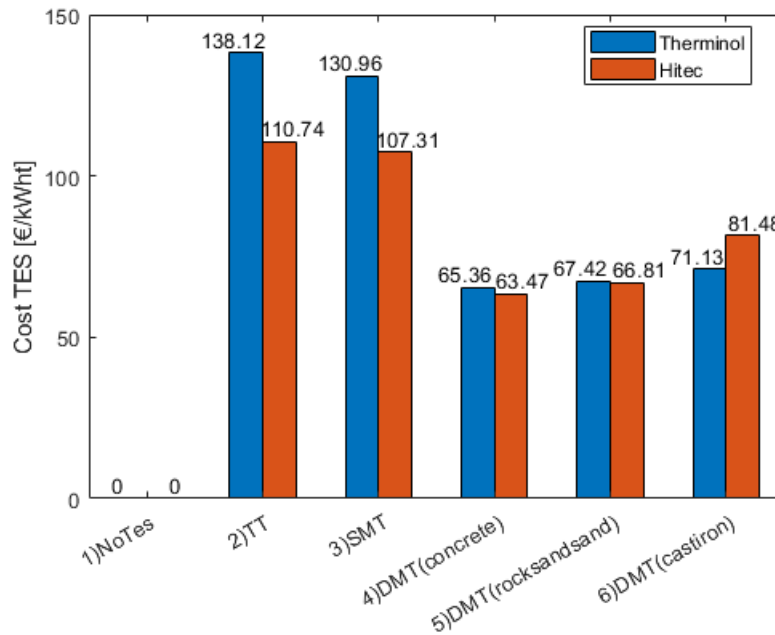


Figure 71 - Cost TES per kWhth of thermal energy storage capacity – SCENARIO 2

The LCOE and NCOTES obtained are now presented.

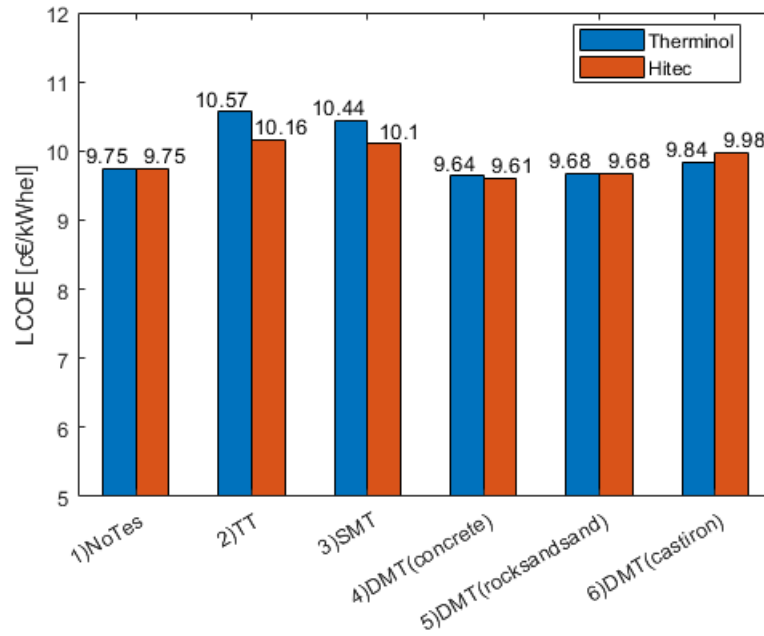


Figure 72 - LCOE results – SCENARIO 2

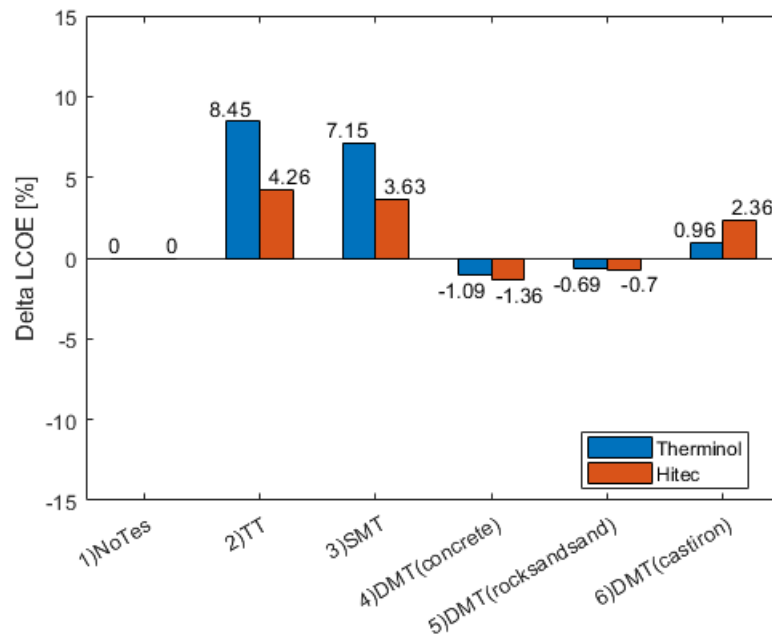


Figure 73 - Deviation of the LCOE respect the conditions without storage – SCENARIO 2

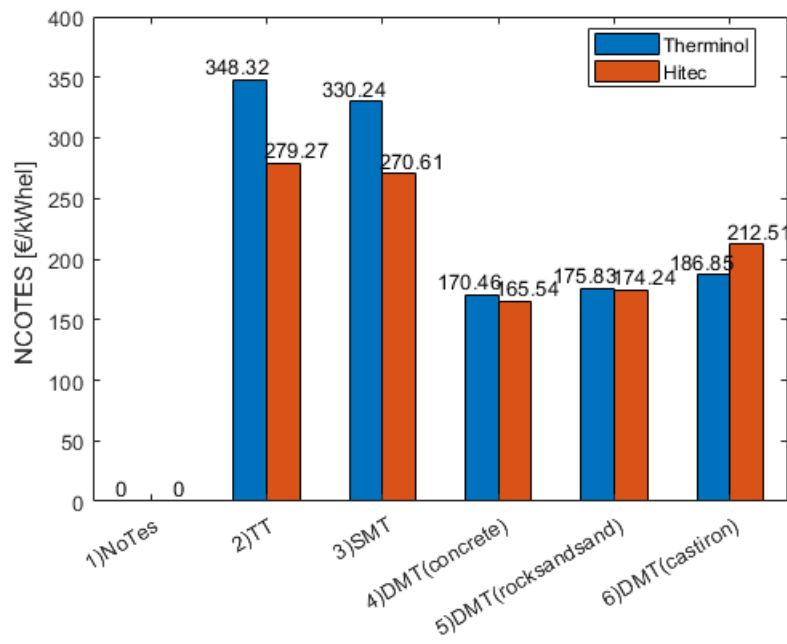


Figure 74 - NCOTES results – SCENARIO 2

Scenario 3

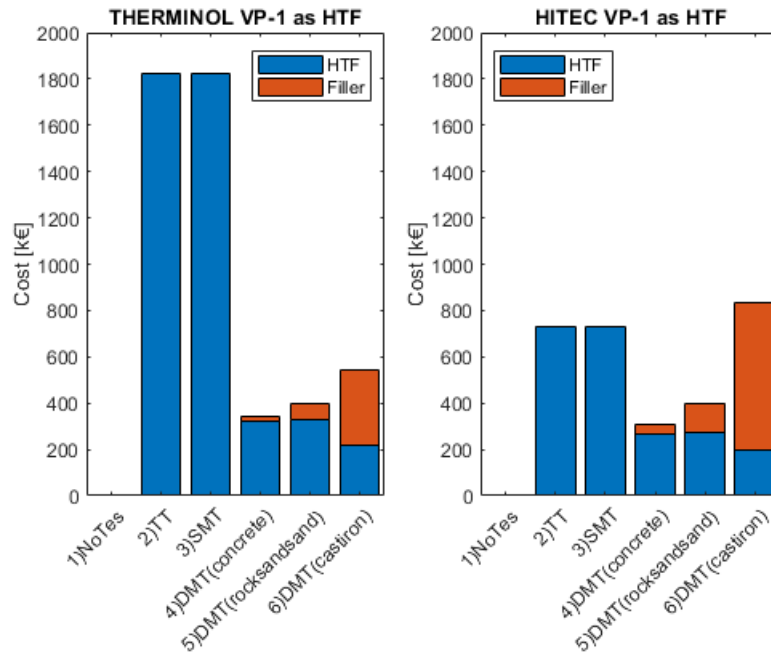


Figure 75 - Cost of the materials for the tank - Breakdown between HTF and Filler – SCENARIO 3

Next graph shows the cost of the storage divided by the thermal capacity of it, the result is a parameter [€/kWhth] which put in evidence a clear advantage of the DMT technology.

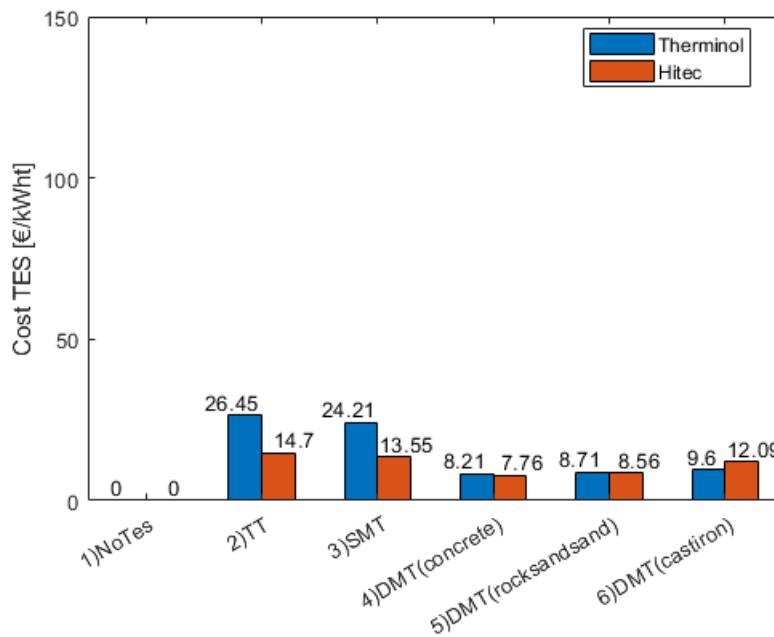


Figure 76 - Cost TES per kWhth of thermal energy storage capacity – SCENARIO 3

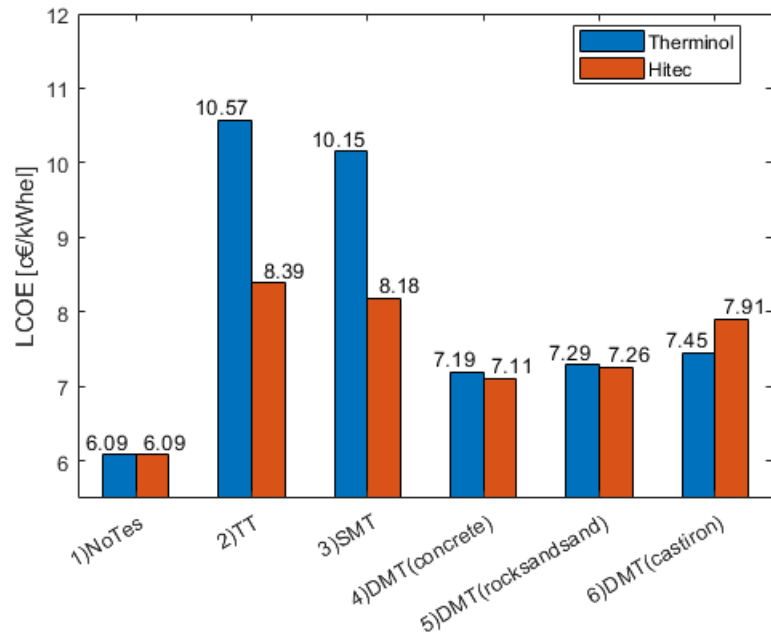


Figure 77 - LCOE results - SCENARIO 3

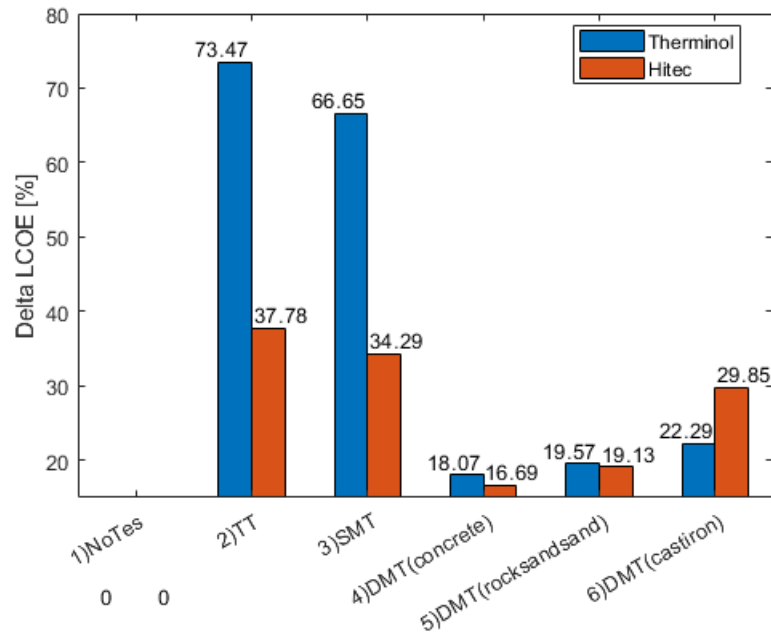


Figure 78 - Deviation of the LCOE respect the conditions without storage – SCENARIO 3

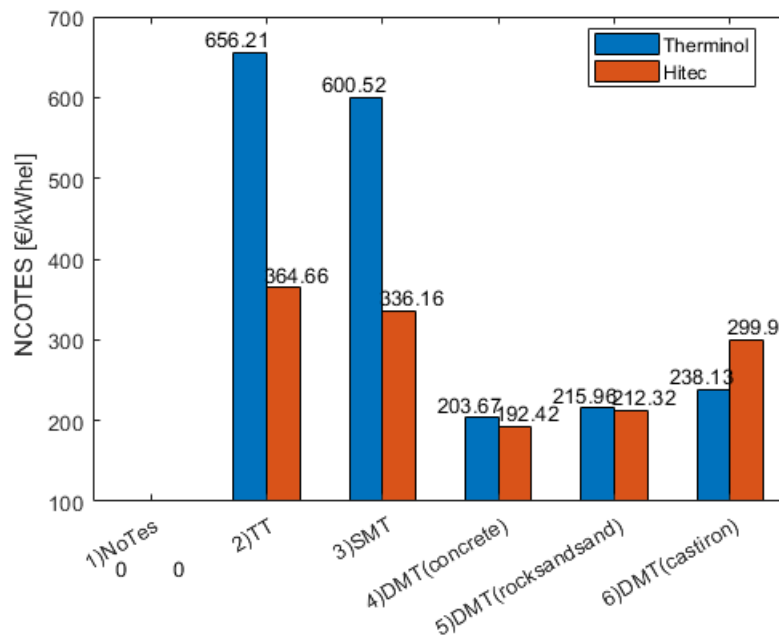


Figure 79 - NCOTES results - SCENARIO 3

5.6.2 Preliminary Study of the investment's feasibility - NPV & PBP evaluation

Scenario 1

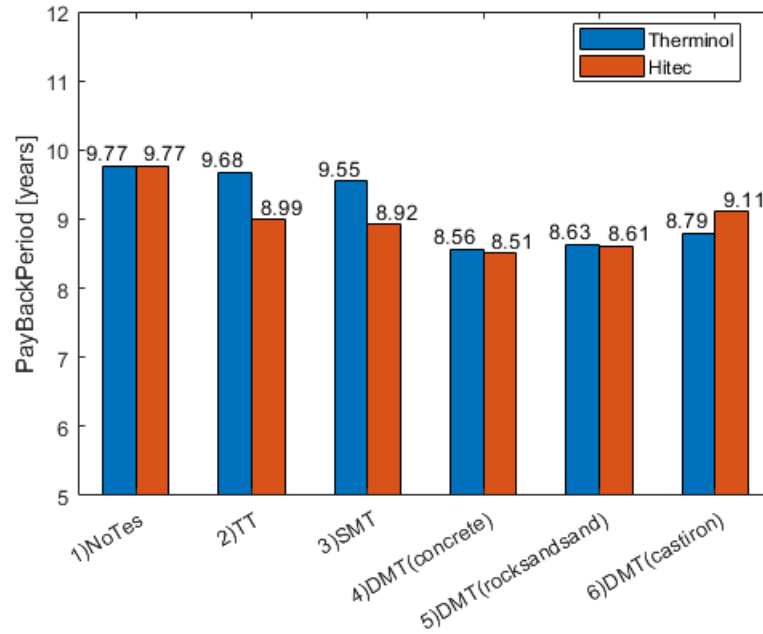


Figure 80 – Pay Back Period results - SCENARIO 1

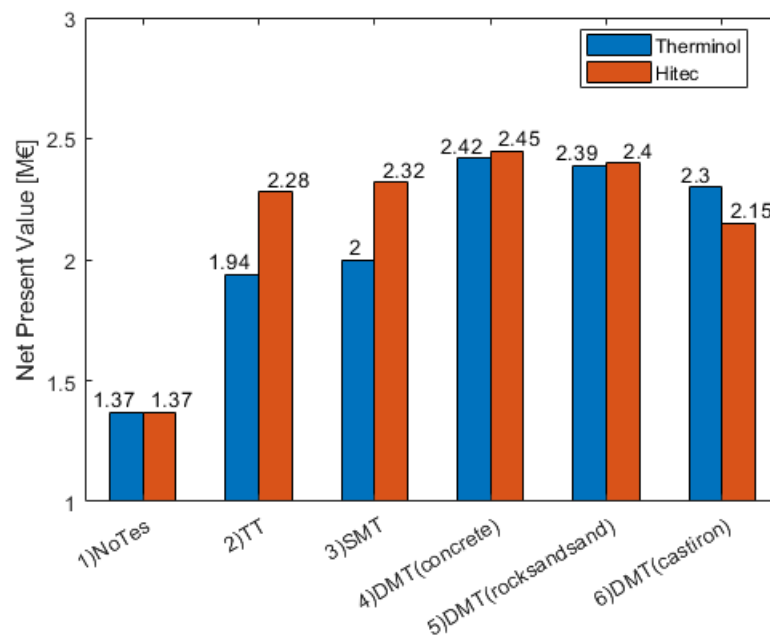


Figure 81 - Net Present Value – SCENARIO 1

Scenario 2

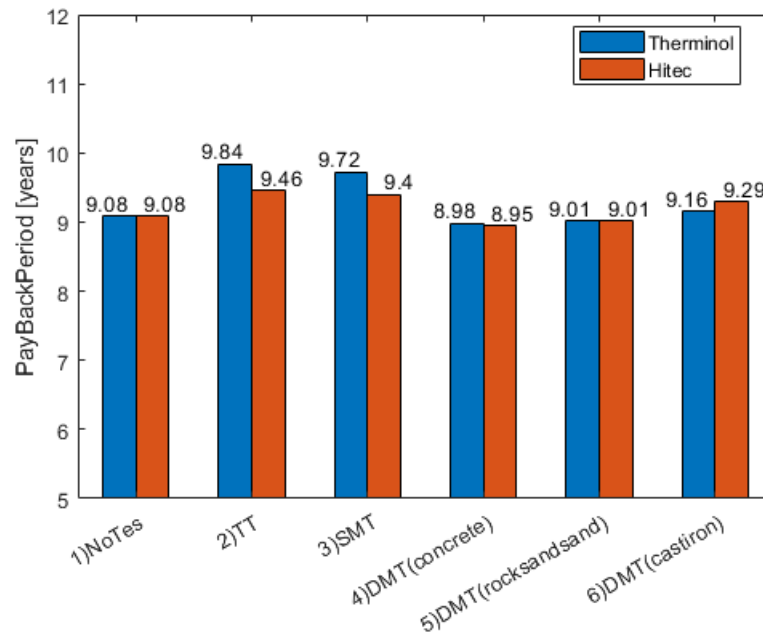


Figure 82 – Pay Back Period results - SCENARIO 2

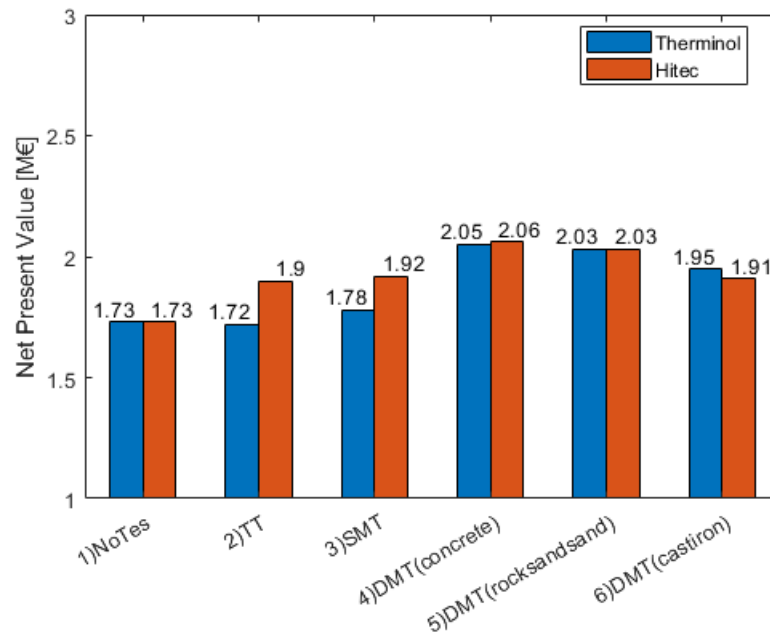


Figure 83 - Net Present Value – SCENARIO 2

Scenario 3

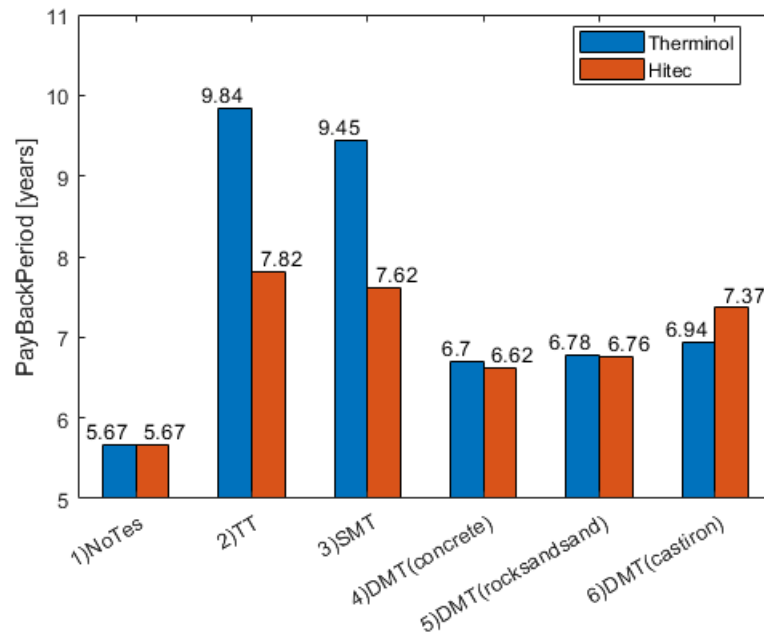


Figure 84 - Pay Back Period results - SCENARIO 3

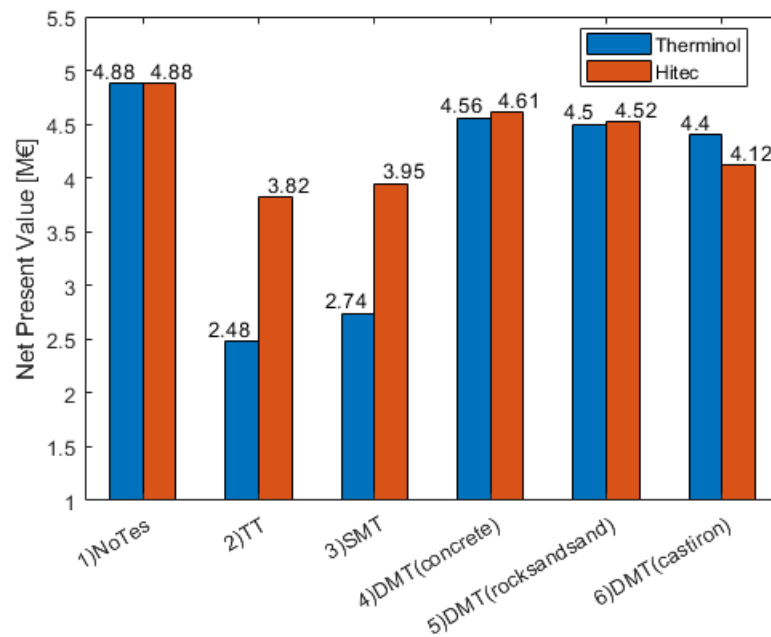


Figure 85 – Net Present Value – SCENARIO 3

5.6.3 Utilisation of the TES

Scenario 1

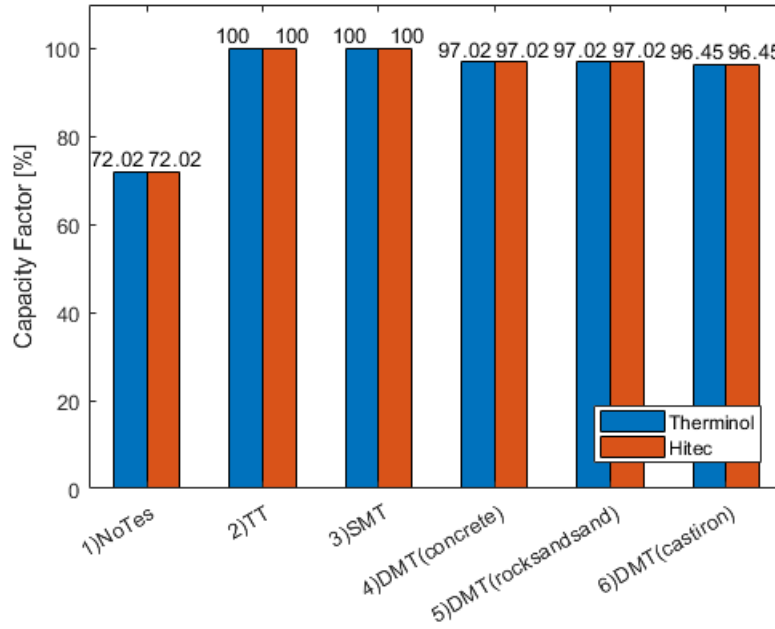


Figure 86 - Capacity factor - Results - SCENARIO 1

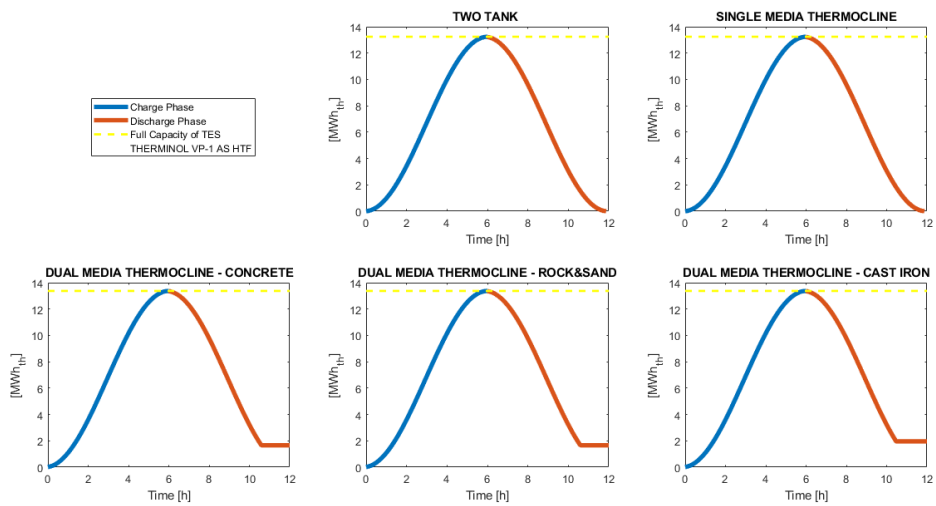


Figure 87 - State of the TESs - Therminol VP-1 - SCENARIO 1

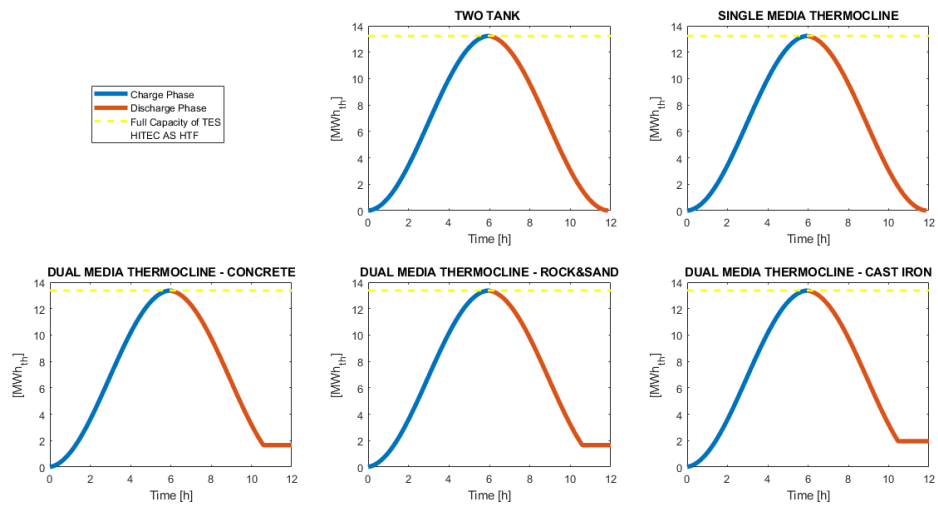


Figure 88 - State of the TESs - Hitec - SCENARIO 1

Scenario 2

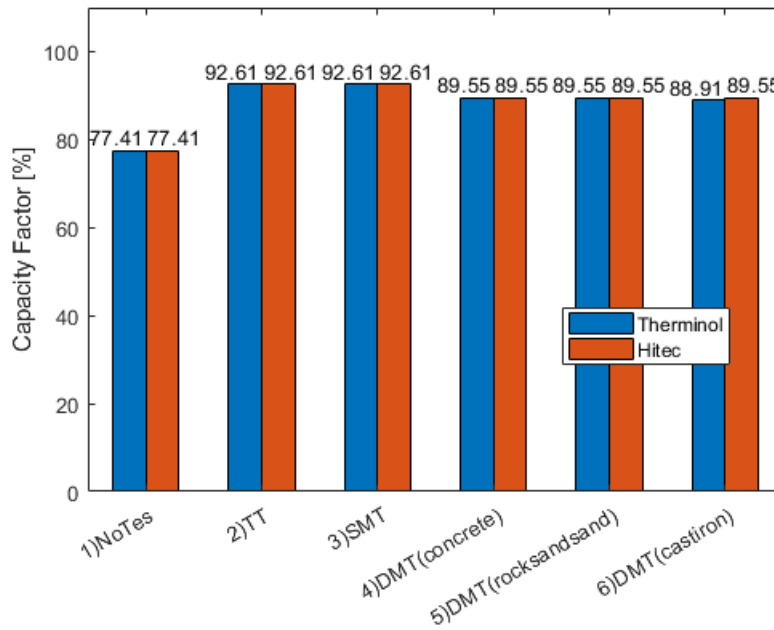


Figure 89 - Capacity factor - Results - SCENARIO 2

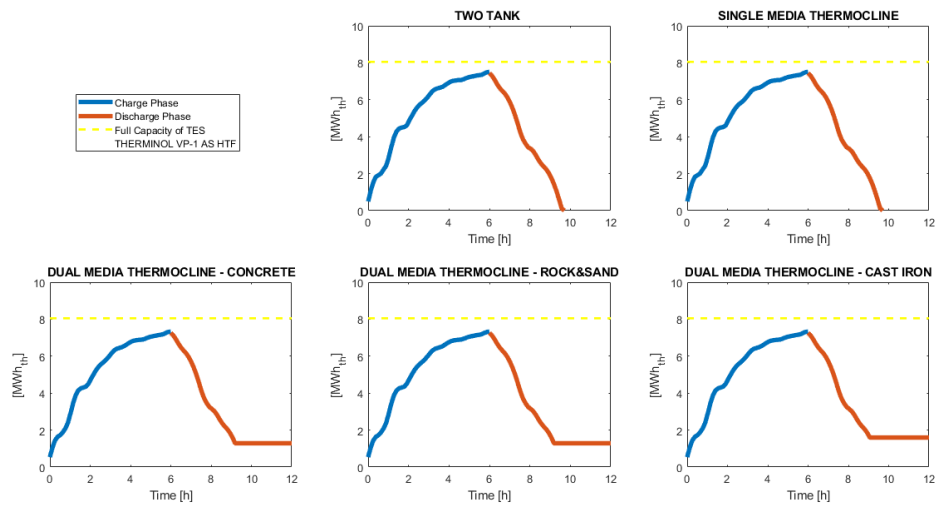


Figure 90 - State of the TESs - Therminol VP-1 - SCENARIO 2

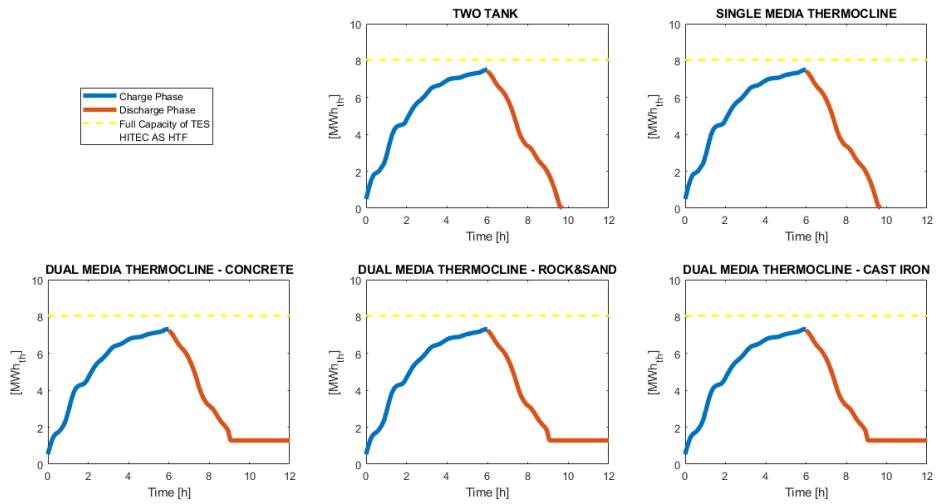


Figure 91 - State of the TESs - Hitec - SCENARIO 2

Scenario 3

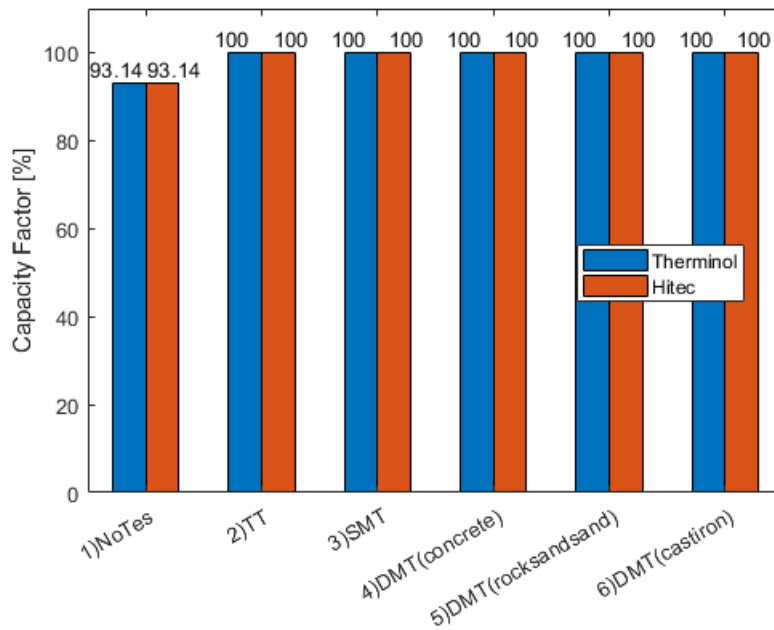


Figure 92 - - Capacity factor - Results - SCENARIO 3

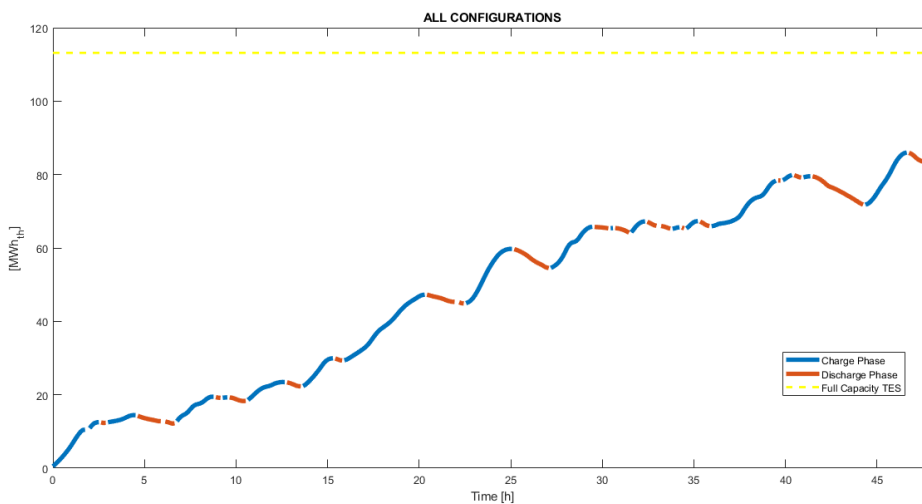


Figure 93 - State of the TESs - SCENARIO 3

It can be seen in the graph in Figure 92 the capacity factor is 100% for all the configurations which means the ability to work always in nominal conditions. Those results were clear also in the graph above (Figure 37, Figure 40, Figure 43, Figure 46, and Figure 61). The similarities are due to the oversizing of the TES related to the predominant OVERLOAD conditions of the industrial process chosen in this work.

5.7 Miscellaneous results – Surface Heat Exchangers

The next table shows the surface heat exchange of all the heat exchangers present in the plant, they are calculated implemented the approach presented in **Errore. L'origine riferimento non è stata trovata.**. All the results are for the nominal conditions regarding the HX present in the ORC and regarding the worst-case scenario for the ones present in the TES-Loop.

Table 23 - Surfaces heat exchange – Nominal Conditions

Surface Heat Exchange	Two-Tank	Single Thermocline	Dual-Media Thermocline
	[m ²]	[m ²]	[m ²]
HX1	378,92	378,92	334.09
HX2	378,92	378,92	370.62
Evaporator/HX3	634,13		
Recuperator	437,68		
Condenser	487,44		

6. Conclusions and future developments

The main motivation for this study was to research, examine and analyze the world of the Thermal Energy Storage in the context of the Waste Heat Recovery in order to find out a different way to produce electrical energy inefficient manner with a fluctuating source. Aim of the models which have been developed was to create a tool able to techno-economically compare the different configuration under investigation. Furthermore, try to find out results with large expandability even in another context to underline the viability and the advantages of the introduction of a powerful device as the TES.

In this regard, were evaluated in detail three typologies of TES: Two-Tank, Single Media Thermocline, and Dual Media Thermocline. For the latter, a model solved by a discretization by applying the explicit-forward difference scheme in time joint with the upwind difference scheme in space. From the validation emerged an average percentage error lower the 1%.

Rather than focusing on TES components alone, another goal of this thesis was achieved by comparing the TES alternatives in the context of electricity generation of an Organic Rankine Cycle. All the results are obtained by a group of the different mathematical model all integrated into one modeling environment. The thesis has been developed bearing in mind that a proper evaluation of the TES's affordability is strictly linked with the performances of all the plant in which is incorporated. Last but not the least, the reliability of the results of the three scenarios presented, especially the economic parameters which are easier to compare and to understand, is strictly dependent on the accuracy of the thermodynamics of the model.

6.1 Resume and discussion of the results

Throughout the whole sector of Energy's production, the most important factor determining whether energy technology can reach commercialization is the cost of energy. The most common standard-parameter which has been developed along the years is the LCOE to properly gauge the cost of a specific energy producing technology. LCOE represents a sort of “break-even” value that a power provider would need to charge in order to justify an investment in a particular energy project. Next table shows the resume of the LCOE results for the different scenarios and configuration analyzed in this work.

Table 24 - LCOE'scenarios results

		SCENARIO 1			SCENARIO 2			SCENARIO 3		
		LCOE [c€/kWhel]								
		Value	Var [%]	✓/X	Value	Var [%]	✓/X	Value	Var [%]	✓/X
Therminol VP-1	NO TES	10,49	-	-	9,75			6,09		
	TT	10,4	-0,87	✓	10,57	8,45	X	10,57	73,47	X
	STT	10,26	-2,23	✓	10,44	7,15	X	10,15	66,65	X
	DMT - Concrete	9,2	-12,35	✓	9,64	-1,09	✓	7,19	18,07	X
	DMT - Rocks&Sand	9,26	-11,7	✓	9,68	-0,69	✓	7,29	19,57	X
	DMT - Cast Iron	9,44	-10,2	✓	9,84	0,96	X	7,45	22,29	X
Hitec	TT	9,65	-7,99	✓	10,16	4,26	X	8,39	37,78	X
	STT	9,58	-8,69	✓	10,1	3,63	X	8,18	34,29	X
	DMT - Concrete	9,13	-12,94	✓	9,61	-1,36	✓	7,11	16,69	X
	DMT - Rocks&Sand	9,24	-11,89	✓	9,68	-0,7	✓	7,26	19,13	X
	DMT - Cast Iron	9,87	-6,77	✓	9,98	2,36	X	7,91	29,85	X

Scenario 1 presents every investment with advantages respect the configuration without energy storage, in particular, the best configuration is with Hitec as HTF and Concrete as filler with a reduction of LCOE of 12.94%. This configuration is the best one even in the other scenarios (-1.36% in 2, and +16.69% in 3). Regarding the third scenario appears clear an increasing value of the LCOE which underline a not-convenience of the investment under the hypothesis of this work but those results put in evidence big improvements considering the Dual Media Thermocline configuration as was expected from the big saving related the utilization of a lower amount of HTF which as a cost relevant in the cost breakdown of the TES (5.6.1).

The Capacity factor defined as in 4.3.4 represents a measure of the closeness of the working conditions to the design-conditions chosen for the energy plant.

Table 25 – Capacity factor’s scenarios results.

		SCENARIO 1			SCENARIO 2			SCENARIO 3		
		CAPACITY FACTOR [%]								
		Value	Var [%]	✓/✗	Value	Var [%]	✓/✗	Value	Var [%]	✓/✗
Therminol VP-1	NO TES	72,02	-	-	77,41			93,14		
	TT	100	38,85	✓	92,61	19,64	✓	100	7,37	✓
	STT	100	38,85	✓	92,61	19,64	✓	100	7,37	✓
	DMT - Concrete	97,02	34,71	✓	89,55	15,68	✓	100	7,37	✓
	DMT - Rocks&Sand	97,02	34,71	✓	89,55	15,68	✓	100	7,37	✓
	DMT - Cast Iron	96,45	33,92	✓	88,91	14,86	✓	100	7,37	✓
Hitec	TT	100	38,85	✓	92,61	19,64	✓	100	7,37	✓
	STT	100	38,85	✓	92,61	19,64	✓	100	7,37	✓
	DMT - Concrete	97,02	34,71	✓	89,55	15,68	✓	100	7,37	✓
	DMT - Rocks&Sand	97,02	34,71	✓	89,55	15,68	✓	100	7,37	✓
	DMT - Cast Iron	96,45	33,92	✓	88,91	14,86	✓	100	7,37	✓

Naturally, there is always an improvement of the CFs, which is one of the clearest aspects of introducing storage in an energy system. As direct consequences, there is a surplus of production in terms of electricity, the main output of the plant, presented in 5.4. The hypothetical trend of the industrial process (n°1) shows higher variation, more than 30% of improvement of the CF per each configuration, and obviously also a higher surplus of power net production. The remaining scenarios, following the real conditions present in literature, have a lower impact due to the shape of the source-profile which have less suitable features to better perform the energy production from a WHR introducing a TES. Furthermore, it should be emphasized that the annual integration results have been analyzed using simply a repetition of the results per each time analysis used (respectively 12h,12h and 48h for the three different scenarios). If for the Scenario 1 and 2 the capacity of the storage is almost empty at the end of the time analysis (empty for the configurations only with HTF, around the 20% of the energy is still stored for the dual media configurations - 5.6.3) as regards the Scenario 3 the around the 70% of the capacity is still unused at the end of the time analysis (Figure 93 - State of the TESs - SCENARIO 3), and when the annual parameters have been calculated, this amount of energy is not used and considered as a release in the environment.

Eventually, as reported in 5.2, the size of the storage is driven by the amount of heat-surplus of the OVERLOAD phase, and if in the first two scenarios the shape of the source profile allows a fully charged condition at the middle of the time analysis, for the third scenarios there is a big oversizing of the tank (more then 110kWh when the maximum value present in the state of the TES is close the 80kWh). Following the resume of the PBP and NPV results.

Table 26 – PBP's scenarios results.

		SCENARIO 1			SCENARIO 2			SCENARIO 3		
		PAYBACK PERIOD [years]								
		Value	Var [%]	✓/✗	Value	Var [%]	✓/✗	Value	Var [%]	✓/✗
Therminol VP-1	NO TES	9,77	-	-	9,08			5,67		
	TT	9,68	-0,92	✓	9,84	8,37	✗	9,84	73,54	✗
	STT	9,55	-2,25	✓	9,72	7,05	✗	9,45	66,67	✗
	DMT - Concrete	8,56	-12,38	✓	8,98	-1,10	✓	6,7	18,17	✗
	DMT - Rocks&Sand	8,63	-11,67	✓	9,01	-0,77	✓	6,78	19,58	✗
	DMT - Cast Iron	8,79	-10,03	✓	9,16	0,88	✗	6,94	22,40	✗
Hitec	TT	8,99	-7,98	✓	9,46	4,19	✗	7,82	37,92	✗
	STT	8,92	-8,70	✓	9,4	3,52	✗	7,62	34,39	✗
	DMT - Concrete	8,51	-12,90	✓	8,95	-1,43	✓	6,62	16,75	✗
	DMT - Rocks&Sand	8,61	-11,87	✓	9,01	-0,77	✓	6,76	19,22	✗
	DMT - Cast Iron	9,11	-6,76	✓	9,29	2,31	✗	7,37	29,98	✗

Table 27 – NPS's scenarios results.

		SCENARIO 1			SCENARIO 2			SCENARIO 3		
		NET PRESENT VALUE [M€]								
		Value	Var [%]	✓/✗	Value	Var [%]	✓/✗	Value	Var [%]	✓/✗
Therminol VP-1	NO TES	1,37	-	-	1,73			4,88		
	TT	1,94	41,61	✓	1,72	-0,58	✗	2,48	-49,18	✗
	STT	2	45,99	✓	1,78	2,89	✓	2,74	-43,85	✗
	DMT - Concrete	2,42	76,64	✓	2,05	18,50	✓	4,56	-6,56	✗
	DMT - Rocks&Sand	2,39	74,45	✓	2,03	17,34	✓	4,5	-7,79	✗
	DMT - Cast Iron	2,3	67,88	✓	1,95	12,72	✓	4,4	-9,84	✗
Hitec	TT	2,28	66,42	✓	1,9	9,83	✓	3,82	-21,72	✗
	STT	2,32	69,34	✓	1,92	10,98	✓	3,95	-19,06	✗
	DMT - Concrete	2,45	78,83	✓	2,06	19,08	✓	4,61	-5,53	✗
	DMT - Rocks&Sand	2,4	75,18	✓	2,03	17,34	✓	4,52	-7,38	✗
	DMT - Cast Iron	2,15	56,93	✓	1,91	10,40	✓	4,12	-15,57	✗

Those are the first two parameters used for the evaluation of an investment. The trend of the results is coherent to the results obtained with the LCOE. The best configuration is again the Hitec-DMT Concrete with a reduction of the PBP of 12.90% and an NPV which increase of 78.83% respect the conditions without storage in the plant. Looking at the results of the third scenario could be evident that some arrangements regarding the thermodynamic and the sizing of the TES could give still positive results.

Following the resume tables of the normalized cost of the storage, respectively divided by the some of the electric production (NCOTES - 4.3.2) and the capacity of the storage (Cost TES - 5.6.1)

Table 28- NCOTES's scenarios results

		SCENARIO 1	SCENARIO 2	SCENARIO 3
		NCOTES [€/kWhel]		
	NO TES	0	0	0
Therminol VP-1	TT	381,44	348,32	656,21
	STT	362,31	330,34	600,52
	DMT - Concrete	188,85	170,46	203,67
	DMT - Rocks&Sand	197,89	175,83	215,96
	DMT - Cast Iron	215,47	186,85	238,13
Hitec	TT	281,26	279,27	364,66
	STT	271,47	270,61	336,16
	DMT - Concrete	180,56	165,54	192,42
	DMT - Rocks&Sand	195,22	174,24	212,32
	DMT - Cast Iron	261,20	212,50	299,90

The values of the NCOTES are severely significant being related to the amount of electrical energy provided at the grid or used by the same companies who produced the waste used as a source of the plant. Per each scenario, is always the Hitec-DMT Concrete configuration the best one, with a lower value of 165.54 €/kWhel for Scenario 2.

Table 29 – Cost TES of scenarios results

		SCENARIO 1	SCENARIO 2	SCENARIO 3
		Cost TES [€/kWhth]		
	NOTES	0	0	0
Therminol VP-1	TT	99,29	138,12	26,45
	STT	94,31	130,96	24,21
	DMT - Concrete	47,69	65,36	8,21
	DMT - Rocks&Sand	49,98	67,42	8,71
	DMT - Cast Iron	54,10	71,13	9,60
Hitec	TT	73,22	110,74	14,70
	STT	70,67	107,31	13,55
	DMT - Concrete	45,60	63,47	7,76
	DMT - Rocks&Sand	49,30	66,81	8,56
	DMT - Cast Iron	65,58	81,48	12,09

Regarding the Cost of TES respect, the Storage capacity is clear a lower value for Scenario 3 having an oversize of the tanks. It should be underlined the decrease of this parameter when the capacity is higher. Even between the Scenario 1 and 2 there is a big difference of the specific cost (average value close the 25%) because the Scenario 1 has a capacity which is almost the double of the one present in Scenario 2.

6.2 Additional Scenarios – Post analysis

Develop a tool for a good Techno-Economic analysis allows to evaluate the performance of various configurations and scenarios but the big advantages of the modeling approach could be related also to the use of it in order to understand the possibility and the chance to achieve great results tuning some parameters helped by the computational work. From the results above, two problems emerged from the analysis:

- Oversizing the TESs's tanks without having the fully charged state along the process is not effective in economic terms.
- Having a source-profile which doesn't allow an almost complete discharge-phase of storage is not convenient in economic terms and thermodynamically as well.

Following will be presented an overview of the results obtained modifying some aspects of the Scenario 3, which is close to the real process present in the world of industry, having large fluctuations in terms of the waste-heat profile from the source, and load profile for the energy system.

6.2.1 Scenario 4 – Periodic Analysis without Oversize of the TESs's tanks (20% of Reduction)

The phase of OVERLOAD defined in this work is clearly the most important phase of exploiting a surplus of energy through a TES. As pointed out from the analysis of Scenario 3, fixing the capacity without a preliminary study of the source-profile and of the performance of the plant is not totally effective. So, in this scenario developed in post-analysis, the capacity of the storage has been reduced by 20% and fixed before the simulations. Next graph shows the differences.

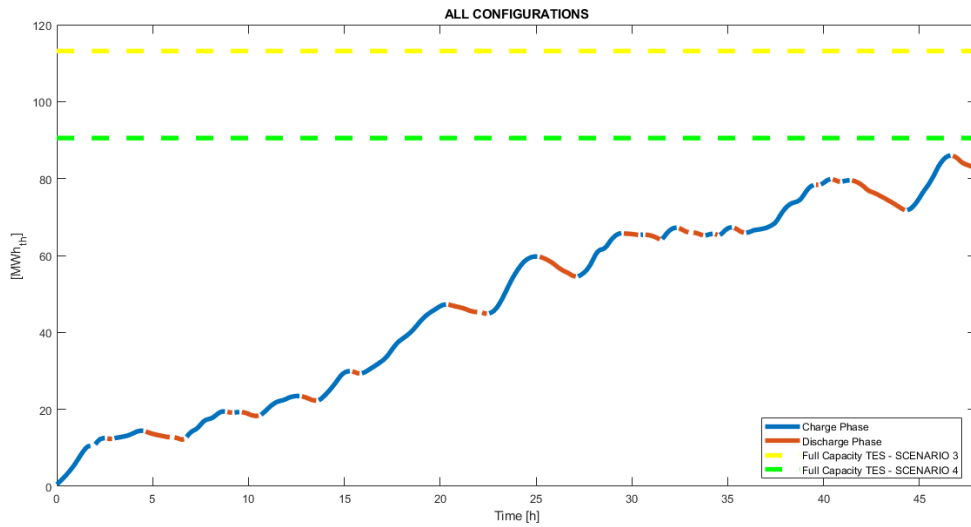


Figure 94 - Differences between Scenario 3 and Scenario 4

Following the main results obtained after that change. LCOE, NPV, and PBP are presented as the most popular and broadly used parameters in the field.

Table 30 - Lcoe's results - Scenario 4

		SCENARIO 3			SCENARIO 4		
		LCOE [c€/kWhel]					
		Value	Var [%]	✓/X	Value	Var [%]	✓/X
Therminol VP-1	NO TES	6,09			6,09		
	TT	10,57	73,47	X	7,72	26,77	X
	STT	10,15	66,65	X	7,21	18,39	X
	DMT - Concrete	7,19	18,07	X	4,96	-18,56	✓
	DMT - Rocks&Sand	7,29	19,57	X	5,03	-17,41	✓
	DMT - Cast Iron	7,45	22,29	X	5,14	-15,60	✓
Hitec	TT	8,39	37,78	X	6,13	0,66	X
	STT	8,18	34,29	X	5,81	-4,60	✓
	DMT - Concrete	7,11	16,69	X	4,91	-19,38	✓
	DMT - Rocks&Sand	7,26	19,13	X	5,01	-17,73	✓
	DMT - Cast Iron	7,91	29,85	X	5,46	-10,34	✓

Table 31 - NPV's results - Scenario 4

		SCENARIO 3			SCENARIO 4		
		NET PRESENT VALUE [M€]					
		Value	Var [%]	✓/X	Value	Var [%]	✓/X
Therminol VP-1	NO TES	4,88			4,88		
	TT	2,48	-49,18	X	4,24	-13,11	X
	STT	2,74	-43,85	X	4,55	-6,76	X
	DMT - Concrete	4,56	-6,56	X	5,93	21,52	✓
	DMT - Rocks&Sand	4,5	-7,79	X	5,89	20,70	✓
Hitec	DMT - Cast Iron	4,4	-9,84	X	5,82	19,26	✓
	TT	3,82	-21,72	X	5,22	6,97	✓
	STT	3,95	-19,06	X	5,41	10,86	✓
	DMT - Concrete	4,61	-5,53	X	5,97	22,34	✓
	DMT - Rocks&Sand	4,52	-7,38	X	5,91	21,11	✓
	DMT - Cast Iron	4,12	-15,57	X	5,63	15,37	✓

Table 32 - PBP's results - Scenario 4

		SCENARIO 3			SCENARIO 4		
		PAYBACK PERIOD [years]					
		Value	Var [%]	✓/X	Value	Var [%]	✓/X
Therminol VP-1	NO TES	5,67			5,67		
	TT	9,84	73,54	X	7,18	21,03	X
	STT	9,45	66,67	X	6,71	15,50	X
	DMT - Concrete	6,7	18,17	X	4,62	-22,73	✓
	DMT - Rocks&Sand	6,78	19,58	X	4,68	-21,15	✓
Hitec	DMT - Cast Iron	6,94	22,40	X	4,79	-18,37	✓
	TT	7,82	37,92	X	5,71	0,70	X
	STT	7,62	34,39	X	5,41	-4,81	✓
	DMT - Concrete	6,62	16,75	X	4,57	-24,07	✓
	DMT - Rocks&Sand	6,76	19,22	X	4,66	-21,67	✓
	DMT - Cast Iron	7,37	29,98	X	5,08	-11,61	✓

Even if the discharged phase doesn't occur for the totality of the capacity of the tank, the investment turns out positive for almost all the configuration with Dual Media Thermocline.

6.2.2 Scenario 5 – Periodic Analysis with a modified UNDERLOAD source-profile (5 % of Reduction)

Over the development of this thesis, during the phase of pre-design of the plant, it was already clear how important was the source-profile shape of the industrial process to choose for the analysis. The main feature of it should be a balance between the phase of UNDERLOAD/OVERLOAD along with the time analysis. Obviously, speaking of a technology related to the waste-heat of a process would be unlikely to think to tune the core-process to have a proper profile which better match the requirements of a TES-technology. In this typology of energy's plant, the randomness is a variable present and scope of the designers is to develop a model able to adapt itself to different working conditions. As pointed out from the analysis developed in this work, the source-profile of the cement industry presented in Scenario 3, has a profile with an UNDERLOAD-phase which doesn't allow to exploit a large part of all the energy stored. Aim of this paragraph is to demonstrate the improvements of the main parameters for the evaluation of the performance and of the investments, related to a reduction of the source-profile in UNDERLOAD of 5%. Those changes have been carried out by modifying the input data of the work of Legmann (5.1.3) before repeating the simulations. Next graphs show the differences in the scenarios.

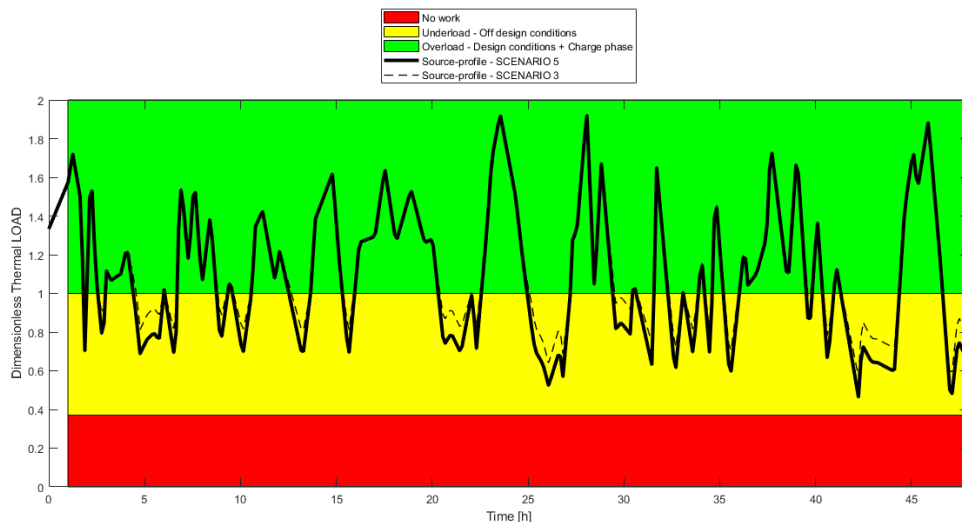


Figure 95 - Differences between Scenario 4 and Scenario 5 – Dimensionless T.L. representation

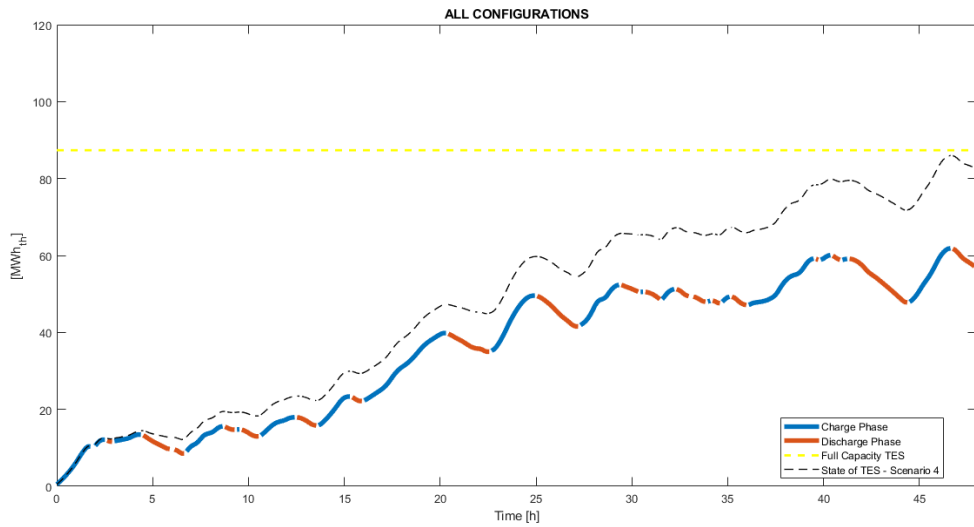


Figure 96 - Differences between Scenario 4 and Scenario 5 – State of TES

Table 33 - Lcoe's results - Scenario 5

		SCENARIO 3			SCENARIO 4			SCENARIO 5		
		LCOE [c€/kWhel]								
		Value	Var [%]	✓/✗	Value	Var [%]	✓/✗	Value	Var [%]	✓/✗
Therminol VP-1	NO TES	6,09			6,09			6,43		
	TT	10,57	73,47	✗	7,72	26,77	✗	7,68	16,28	✗
	STT	10,15	66,65	✗	7,21	18,39	✗	7,18	10,45	✗
	DMT - Concrete	7,19	18,07	✗	4,96	-18,56	✓	4,88	-31,76	✓
	DMT - Rocks&Sand	7,29	19,57	✗	5,03	-17,41	✓	4,93	-30,43	✓
	DMT - Cast Iron	7,45	22,29	✗	5,14	-15,60	✓	5,29	-21,55	✓
Hitec	TT	8,39	37,78	✗	6,13	0,66	✗	6,56	1,98	✗
	STT	8,18	34,29	✗	5,81	-4,60	✓	6,09	-5,58	✓
	DMT - Concrete	7,11	16,69	✗	4,91	-19,38	✓	4,90	-31,22	✓
	DMT - Rocks&Sand	7,26	19,13	✗	5,01	-17,73	✓	4,90	-31,22	✓
	DMT - Cast Iron	7,91	29,85	✗	5,46	-10,34	✓	5,76	-11,63	✓

Table 34 - NPV's results - Scenario 5

		SCENARIO 3			SCENARIO 4			SCENARIO 5		
		NET PRESENT VALUE [M€]								
		Value	Var [%]	✓/✗	Value	Var [%]	✓/✗	Value	Var [%]	✓/✗
Therminol VP-1	NO TES	4,88			4,88			4,44		
	TT	2,48	-49,18	✗	4,24	-13,11	✗	4,26	-4,05	✗
	STT	2,74	-43,85	✗	4,55	-6,76	✗	4,57	2,92	✓
	DMT - Concrete	4,56	-6,56	✗	5,93	21,52	✓	5,98	34,68	✓
	DMT - Rocks&Sand	4,5	-7,79	✗	5,89	20,70	✓	5,96	34,23	✓
	DMT - Cast Iron	4,4	-9,84	✗	5,82	19,26	✓	5,73	29,05	✓
Hitec	TT	3,82	-21,72	✗	5,22	6,97	✓	4,95	11,49	✓
	STT	3,95	-19,06	✗	5,41	10,86	✓	5,24	18,01	✓
	DMT - Concrete	4,61	-5,53	✗	5,97	22,34	✓	5,97	34,46	✓
	DMT - Rocks&Sand	4,52	-7,38	✗	5,91	21,11	✓	5,97	34,46	✓
	DMT - Cast Iron	4,12	-15,57	✗	5,63	15,37	✓	5,44	22,52	✓

Table 35 - PBP's results - Scenario 5

		SCENARIO 3			SCENARIO 4			SCENARIO 5		
		PAYBACK PERIOD [years]								
		Value	Var [%]	✓/✗	Value	Var [%]	✓/✗	Value	Var [%]	✓/✗
Therminol VP-1	NO TES	5,67			5,67			5,59		
	TT	9,84	73,54	✗	7,18	21,03	✗	7,15	21,82	✗
	STT	9,45	66,67	✗	6,71	15,50	✗	6,69	16,44	✗
	DMT - Concrete	6,7	18,17	✗	4,62	-22,73	✓	4,55	-22,86	✓
	DMT - Rocks&Sand	6,78	19,58	✗	4,68	-21,15	✓	4,59	-21,79	✓
Hitec	DMT - Cast Iron	6,94	22,40	✗	4,79	-18,37	✓	4,63	-20,73	✓
	TT	7,82	37,92	✗	5,71	0,70	✗	5,51	-1,45	✓
	STT	7,62	34,39	✗	5,41	-4,81	✓	5,37	-4,10	✓
	DMT - Concrete	6,62	16,75	✗	4,57	-24,07	✓	4,56	-22,59	✓
	DMT - Rocks&Sand	6,76	19,22	✗	4,66	-21,67	✓	4,56	-22,59	✓
	DMT - Cast Iron	7,37	29,98	✗	5,08	-11,61	✓	5,06	-10,47	✓

6.3 Future work

As was briefly mentioned in many chapters of this work, there is still the possibility of improving the models following the TEA approach. Thus, suggestions and recommendations which are useful for easily understand the weakness of the project and on the other hand for any possible future work based on the activity of research of this Thesis are presented below:

- Regarding the properties of the fluid used as a source of the plant, the simulations have been carried out using Air modeled by the intern library of EES. Having much more information from the industry considering the real chemical composition of the fluid used for the WHR could improve the accuracy of the results.
- The ORC could investigate much more, for example, an algorithm of optimization could be implemented in order to understand the best working fluid.
- The turbine and the evaporator, which are the most important components for the ORC, are severely addressed in the literature. Adding a more detailed model of them in this systematic approach could improve the reliability of the model.
- The off-design of the ORC must be further analyzed even in terms of operational and maintenance cost as well as from a life cycle viewpoint.
- Introduce in the model the world of PCM which is a well-established technology that has revolutionized the TES sector.

- More accurate geometrical observations regarding the design of the tanks.
- For the Dual Media Thermocline, a value of void factor of 0.3 has been adopted. A study with the variability of this value could be done in order to find out the best techno-economic configuration.
- During the breakdown of the Cost of the TES, Installation cost hasn't been considered. Especially when the size of the devices is higher and varies between the scenarios under investigation, its impact could be relevant.
- The cost of the components included some assumptions, introducing a much more detailed economic study should enrich the impact and viability of the results.
- A joint collaboration with some companies could be useful. Having proper data of real processes, not widely present in literature, will return real results and even the phase of pre-design of the system could return positive improvements to the integrated model.
- The Techno-Economic Approach followed in this work, may be extended to different sectors. A model able to sweep through a large range of temperatures can enrich the results obtained. Obviously, a proper model of different typologies of TES must be provided in order to match the various temperatures (from the world of cooling to the high range temperature)

7. References

- [1] N. H. Afgan and M. G. Carvalho, "Multi-criteria assessment of new and renewable energy power plants," vol. 27, pp. 739–755, 2002.
- [2] M. Fernández-torrijos, C. Sobrino, and J. A. Almendros-ibáñez, "Simplified model of a dual-media molten-salt thermocline tank with a multiple layer wall," vol. 151, pp. 146–161, 2017.
- [3] G. Walther *et al.*, "change," pp. 389–395, 2002.
- [4] J. Spelling and T. Fransson, "A Comparative Thermo-economic Study of Hybrid Solar Gas-Turbine Power Plants," vol. 136, no. January 2014, pp. 1–10, 2018.
- [5] E. Iakovou, A. Karagiannidis, D. Vlachos, A. Toka, and A. Malamakis, "Waste biomass-to-energy supply chain management : A critical synthesis," *Waste Manag.*, vol. 30, no. 10, pp. 1860–1870, 2010.
- [6] C. Clouser and M. Ewert, "The renewables cost challenge: Levelized cost of geothermal electric energy compared to other sources of primary energy – Review and case study," *Renew. Sustain. Energy Rev.*, vol. 82, no. October 2017, pp. 3683–3693, 2018.
- [7] S. Brückner, S. Liu, L. Miró, M. Radspieler, L. F. Cabeza, and E. Lävemann, "Industrial waste heat recovery technologies: An economic analysis of heat transformation technologies," *Appl. Energy*, vol. 151, pp. 157–167, 2015.
- [8] I. B. Page, "No Title."
- [9] B. Saleh, G. Koglbauer, M. Wendland, and J. F. Å, "Working fluids for low-temperature Organic Rankine Cycles Working fluids for low-temperature organic Rankine cycles," no. July, 2007.
- [10] Y. Fang, F. Yang, and H. Zhang, "Comparative analysis and multi-objective optimization of organic Rankine cycle (ORC) using pure working fluids and their zeotropic mixtures for diesel engine waste heat recovery," *Appl. Therm. Eng.*, vol. 157, no. April, p. 113704, 2019.
- [11] H. Chen, D. Y. Goswami, and E. K. Stefanakos, "A review of thermodynamic cycles and working fluids for the conversion of low-grade heat," *Renew. Sustain. Energy Rev.*, vol. 14, no. 9, pp. 3059–3067, 2010.
- [12] P. Arvay, M. R. Muller, and V. Ramdeen, "Economic Implementation of the Organic Rankine Cycle in Industry," pp. 12–22, 2011.
- [13] K. Park, S. Oh, and W. Won, "Techno-economic optimization of the integration of an organic Rankine cycle into a molten carbonate fuel cell power plant," vol. 36, no. 3, pp. 345–355, 2019.
- [14] S. M. Camporeale, A. M. Pantaleo, P. D. Ciliberti, and B. Fortunato, "Cycle configuration analysis and techno-economic sensitivity of biomass externally fired gas turbine with bottoming ORC Internal Rate of Return," *ENERGY Convers. Manag.*, vol. 105, pp. 1239–1250, 2015.
- [15] A. D. Akbari and S. M. S. Mahmoudi, "Thermo-economic analysis & optimization of the combined supercritical CO₂ (carbon dioxide) recompression Brayton / organic Rankine cycle," *Energy*, vol. 2, 2014.
- [16] R. Pili, A. Romagnoli, H. Spliethoff, and C. Wieland, "Techno-Economic Analysis of Waste Heat Recovery with ORC from Fluctuating Industrial Sources," *Energy*

- Procedia*, vol. 129, pp. 503–510, 2017.
- [17] C. S. Iii and C. Depcik, “Review of organic Rankine cycles for internal combustion engine exhaust waste heat recovery,” *Appl. Therm. Eng.*, vol. 51, no. 1–2, pp. 711–722, 2013.
- [18] Q. Li, S. S. M. Tehrani, and R. A. Taylor, “Techno-economic analysis of a concentrating solar collector with built-in shell and tube latent heat thermal energy storage,” *Energy*, vol. 121, pp. 220–237, 2017.
- [19] S. Lecompte, H. Huisseune, M. van den Broek, S. De Schampheleire, and M. De Paepe, “Part load based thermo-economic optimization of the Organic Rankine Cycle (ORC) applied to a combined heat and power (CHP) system,” *Appl. Energy*, vol. 111, pp. 871–881, 2013.
- [20] F. Heberle and D. Brüggemann, “Thermoeconomic Analysis of Hybrid Power Plant Concepts for Geothermal Combined Heat and Power Generation,” pp. 4482–4497, 2014.
- [21] J. Orbie, “Modeling of part load behavior of an Organic Rankine Cycle (ORC) with a direct evaporator,” 2014.
- [22] Y. Dai, J. Wang, and L. Gao, “Parametric optimization and comparative study of organic Rankine cycle (ORC) for low grade waste heat recovery,” *Energy Convers. Manag.*, vol. 50, no. 3, pp. 576–582, 2009.
- [23] Z. Q. Wang, N. J. Zhou, J. Guo, and X. Y. Wang, “Fluid selection and parametric optimization of organic Rankine cycle using low temperature waste heat,” *Energy*, vol. 40, no. 1, pp. 107–115, 2012.
- [24] L. Pierobon, T. Nguyen, U. Larsen, F. Haglind, and B. Elmegaard, “Multi-objective optimization of organic Rankine cycles for waste heat recovery : Application in an offshore platform,” *Energy*, vol. 58, pp. 538–549, 2013.
- [25] L. Branchini, A. De Pascale, and A. Peretto, “Systematic comparison of ORC configurations by means of comprehensive performance indexes,” vol. 61, 2013.
- [26] R. T. Jacobsen, “‘Thermodynamic Properties of Air and Mixtures of Nitrogen, Argon, and Oxygen from 60 to 2000 K at Pressures to 2000 MPa’, J. Phys. Chem. Ref. Data, Vol. 29, No. 3, 2000.,” 2000.
- [27] F. Calise, M. Dentice, M. Vicidomini, and M. Scarpellino, “Design and simulation of a prototype of a small-scale solar CHP system based on evacuated flat-plate solar collectors and Organic Rankine Cycle,” *Energy Convers. Manag.*, vol. 90, pp. 347–363, 2015.
- [28] A. Cavallini, *13 - Heat transfer and heat exchangers*. Elsevier Ltd, 2017.
- [29] M. E. Mondejar, F. Ahlgren, M. Thern, and M. Genrup, “Quasi-steady state simulation of an organic Rankine cycle for waste heat recovery in a passenger vessel,” *Appl. Energy*, vol. 185, pp. 1324–1335, 2017.
- [30] D. H. Cooke, “Copyright © 1984 by ASME,” 2019.
- [31] C. Zhang *et al.*, “A novel methodology for the design of waste heat recovery network in eco-industrial park using techno-economic analysis and multi-objective optimization,” *Appl. Energy*, vol. 184, pp. 88–102, 2016.
- [32] R. Chacartegui, L. Vigna, J. A. Becerra, and V. Verda, “Analysis of two heat storage integrations for an Organic Rankine Cycle Parabolic trough solar power plant,” *Energy Convers. Manag.*, vol. 125, pp. 353–367, 2016.
- [33] M. Khaljani, R. K. Saray, and K. Bahlouli, “Comprehensive analysis of energy , exergy

- and exergo-economic of cogeneration of heat and power in a combined gas turbine and organic Rankine cycle,” *Energy Convers. Manag.*, vol. 97, pp. 154–165, 2015.
- [34] M. Y. S. M. S. Mahmoudi, “ORIGINAL RESEARCH PAPER A thermodynamic study of waste heat recovery from GT-MHR using organic Rankine cycles,” pp. 181–196, 2011.
- [35] H. Legmann, “Recovery of industrial heat in the cement industry by means of the orc process,” pp. 29–35.
- [36] A. Gil, A. Castell, E. Oro, B. L. F. Cabeza, and C. Sole, “Review of Solar Thermal Storage Techniques and Associated Heat Transfer Technologies,” vol. 100, no. 2, pp. 525–538, 2012.
- [37] G. Alva, Y. Lin, and G. Fang, “An overview of thermal energy storage systems,” *Energy*, vol. 144, pp. 341–378, 2018.
- [38] M. Longeon, A. Soupart, J. Fourmigué, A. Bruch, and P. Marty, “Experimental and numerical study of annular PCM storage in the presence of natural convection,” *Appl. Energy*, vol. 112, pp. 175–184, 2013.
- [39] PEI-WEN LI, *Thermal Energy Storage Analyses and Designs*. 2017.
- [40] A. M. Papadopoulos, “State of the art in thermal insulation materials and aims for future developments,” vol. 37, pp. 77–86, 2005.
- [41] M. M. Kenisarin, “High-temperature phase change materials for thermal energy storage,” vol. 14, pp. 955–970, 2010.
- [42] J. T. Van Lew, P. Li, and J. Stephens, “Analysis of Heat Storage and Delivery of a Thermocline Tank,” no. April 2016, 2011.
- [43] M. Hänchen, S. Brückner, and A. Steinfeld, “High-temperature thermal storage using a packed bed of rocks e Heat transfer analysis and experimental validation,” *Appl. Therm. Eng.*, vol. 31, no. 10, pp. 1798–1806, 2011.
- [44] D. Energetica, “Economic and Scenario Analyses of New Gas Turbine Combined Cycles With No Emissions of,” vol. 127, no. July 2005, 2019.
- [45] S. Lemmens, “Cost engineering techniques & their applicability for cost estimation of organic rankine cycle systems,” *Energies*, vol. 9, no. 7, 2016.
- [46] S. S. Mostafavi, R. A. Taylor, K. Nithyanandam, and A. Shafiei, “Annual comparative performance and cost analysis of high temperature , sensible thermal energy storage systems integrated with a concentrated solar power plant,” *Sol. Energy*, vol. 153, pp. 153–172, 2017.
- [47] R. Jacob, W. Saman, and F. Bruno, “Capital cost expenditure of high temperature latent and sensible thermal energy storage systems,” *AIP Conf. Proc.*, vol. 1850, 2017.
- [48] P. Li, J. Van Lew, C. Chan, W. Karaki, J. Stephens, and J. E. O. Brien, “Similarity and generalized analysis of ef fi ciencies of thermal energy storage systems,” *Renew. Energy*, vol. 39, no. 1, pp. 388–402, 2012.

